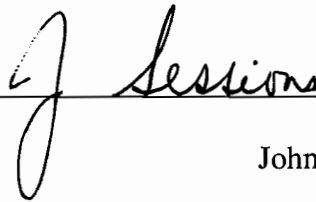


AN ABSTRACT OF THE DISSERTATION OF

Abdullah E. Akay for the degree of Doctor of Philosophy in Forest Engineering
presented on March 31, 2003.

Title: Minimizing Total Cost of Construction, Maintenance, and Transportation Costs
with Computer-Aided Forest Road Design.

Abstract approved: _____



John Sessions

The systems currently available for forest road design are not capable of making computer-aided design judgments such as: 1) automated generation of alternative grade lines, 2) optimizing vertical alignment, 3) minimizing total cost of construction, maintenance, and transportation costs, and 4) aiming for least environmental impacts. In recent years, advances in the processing speed and real-time rendering and viewing of high-resolution three dimensional (3D) graphics on microcomputers, combined with improved resolution in mapping technologies have made it possible to locate a route interactively between two given points on a 3D display of a ground surface. A 3D forest road alignment model, TRACER, aided by an interactive computer system, was developed to help a designer with rapid evaluation of alternatives. The road design objective is to design a path with the

lowest total construction, maintenance, and transportation costs, while conforming to design specifications, environmental requirements, and driver safety.

The model relies on a high-resolution digital elevation model (DEM) to provide terrain data for supporting the analysis of road design features such as ground slope, topographic aspect, and other landform characteristics. Light Detection and Ranging (LIDAR) system is one of the systems that provide high-resolution and accurate DEM data. The contributions of the TRACER program are: (1) data input is enhanced through a 3D graphic interface, (2) user efficiency is enhanced through automated horizontal and vertical curve fitting routines, cross section generation, and cost routines for construction, maintenance, and vehicle use, (3) road feasibility is ensured by considering terrain conditions, geometric specifications, and driver safety, (4) design time is reduced in the early stage of the forest road design by allowing the designer to quickly examine alternative routes, (5) economic efficiency is enhanced by combining modern optimization techniques to minimize earthwork allocation cost using linear programming and to optimize vertical alignment using a heuristic technique (Simulated Annealing), and (6) environmental impacts are considered by estimating the average annual volume of sediment delivered to a stream from the road section. It is anticipated that the computer-aided analysis of route selection will improve the efficiency of road designers in identifying road alignment alternatives that are best suited to local conditions considering costs, environmental impacts, and driver safety.

©Copyright by Abdullah E. Akay
March 31, 2003
All Rights Reserved

Minimizing Total Cost of Construction, Maintenance, and Transportation

Costs with Computer-Aided Forest Road Design

by
Abdullah E. Akay

A DISSERTATION

submitted to

Oregon State University

in partial fulfillment of
the requirements for the
degree of

Doctor of Philosophy

Presented March 31, 2003
Commencement June 2003

ACKNOWLEDGEMENTS

I would have never finished this dissertation without the help and wishes of Allah, the most Merciful, and the most Compassionate. I would like to express my gratitude to people of my country, Turkey, for providing me this rare opportunity to pursue my academic career in the United States of America.

This dissertation can be presented because of the help and support of many people. I would first like to thank the chair of my graduate committee, Dr. John Sessions, for his guidance and advice in completing my doctorate. I am deeply indebted to him from the beginning to the end of my graduate study. I could not have had a better advisor and colleague.

I would like to thank the other members of my committee: Dr. Jon Kimerling, Dr. Kevin Boston, Dr. Loren Kellogg, and Dr. Darrell Ross. I would also like to thank Dr. Pete Bettinger and Dr. Ward Carson for the discussions we had concerning the direction of this dissertation. I want to thank Jeff Starnes and Dave Young at the Oregon State University Research Forest for providing me with their valuable experiences in forest road design. I also want to thank the faculty and graduate students who I have associated with at Oregon State University. They have made the time I have spent here enjoyable.

I would like to express my sincere appreciation to my dear wife, Tuba, whose patience and support enabled me to complete this dissertation. I want to thank my

charming daughter, Alanur, for giving me love, laughter, and enjoyment when I needed it most.

Furthermore, I would like to mention some of my friends who provided me with helpful comments: Cumhuriyet A. Gelogullari and Serdar Turan. Many people contributed to this work, either directly or indirectly. Thanking every one by name would take many pages. Therefore, for the people I did not mention in this acknowledgment, thank you.

TABLE OF CONTENTS

	<u>Page</u>
INTRODUCTION.....	1
CAN AN EXPERT DESIGN SYSTEM HELP FOREST ROAD DESIGN AND CONSTRUCTION?	6
Abstract.....	7
Introduction.....	8
Highway Design Systems	9
Roadway Design	9
Earthwork Allocation	19
Forest Road Design Systems	31
Current Methods	32
TRACER, a Decision Support System	33
Applying TRACER to Forest Road Design.....	43
Conclusions and Extensions	47
Literature Cited	50
A METHOD FOR MINIMIZING CONSTRUCTION, MAINTENANCE, AND TRANSPORTATION COSTS WITH COMPUTER-AIDED FOREST ROAD DESIGN.....	53
Abstract.....	54
Introduction.....	55
Method	59
Data Preparation.....	59
Design Constraints	64
Cross Sections	79
Total Cost.....	80
Construction Costs	81

TABLE OF CONTENTS (Continued)

	<u>Page</u>
Maintenance Costs	90
Transportation Costs	92
Sediment Production	94
Vertical Alignment Optimization	94
Model Application	96
Conclusions and Extensions	100
Literature Cited	103
APPLYING THE DECISION SUPPORT SYSTEM, TRACER, TO FOREST ROAD DESIGN	106
Abstract	107
Introduction	108
Program Features	110
Model Application	116
Data Preparation	116
Road Design Specifications	118
Example A	124
Example B	126
Results and Discussion	128
Conclusions and Extensions	131
Literature Cited	133
CONCLUSIONS	135
BIBLIOGRAPHY	142
APPENDICES	148

LIST OF FIGURES

<u>Figure</u>	<u>Page</u>
2.1. Profile View of the Highway Section.	10
2.2. Chematic diagram of a terrain on a square grid.	12
2.3. Alternative Routes Within Alternative Bands of Interest.	15
2.4. Profile-Grade Line and Mass Diagram.	20
2.5. The Theory of the forest road alignment optimization model, TRACER.	34
2.6. Graphical user interface of the model, displaying 3D image of the terrain.	38
2.7. Locating a feasible trial route between two given points.	39
2.8. Generation of a vertical and horizontal alignment.	40
2.9. Road Profile indicating gradient and vertical alignment in Example A.	45
2.10. Road Profile indicating gradient and vertical alignment in Example B.	46
3.1. Theory of the forest road alignment optimization model, TRACER.	60
3.2. Locating a feasible trial route between two given points.	63
3.3. Elements of horizontal and vertical roadway (tangent) grades.	65
3.4. Geometry of a symmetrical vertical curve (crest) used in the model.	68
3.5. Geometry of a simple horizontal circular curve used in the model.	72
3.6. Road elements on the cross section.	79
3.7. Profile view showing road gradient and vertical alignment in Example A.	97
3.8. Profile view showing road gradient and vertical alignment in Example B.	98
4.1. Locating a feasible trial route between two given points.	112
4.2. Optimized vertical alignment.	115

LIST OF FIGURES (Continued)

<u>Figure</u>	<u>Page</u>
4.3. 3D image of the terrain.	117
4.4. Example A: Profile view showing road gradient and vertical alignment.....	124
4.5. Example A: Feasible solutions during the search to identify the best vertical alignment.....	125
4.6. Example A: The summary table indicating cost components and sediment..	126
4.7. Example B: Profile view showing road gradient and vertical alignment.	127
4.8. Example B: Feasible solutions during the search to identify the best vertical alignment.....	128
4.9. Example B: The summary table indicating cost components and sediment..	129

LIST OF TABLES

<u>Table</u>	<u>Page</u>
2.1. The data format of the digital elevation model (DEM) data format.....	36
2.2. Specifications for the aggregate surfacing material.....	44
3.1. Road specifications for the surfacing material used in design examples.....	96
4.1. Specifications for surfacing material used in the model application.....	119
4.2. Road design specifications for elements other than road surfacing.....	120

LIST OF APPENDICES

	<u>Page</u>
A 1. Displaying and Rendering 2D and 3D Image of the Terrain	149
A 2. Determining the Length of a Vertical Curve	152
A 3. Safe Stopping Distance on a Horizontal Curves.....	154
A 4. Stream Crossing Angle	156
A 5. Locating Station Points Along the Roadway	157
A 6. Extracting Ground Elevations from the DEM	162
A 7. Determining Cross Section Types.....	163
A 8. Computing Cut and Fill Areas on Cross Sections.....	168
A 9. Earthwork Volume.....	188
A 10. Offtracking around the Horizontal Curve	191
A 11. Clearing the Middle Ordinate Distance for SSD	193
A 12. Clearing and Grubbing Limits	198
A 13. Locating ditch relief culverts	199
A 14. Surfacing Cost Components.....	206
A 15. Seeding and Mulching Area.....	210
A 16. Vehicle Performance.....	211
A 17. Vehicle Cost Calculation.....	219
A 18. Road Sediment Delivery Prediction.....	222
A 19. Optimizing Vertical Alignment.....	227
A 20. Turnout Design Geometry.....	229

LIST OF APPENDIX FIGURES

<u>Figure</u>	<u>Page</u>
A1-1. 2D image of the terrain.	149
A1-2. 3D image of the terrain.	150
A1-3. 2D images of the terrain squeezed in above-below display format.	151
A2-1. SSD is greater than t the length of a vertical curve.	153
A2-2. SSD is less than t the length of a vertical curve.	153
A3. Safe stopping distance on a horizontal curve.	155
A4. Elements of stream-crossing angle.	156
A5-1. Layout elements of a vertical curve (crest).	157
A5-2. Layout elements of a horizontal circular curve (right-centered).	159
A5-3. Layout elements of a straight roadway (tangent).	161
A6. Estimation of the ground elevation at a station point.	162
A7-1. The types of cross sections.	164
A7-2. A crowned type road surface used as a scale in the model.	165
A7-3. Geometry of a cross section on a straight roadway (tangent).	165
A7-4. Geometry of a cross section on a right centered horizontal curve.	166
A8-1. Plan view of the cut and fill cross section.	168
A8-2. Profile view of the cut and fill cross section.	168
A8-3. Cut and fill areas on right road side.	169
A8-4. Case 1: Cut and fill area on right road side.	170
A8-5. Case 3: Cut and fill area on right road side.	172

LIST OF APPENDIX FIGURES (Continued)

<u>Figure</u>	<u>Page</u>
A8-6. Cut and fill areas on left road side.....	173
A8-7. Cut and fill areas on ditch section.....	174
A8-8. Case 1: Cut and fill area on ditch section.	175
A8-9. Case 3: Cut and fill area on ditch section.	176
A8-10. Cut and fill areas on the catch basin.	177
A8-11. Case 1: Cut and fill area on a catch basin.....	178
A8-12. Cut and fill areas on cut slope section.	180
A8-13. Locating curtain fence over the cut slope.	182
A8-14. Geometry of a retaining wall.	183
A8-15. Cut and fill areas on fill slope section.	185
A9-1. Earthwork Volume: cut and fill section to through cut section.	189
A9-2. Earthwork Volume: through fill to through cut section.....	190
A10. Maximum offtracking on a horizontal curve.	191
A11-1. Clearing the middle ordinate distance for SSD.	194
A11-2. Computing M_p distances.	195
A11-3. $a_{p=2}$ distance between PC and the second station point on the curve.....	196
A11-4. $a_{p=3}$ distance between PC and the third station point on the curve.	197
A12. Clearing and grubbing limits.....	198
A13-1. The low point on the vertical (sag) curve.	199
A13-2. Plan view of the culvert on the cut and fill cross section.	200

LIST OF APPENDIX FIGURES (Continued)

<u>Figure</u>	<u>Page</u>
A13-3. Scenario 1: Geometry of a ditch relief culvert.....	201
A13-4. Scenario 2: Geometry of a ditch relief culvert.....	202
A13-5. Hand-placed riprap material.	204
A13-6. Machine-placed riprap material.	205
A14. Elements of the aggregate surfacing.	206
A15. Seeding and mulching area.	210
A16-1. Dynamic wheel load distribution on stinger type truck (loaded).	211
A16-2. Determining subsections using vehicle speed.....	213
A16-3. Case 1: Determining travel time.....	214
A16-4. Case 2: Determining travel time.....	215
A16-5. Case 3: Determining travel time.....	217
A16-6. Case 4: Determining travel time.....	217
A18. Determining stream distance.....	224
A19. Flow of the simulated annealing method.....	228
A20. Elements of a turnout geometry.....	229

DEDICATION

This dissertation is dedicated to my parents,
Safiye and Ahmet Akay

Minimizing Total Cost of Construction, Maintenance, and Transportation Costs with Computer-Aided Forest Road Design

Chapter 1

Introduction

The main factors determining the location of a road are construction and maintenance costs, transportation costs, environmental requirements, and driver safety. A designer has to carefully determine a route with the lowest construction, maintenance, and transportation costs while conforming to protection of soil and water resources, and providing driver safety. For low volume forest roads in mountainous terrain, construction and maintenance are the largest cost components (Pearce, 1974). Transportation cost is also a factor and varies with truck performance and equipment costs, as well as road gradient and curvature.

Traditional manual methods of road design analysis depend upon a designer's intuition and judgment. Computers have been used in forest road design since the 1960's, but have largely been applied to automate the computational tasks of earthwork calculation and computer aided drafting. The mass diagram is employed to balance the required quantities of cut and fill.

The systems currently available for forest road design are not intended to make computer-aided design judgments such as generation of alternative grade lines, best fitting vertical alignment for minimizing earthwork, minimizing the total cost of construction, maintenance, and transportation, and aiming for the least environmental

impact. They are generally used as a tool to make the mathematical calculations required to do basic manual road design. Since the manual method is “trial-and-error” and there are many possible alignments, it is highly conceivable that the manual design might not yield the best result. In many cases, data input is cumbersome in current programs. The road designer must enter many set-up parameters and input traverse notes into the related modules.

After entering the survey data and design parameters, some programs manipulate geometric road design and earthwork balance calculations by allowing the designer to work in plan, profile or cross section view simultaneously, using a visual display screen (RoadEng, 2002 and Lumberjack, 1995). However, the designer has to make these manipulations in such a way that all the constraints of horizontal and vertical alignments are satisfied, which can be very time consuming. The designer has to examine a number of alternatives to be sure that the final route location is “reasonably” cost effective among the infinite number of alternative grade lines.

In recent years, advances in the processing speed and real-time rendering and viewing of high-resolution three dimensional (3D) graphics on microcomputers have made it possible to locate a route interactively on a 3D display of a ground surface generated by a high-resolution digital elevation model (DEM). LIDAR (Light Detection and Ranging) is one of the fastest growing systems that provide high-resolution and accurate DEMs. The accuracy of each point on the ground is approximately 15 cm in the vertical, and 1.0 meter in the horizontal (Ahmed et al. 2000).

A three-dimensional forest road alignment optimization model, TRACER, aided by an interactive computer system, was developed to help the designer with rapid evaluation of alternatives for the most economical path selection problem. The objective is to locate a path with the lowest sum of construction, and future maintenance and transportation costs, while conforming to design specifications, environmental requirements, and providing driver safety. The designer generates the alternative road alignments by tracing the possible paths using computer cursor on a 3D image of the terrain. The model relies on a digital elevation model (DEM) to provide terrain data for supporting the analysis of road design features such as ground slope, topographic aspect, and other landform characteristics used during the development of the forest road design.

The model has three stages. The first stage involves the road designer generating a trial route between two given points by establishing a series of intersection points on the 3D image of the terrain, subject to a wide range of geometric specifications and environmental requirements. The geometric specifications are maximum allowable road grade, minimum radius of the horizontal curves, minimum length of the vertical curves, minimum distance between curves, and minimum safe stopping distance for driver safety. It is also required that horizontal and vertical curves do not overlap each other. The environmental requirements include minimum allowable road grade and rolling road grades to provide proper drainage, minimum distance from riparian zones to protect stream

channels, minimum stream-crossing angle to reduce damage to riparian zones, and maximum height of cuts and fills at any section to reduce potential soil movement.

In the second stage, the model generates the horizontal and a preliminary vertical alignment by locating station points between the intersection points that were established in the first stage. The model locates the cross sections, computes earthwork volumes between stations using the average end-area technique, minimizes earthwork costs using a linear programming (LP) formulation, computes total cost of the road section including construction, maintenance and transportation costs, and estimates the average annual volume of sediment delivered to a stream from the road section, using the method of a GIS-based road erosion/delivery model.

In the third stage, the model adjusts the vertical alignment to find the lowest total cost. This is accomplished using a combinatorial optimization technique (Simulated Annealing) to select the best vertical alignment that minimizes the sum of construction, maintenance and transportation costs considering technically feasible grades within the specified elevation ranges of the intersection points of the vertical alignment. For each trial vertical alignment, the model calculates cross sections, earthwork volumes, and sediment delivery, and minimizes earthwork costs using LP.

The model presented here has the advantages of providing a good quality/near optimum solution, and it is easily applied by the forest engineer. By incorporating modern computer software languages with displaying and rendering high-resolution 2D and 3D images of the terrain in real-time, and using GIS technologies and optimization techniques, a forest road designer can quickly evaluate alternatives and

design a path with the approximately lowest total cost considering construction and future maintenance and transportation costs, while conforming to design specifications, environmental requirements, and providing driver safety.

This dissertation is presented in manuscript format with three papers to be submitted to professional engineering journals or conference proceedings. As such, some repetition of subject matter is inevitable. The chapter headings are

1. Introduction: Presents the objective and scope of the thesis.
2. Manuscript 1: Can An Expert Design System Help Forest Road Design and Construction? This synthesizes the methods that are currently available for road design and construction, and investigates if a decision support system may help forest road designers.
3. Manuscript 2: A Method for Minimizing Construction, Maintenance, and Transportation Costs with Computer-Aided Forest Road Design. This covers the methodology behind TRACER and summarizes the results of its application.
4. Manuscript 3: Applying The Decision Support System, TRACER, to Forest Road Design. This presents the features of the TRACER and the application of the program.
5. Conclusions: Summarizes the entire thesis and presents recommendations for implementation and further development.

Bibliography

Appendices

Chapter 2

Can An Expert Design System Help Forest Road Design and Construction?

Abdullah E. Akay
John Sessions

Department of Forest Engineering
Oregon State University
Corvallis, OR 97331

Abstract

Advances in the processing speed of microcomputers have increased interest in computer-aided design systems employing modern optimization techniques to provide rapid evaluation of road alignments in a more systematic manner than traditional manual methods. Such systems are available to designers in the field of highway engineering. However, current forest road design systems are incapable of making computer-aided design judgments such as automated generation of alternative grade lines, minimizing total costs, and aiming for least environmental impacts. They are generally used as a tool to make the mathematical calculations required to do basic manual road design. In this study, optimal route location systems currently available for highway design were synthesized. A 3D forest road alignment model, TRACER, was developed to help a forest road designer with quick evaluation of alternatives and to design a path with the lowest total cost considering construction and future maintenance and transportation costs, while conforming to design specifications, environmental requirements, and driver safety. This paper synthesizes the optimal route location systems in highway design and demonstrates how TRACER might help a forest road designer determine horizontal and vertical road alignments considering all of costs and impacts simultaneously.

Introduction

The design of a road between two end points of known locations and elevations is a complex problem that must consider economic and environmental factors. The designer has to carefully determine a route with the lowest sum of construction, and future maintenance and transportation costs while protecting soil and water resources. Road construction is a significant portion of the total cost of harvesting the timber and transporting them from stump to the mills. The major cost component in the construction of a road is the earthwork cost involved in establishing the position of the roadway.

There has been increasing interest in computer-aided analysis of route selection, as it could lead to considerable time savings in road design. Road design analysis by computer also provides quick evaluation of alternatives in a more systematic manner than traditional manual methods. Many systems using optimization techniques have been developed for optimal route location in the field of highway design. There are no optimization techniques applied in forest road construction. The fundamental route location problem of finding the best or optimum path between two points as a function of physical, economical, and environmental factors, normally involves similar stages for both highways and forest roads. The objective of this paper is to provide a synthesis of the optimal route location systems that are currently available for highway design and to investigate if a decision support system, TRACER, might help a forest road designer determine the best route between

two chosen points that minimizes the total cost of construction plus the future cost of maintaining and using the road.

Highway Design Systems

Route location is one of the major decisions in road design to minimize total cost. There are an infinite number of possible combinations of line and grade to connect two given points on a surface. In order to be sure that designer's final route location is the most cost effective one with minimum environmental damage, the designer has to examine many alternatives. Such a problem with many solutions can be solved using one of the optimization techniques that systematically search for the solution with minimum cost among the acceptable solutions. Cost of the earthmoving operation has a significant effect on the total costs and productivity of an entire road design project. The following discussion is divided into two sections. The first section summarizes roadway design systems and the second section focuses specifically on earthwork allocation methods.

Roadway Design

Roberts (1957) developed a computer-aided system that integrated photogrammetric methods and air photo analysis techniques with the rapidly advancing microcomputers to solve the optimal highway location problem. As the problem became increasingly complex, he suggested dividing highway costs into components that affect the location and analyze these components separately. Some of the more important cost components were land cost, earthwork, traffic design, and soil and hydrological conditions. For each cost component, the system generated a set

of base maps, rasterized with an appropriate grid size, and converted to unit cost maps containing isolines of equal cost. At the final stage, all the unit cost maps were added to generate the final economic surface model of the study area. The total highway cost between two known locations was computed based on the area under the line connecting these two locations. The best highway location was the minimum cost path through this cost model.

To locate a road in rough terrain, a smooth (average) terrain model was developed by taking the mean elevation of the actual terrain model, which was subdivided into square zones. The arithmetic difference between the actual terrain elevation and smoothed elevation was used to calculate earthwork, positive difference being cut and negative difference being fill (Figure 2.1). This model, using a

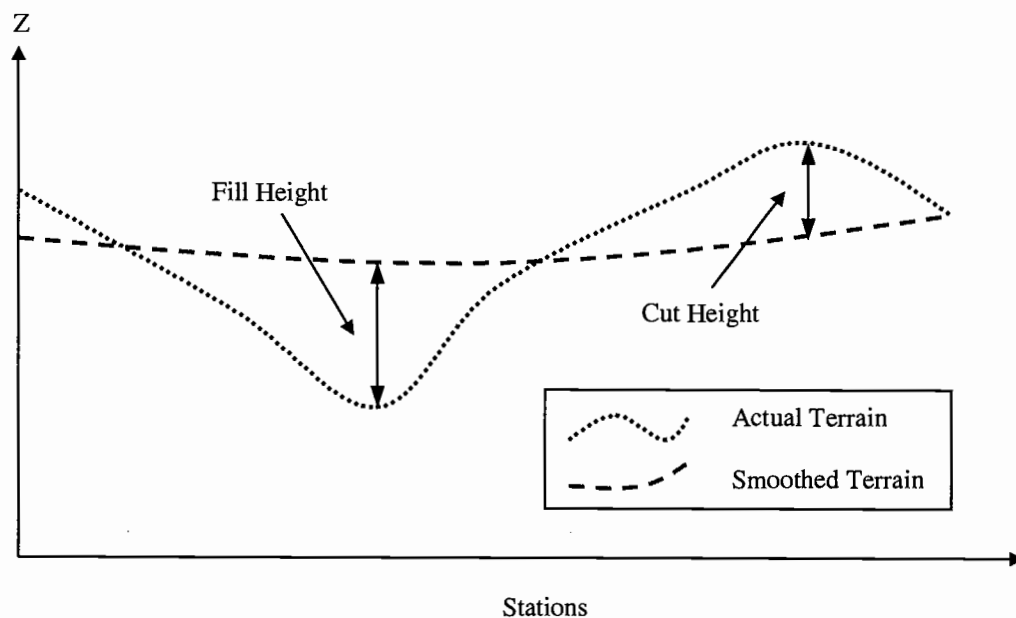


Figure 2.1. Profile View of the Highway Section.

simplified cost model, was limited when the terrain is mountainous since the costs also depend on the direction of the highway. The minimum cost path should be calculated considering not only the cost of putting a highway at a certain terrain point, but also the direction. Therefore, this model can be used only in the early stages of the route location procedure. However, it was probably the earliest important study using a computer-aided system to locate the best route with minimum cost.

In 1964, Gladding suggested combining earthwork estimation with shortest path techniques and developed the Terrain Algorithm System (TAS). It was an extension of Roberts' (1957) cost model, except the cost of putting a highway at each terrain point was based on both the cost and the direction of the highway. The model first generates the terrain model using square grids (Figure 2.2) with respect to the baseline, then, smoothes the terrain in four directions by evaluating the current grid under consideration and three grids to each side of current grid.

Alternative highway alignments were generated to minimize total cost. The model computed the total cost based on construction, user, and maintenance costs. To find the minimum cost path between two known locations, the model generates the economic relief model by considering cost in four directions at each grid cell.

This model was developed to assist the engineer by searching and generating alternative alignments automatically. The limitation of the model was that the maximum grade requirements were not directly considered in developing the smoothed terrain model. Even though grade control was not addressed, TAS was the first model combining cut and fill estimates with a shortest path technique.

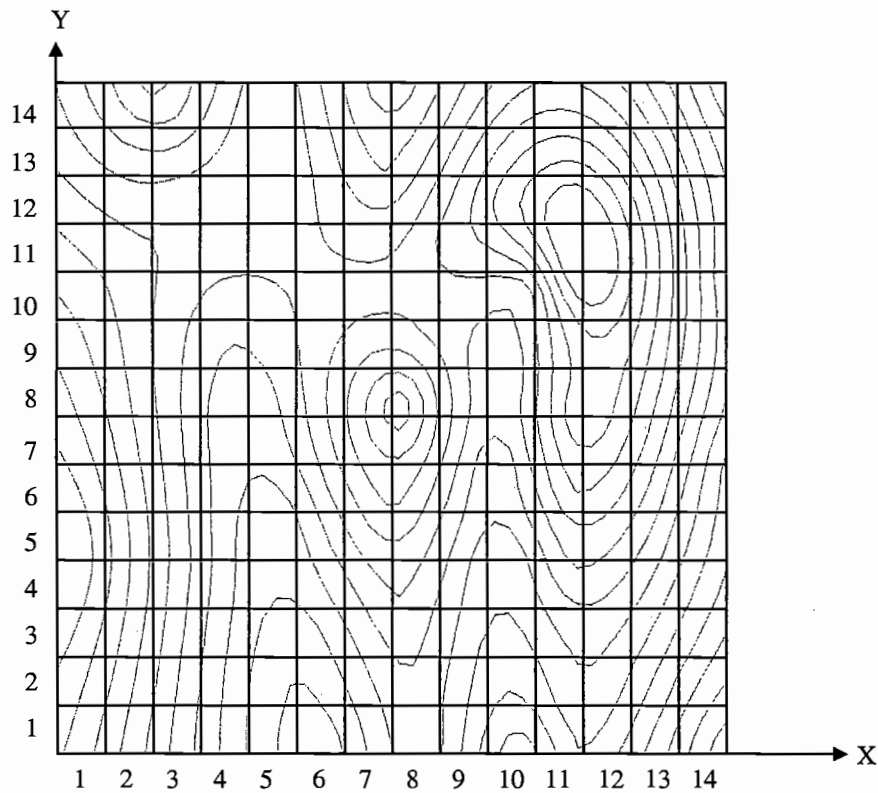


Figure 2.2. Schematic diagram of a terrain on a square grid.

Turner (1968) developed the Generalized Computer Aided Route Selection (GCARS) system to generate a series of ranked alternatives using minimum path analysis techniques. The model included three main procedures: (1) data preparation; (2) search for alternative paths; and (3) selection of the best route with the lowest cost. Alternative paths were located based on physical and socioeconomic constraints, called highway location factors. There were two sets of factors: route-independent factors (topography, soil, geology, land use etc.) and route-dependent factors (user costs, socioeconomic considerations, aesthetic factors etc.). Once a preliminary set of

alternative locations was developed using the first set of factors, the second set of factors was used to modify the preliminary alternative to generate a final set of alternatives.

For each factor, the available data were collected and converted into formats that were acceptable by the computer systems. The model used topographic maps, engineering soils maps, and aerial photography to measure the earthwork cost factor, surface cost factors and land use data, respectively. A unique smoothed surface was constructed for each cost factor, which was assigned to each square search grid using standard regression techniques. Then, the model generated a combined surface by summing all the individual surfaces for each factor. Using minimum path analysis techniques, a series of alternative route alignments were generated automatically. After determining the alternatives, the selection of the best route was done by the designer. The outputs from the model included cost maps, each indicating a particular cost factor.

Turner's model provided the best route location as a shortest path upon the grid. However, the grades of the road still did not satisfy the road grade requirements and highway direction was determined by ground slope without explicit consideration of construction cost.

To locate a highway route, Howard et al. (1968) suggested the optimum curvature principle (OCP) that optimized the specified criteria including cut-and-fill, right-of-way, construction cost, maintenance cost, and user's cost. In this study, each criterion was defined by the term of a function, which was determined using a bicubic

spline interpolation technique. The OCP used the logarithmic directional derivative of the criterion function perpendicular to the highway route to generate the curvature of an optimum highway location. Even though it was for practical applications, the OCP with more accurate data had a great potential to provide the engineer with an optimum route location in less time and at less cost.

In 1969, O'Brien and Bennett proposed the Optimal Rural Highway Location system (POTLOC) using dynamic programming with a 3D search grid to solve the problem of minimizing construction, maintenance, and users' costs, subject to specified constraints including grades, curvature and location. The inputs to the POTLOC system were divided into two groups: network dependent inputs (design standards, traffic volume, budgetary constraints etc.) and link dependent inputs (terrain data, location constraints, and user costs).

To reduce the infinite number of feasible routes to finite proportions, alternative horizontal and vertical alignments within bands of interest were located using 3D grids. The resolution of the grids, reflected by density and accuracy of the terrain model, was kept small enough to detect the optimum route. On the other hand, the resolution could not be too small since the computational time and expense increases with the number of grid cells. After identifying the set of alternative routes within a band of interest (Figure 2.3), dynamic programming was applied to establish the optimal route with the minimum costs. In this system, roadway line and grade alternatives were controlled for both horizontal and vertical curvature.

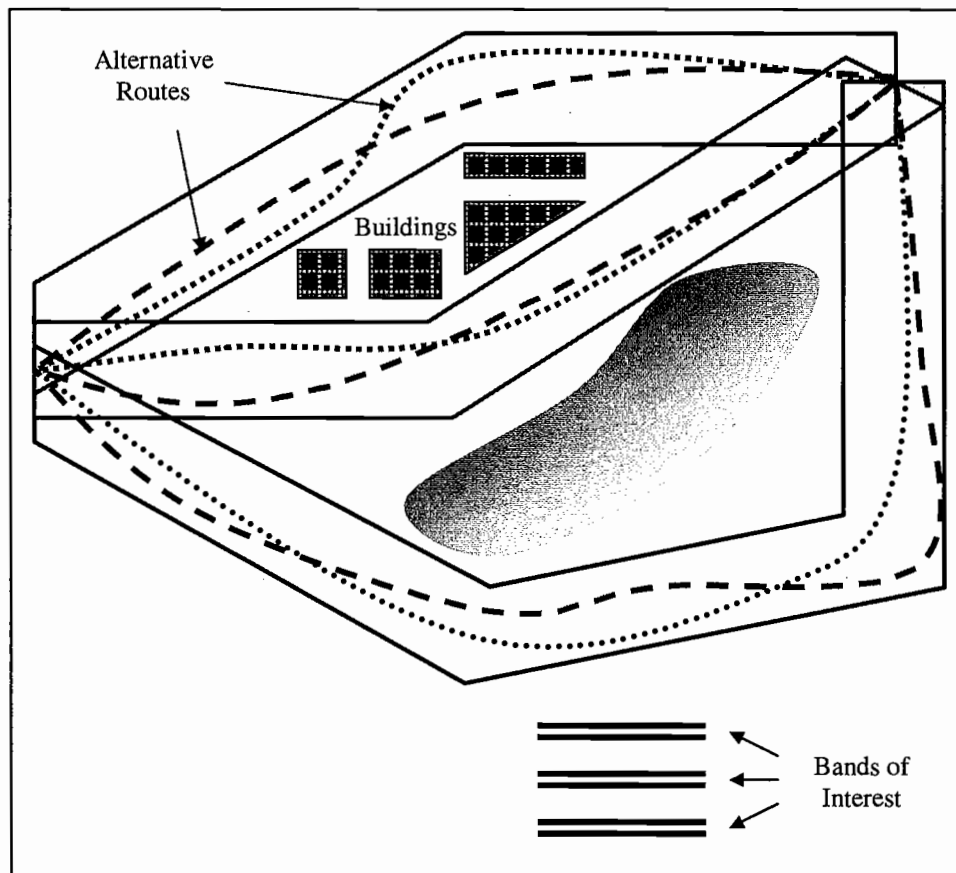


Figure 2.3. Alternative Routes Within Alternative Bands of Interest.

Nicholson (1974) proposed an improvement by developing two computer programs that simultaneously searched for optimization of horizontal and vertical alignments. The first program, Extremal Field Method of Optimal Route Location (EFMORL), used dynamic programming to determine a band of interests within a feasible area. Once the coordinate system and the end points of the route were located

within the feasible area, the route was divided into N number of stages. The ground surface was represented by a limited number of grid points in order to make the program possible to evaluate a large number of alternatives without exceeding the computer storage capacity. However, this decreases the efficiency of the program in the case of steep or broken ground.

The second program, Variational Calculus Method of Optimal Route Location (VCMORL), was used to produce the optimum alignment, which minimized the total costs of constructing and using a road. The application of the model to a real problem indicated this model was superior to the traditional approach for determining route location. However, the method could not easily deal with curvature limitations and gradient change since the constraints on the permitted horizontal or vertical curvature restricted the change of route direction at any stage.

Parker (1977) also used a two-stage approach to select the optimal path that minimizes the construction costs and satisfies the grade constraints anywhere on this path. Linear programming was used to select a smooth surface covering the area of interest that minimized the total earthwork costs. In order to compute the construction cost, the area was subdivided into square zones and the differences between the elevations of the selected surface and the original ground were computed for each zone. The output from the first step plus a user-specified number of desired alternatives were the inputs to the second stage. The second stage used the multiple-path selection program to determine the location of the optimal path on the selected surface that has the minimum cost. Parker used a square search grid similar to

Turner's method. The selection program consisted of a shortest path algorithm (Whiting and Hillier, 1960) and next-best path approach (Hoffman and Pavley, 1959). After a number of applications of this method to an actual route location project, results indicated that it was certainly a quicker way to search for alternative route locations than the present manual approaches. In this model, users' costs were not calculated.

Goh et al. (1988) compared a dynamic programming with a state parameterization model to solve the three-dimensional highway location problem. To minimize the sum of certain predefined cost items, the method selected an optimal vertical profile between two given end points of known locations, once horizontal alignment was predetermined and fixed. The cost items considered in the methods were pavement costs, land usage costs, vehicle operating costs, and earthwork costs. The dynamic programming and state parameterization models were applied to a numerical example to compare their performances.

In the dynamic programming approach, the highway section was subdivided into stages. Rectangular grids were used to cover the cross sections along the central axis. " N " number of vertical grid lines were drawn to subdivide the grids into uniformly spaced rectangular elements. The highway profile was then approximated by a series of linear segments connecting grid points from the start point to end point of the road. Finally, the problem was solved by minimizing sum of the construction costs. To ensure safe and smooth traffic movement, the vertical alignment was selected subject to maximum gradient control, curvature requirements, and control

points with fixed levels. The dynamic programming model was limited by computer memory capacity for the two-dimensional problem. Therefore, it was even more difficult to apply dynamic programming for solving a three-dimensional problem due to the significant increase in memory requirements as well as computation time.

In the state parametrization model total construction cost of the highway section was expressed as a continuous function $y(x)$, thus formulated as a calculus of variation problem. The road profile was approximated as a series of cubic spline functions to transform the functional optimization problem into a constrained mathematical programming problem. Since a certain degree of smoothness was necessary for satisfying the gradient constraints, the parameterization of $y(x)$ was followed by its first and second derivatives. The results of the numerical example indicated that the state parametrization model had better flexibility to solve a three-dimensional problem, while the dynamic programming method was superior in terms of ease of formulation and computational CPU time.

Chew et al. (1989) developed a Continuous State Parameterization Model, a follow-up to the study of Goh et al (1988), to solve a three-dimensional highway alignment problem. The optimum profile is determined by locating the optimal horizontal and vertical alignment simultaneously while satisfying constraints such as road grade, curvature, and inaccessible regions. A Cartesian coordinate system was used to represent the road profile and the ground profile by a continuous function. The ground profile was approximated as a series of right angle planar triangular surfaces. The vertical coordinates of the ground elevation was a function of its x and

y coordinates on the horizontal plane. The optimization program was applied to perform an optimal vertical and horizontal alignment analysis simultaneously. The results indicated that the model was satisfactory in solving practical problems. To generate a good solution in a reasonable computation time, a scaling technique for choosing dimension variables was also proposed in this study. However, for large problems where there is no chance of selecting the initial values of these variables; the designer had to rely on accumulated experience.

Earthwork Allocation

To minimize the earthmoving cost involved in excavating soil from various cut areas and hauling it to various areas for fill and compaction, the cut and fill quantities of soil must be distributed in the most economical combination. The decision variables in earthmoving operations are the cut and fill quantities at various locations, distance between these locations, soil characteristics, and the unit costs for excavation, haul, and embankment.

Several methods have been developed for earthwork allocation. The mass diagram method, introduced by Hickerson (1964), has been used to determine the minimum amount of haul, direction of the haul, and minimum economic distribution of earthwork. It assumes that the haul costs are directly proportional to the distance traveled. A mass diagram is a continuous curve illustrating the cumulative volume of the earth from an initial station to any succeeding station. The points on the curve are plotted with reference to a horizontal scale of distance and a vertical scale of the accumulated earthwork along the centerline of the project (Figure 2.4).

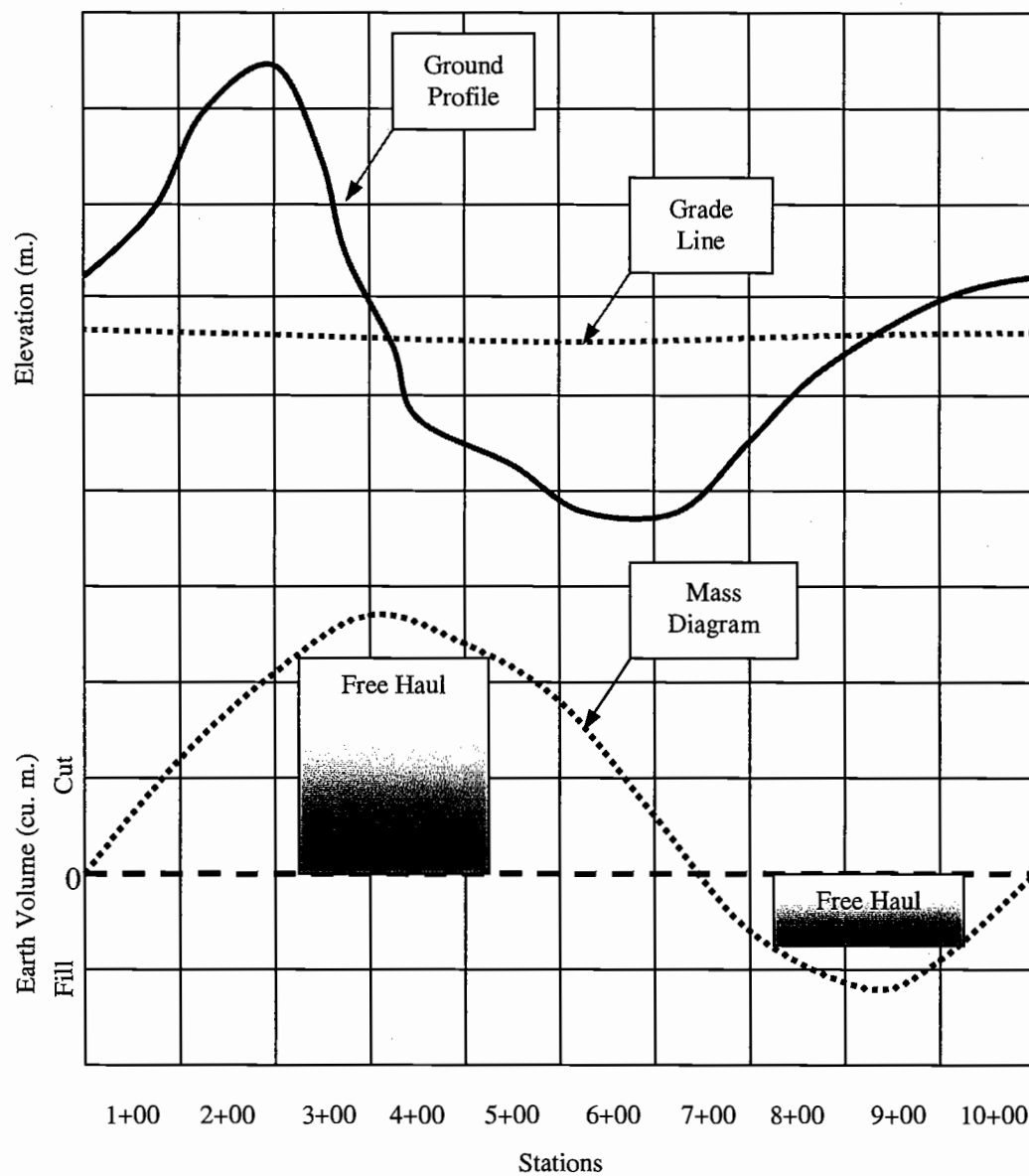


Figure 2.4. Profile-Grade Line and Mass Diagram.

The horizontal line is called the “zero line” or “balance line” when the adjusted positive cut and negative fill are equal. On the mass curve, decreasing lines

represent the fill quantities exceeding cut quantities, whereas increasing lines indicate the opposite. The area between the balance line and the mass curve indicates the total volume of material moved a given distance ($\text{m}^3\text{-km}$). Hauling the material within a certain distance is called “free haul”, when it is moved with no extra cost above the excavation cost. The rest of the hauling, which is beyond the free haul distance limits is called “overhaul”. The cut and fill quantities are balanced using estimated shrinkage or swell factors before accumulating them in the mass curve.

The disadvantage of this procedure is that all overhaul materials and waste and borrow quantities have to be readjusted before cost analysis, unless the entire road section has only one adjustment factor. Also, based on the detailed investigations made in several studies, the usefulness of the mass diagram is decreased where hauling costs are not linearly proportional to the hauling distance, soil characteristics vary along the roadway, and additional quantities of material are required to be borrowed from borrow areas or wasted at landfill areas. The main variables in earthmoving operations can be estimated before the excavation of the earthwork. Therefore, various optimization models have been developed for the earthwork allocation problem to overcome the limitations of the mass diagram and improve the accuracy of the estimates. The following discussion focuses on the syntheses of these models.

Willonbrock (1972) suggested a method to determine the optimal selection of the equipment fleet that minimizes the costs of the earth moving operation. A computer simulation program was generated for an experimental project where a

loader and a fleet of earth moving trucks were analyzed. The cycle time of the operation consisted of two groups of activities: (1) loading time including excavation and loading and (2) travel time including hauling, dumping, spreading, and returning to loader. In this method, the variation associated with each of the activities in a cycle and the interaction delays between loader and trucks were considered to generate a more accurate simulation of reality. A simple example problem was solved to test the productivity of the method. The results indicated that the rate of increase in production for the system was non-linear as more trucks were added to the system due to extra time spent in the waiting line at the loader. Since the cost of the earthmoving operation is the main factor in the overall highway construction project, this method provided the estimators with an accurate simulation of the operation.

Trypia (1979) developed a mixed-integer programming model to minimize the total construction cost subject to certain conditions, including desired gradient for keeping the road grade between acceptable limits and the required road elevation for minimizing the earthwork at specified road points. The density of the search grid points along the road section was determined by the designer based on the type of terrain. At any specified ground point (i), the cost functions of filling (C_{i1}) and excavation (C_{i2}) were formulated based on the terrain conditions, type of machinery and equipment used. In the model, the road elevation (r_i) was equal to $h_i + x_{i1} - x_{i2}$ where h_i was the ground elevation and x_{i2} and x_{i1} were the cut and fill heights, respectively. x_{i1} and x_{i2} were limited by the upper (u_i) and lower limits (l_i). A binary variable (δ) was used to assign the section as either cut or fill at a specified point. The

gradient constraint was introduced into the program by using the road elevations of two consecutive points (Equation 1), the distance between these two points (d_i), and the maximum acceptable road gradient (s).

$$|r_{i+1} - r_i|/d_i \leq s \quad 1.$$

Then, the objective function of minimizing the total cost (Z) was formulated as follows:

$$\text{Min } Z = \sum_i (c_{i1}x_{i1} + c_{i2}x_{i2}) \quad 2.$$

Subject to:

$$\begin{aligned} x_{i1} &\leq u_i \delta \\ x_{i2} &\leq l_i(1-\delta) \\ x_{i1}, x_{i2} &\geq 0 \\ \delta &\in (0,1) \end{aligned} \quad 3.$$

where c_{i1} and c_{i2} are the unit cost of filling and excavation, respectively. Once the horizontal alignment of a road has been determined, the model provided a preliminary vertical alignment solution to find the road elevations at the specified points using a simple form of optimization technique that provided a designer with a good decision making tool.

To optimize the earthwork allocation cost, the technique of transportation model analysis from operations research was developed by Nandgaonkar (1981). The transportation model was formulated as a linear optimization model, in which the objective was to minimize the sum of the costs of moving earth from cut sections to

fill sections and disposal sites. Using the amount of cut, X_{ij} , from cut section i to fill section j , and the unit hauling cost, C_{ij} , the objective function was stated as follows:

$$\text{Min } Z = \sum_i \sum_j C_{ij} X_{ij} \quad 4.$$

Subject to (Equations 5 and 6):

$$\sum_j X_{ij} = a_i \quad 5.$$

where the total amount of cut (a_i) moved from cut section i to all fill sections and landfill areas is equal to the available amount of cut at cut section i :

$$\sum_i X_{ij} = b_j \quad 6.$$

where the total amount of fill (b_j) moved to fill section j from all cut sections equals the amount of fill required at fill section j . Finally, a non-negative condition completed the formulation, $X_{ij} \geq 0$.

The application of the model indicated that the operations research model was suitable to optimize earthwork cost. However, there were some limitations of the model including neglecting the shrinkage and swell properties of the soil and assuming that the cost of earthwork operation did not vary with excavation, transportation, fill and compaction cost.

A linear programming model was developed by Mayer and Stark (1981) to minimize the cost of the earthmoving operation. Swell factor (s_i^h) of the material moved from cut section i , and shrinkage factor (s_j^f) of the material compacted into fill section j , were considered to properly determine haul and fill quantities. The cost

of borrowing the material from borrow areas and the cost of wasting the material to landfill areas were computed separately while the cost of earthwork from cut section to fill sections was represented in a manner similar to the previous reference. The specific unit costs for excavation, haul, and embankment were used based on estimated soil characteristics of each section. Therefore, the objective function and the constraints were stated as follows:

$$\begin{aligned} \text{Min } Z = & \sum_i \sum_j C(i, j) X(i, j) + \sum_i \sum_k C_D(i, k) X_D(i, k) + \\ & \sum_p \sum_j C_B(p, j) X_B(p, j) \end{aligned} \quad 7.$$

Subject to (Equation 8 and 9):

$$\sum_j X(i, j) + \sum_k X_D(i, k) = Q_c(i) \quad 8.$$

where $X(i, j)$ (the amount of cut moved from cut section i to fill section j) plus $X_D(i, k)$ (the amount of cut moved from cut section i to landfill area k) are to be equal to the available amount of cut, $Q_c(i)$, at cut section i .

$$\sum_i s_{ij}^f X(i, j) + \sum_p s_{pj}^f X_B(p, j) = Q_f(j) \quad 9.$$

where $s_{ij}^f X(i, j)$ (the adjusted amount of cut moved from cut section i to fill section j) plus $s_{pj}^f X_B(p, j)$ (the adjusted amount of material moved from borrow area p to fill section j) are equal to the amount of fill required, $Q_f(j)$, at fill section j . The shrinkage factors for material moved from cut section i and borrow area p were defined as s_{ij}^f and s_{pj}^f , respectively.

The capacities of the landfill and borrow areas were also taken into the account in the formulation of constraints (Equation 10):

$$\begin{aligned} \sum_i s_{ik}^f X_D(i, k) &\leq Q_D(k) \\ \sum_j X_B(p, j) &\leq Q_B(p) \end{aligned} \quad 10.$$

where $s_{ik}^f X_D(i, k)$ (the adjusted amount of cut moved from cut section i to landfill area k) was equal to or less than the capacity of the landfill k , $Q_D(i)$. In the same manner, $X_B(p, j)$ (the amount of material moved from borrow area p to fill section j) was equal to or less than the material available in borrow area p , $Q_B(p)$. s_{ik}^f was the swell factor for material moved from cut section i and wasted in landfill area k . Non-negative conditions added into the formulation were $X(i, j)$, $X_D(i, k)$, and $X_B(p, j) \geq 0$.

The unit cost of moving and compacting the material from cut section i to fill section j , $C(i, j)$, was estimated based on unit cost of each operation including excavation (u_e), hauling (u_h), and compacting (u_c), assuming that the costs were linearly proportional to the quantities. The formulation for adjusted quantities was as follows:

$$C(i, j) = u_e + s_i^h (u_h d_{ij} + u_c) \quad 11.$$

where d_{ij} was the distance between the center of cut section i and the fill section j .

The unit cost of borrow, $C_B(p, j)$, and disposal, $C_D(i, k)$, were determined similarly.

This model showed that a linear programming model of earthwork allocation could be used to overcome the limitation of the mass diagram on roadway sections with various soil characteristics. However, increasing the number of sections along

the roadway might increase the time required to collect data. It was also assumed that the unit cost of earthwork activities were constant and not reflected by the quantity moved.

Easa (1987) suggested that the unit cost of purchasing and excavating earthwork from borrow areas consisting of many types of soil with different unit costs of excavation was the only unit cost reflected by the quantity moved, while the unit cost of other earthwork activities were constant. After a detailed investigation of possible variations of unit costs, a unit cost function of purchase and excavation for a borrow area was formulated as a three-component stepwise function, using a mixed-integer linear programming model. This model was proposed as an extension of Mayer and Stark's linear programming model. A stepwise unit cost function was generated by adding the unit cost function of purchase and excavation with respect to the quantity moved from borrow area. Q_p and R_p represented the two break points of specified quantities. The total quantity moved from borrow area (Y_p), consisting of three quantities (Y_{1p} , Y_{2p} , Y_{3p}) with associated unit costs (C_{1p} , C_{2p} , C_{3p}), was equal to the sum of the quantities hauled to the required fill sections ($\sum_j X_B(p, j)$). In a case where $Y_p < Q_p$, the total cost was $C_{1p}Y_{1p}$. If $Y_p > R_p$, it was $(R_p + Y_{3p})C_{3p}$. For any other cases, it was $(Q_p + Y_{2p})C_{2p}$. In order to satisfy these equations, additional constraints were included into the model using binary variables, λ_p and γ_p . Then, the objective function was stated as follows:

$$\text{Min } Z = \sum_i \sum_j C(i, j) X(i, j) + \sum_i \sum_k C_D(i, k) X_D(i, k) +$$

$$\sum_p \sum_j C_B(p, j) X_B(p, j) + \sum_p \{C_{1p} Y_{1p} + C_{2p} Y_{2p} + C_{3p} Y_{3p} + (C_{2p} - C_{1p}) Q_p \lambda_p + [(C_{2p} - C_{1p}) Q_p + (C_{3p} - C_{2p}) R_p] \gamma_p\} \quad 12.$$

where the first and the second terms of the objective function were stated as in the preceding formulation of Mayer and Stark (1981). The third term indicated the cost of haul and compaction for earthwork moved from a borrow area p to fill section j . The cost of purchase and excavation for this borrow area was represented by the last term. The objective function was subject to the similar constraints presented by Mayer and Stark (1981) (Equation 13):

$$\begin{aligned} \sum_j X(i, j) + \sum_k X_D(i, k) &= Q_c(i) \\ \sum_i s_{ij}^f X(i, j) + \sum_p s_{pj}^f X_B(p, j) &= Q_f(j) \\ \sum_i s_{ik}^f X_D(i, k) &\leq Q_D(k) \\ Y_{1p} + Y_{2p} + Y_{3p} &= \sum_j X_B(p, j) \\ X(i, j), X_D(i, k), \text{ and } X_B(p, j) &\geq 0 \end{aligned} \quad 13.$$

The application of the model indicated that it was capable of providing the minimum earthwork cost in a case where the unit cost of purchase and excavation for a borrow area depended on the unknown quantity of earthwork.

In 1988, Easa proposed another linear programming model for the selection of roadway grades that minimized the earthwork cost. The model consisted of three different stages including selecting all technically feasible grades, calculating cut and fill requirements for each grade alternative, and determining the best alternative that

minimized earthwork cost. This model allowed variations in swell and shrinkage of soil along the roadway and guaranteed the minimum earthwork cost within the feasible solutions. The model also satisfied the geometric specifications such as the elements of the vertical alignment, elevation of the grade line, horizontal and vertical alignment relations, and type of vertical curve. In this study, Easa (1988) adopted the linear programming method of Mayer and Stark (1981), assuming that the unit hauling cost was linearly proportional to the hauling distance and the unit cost of purchase and excavation for the borrow area was constant. The results of the example applications indicated that this model provided the designer with the global minimum, which was 23% better than local minimum costs.

Easa (1988b) presented a quadratic programming model of earthwork allocation, in which the last term of the objective function, indicating the total cost purchase and excavation of materials from borrow areas, was a linear function of the quantity used. Thus, the objective function was modified as follows:

$$\begin{aligned} \text{Min } Z = & \sum_i \sum_j C(i, j) X(i, j) + \sum_i \sum_k C_D(i, k) X_D(i, k) + \\ & \sum_p \sum_j C_B(p, j) X_B(p, j) + \sum_p (\alpha_p + \beta_p x_p) x_p \end{aligned} \quad 14.$$

where x_p , α_p , and β_p represented the quantity used from borrow area p , the intercept and slope of the linear unit cost function, respectively. The limitations for the decision variables of $X(i, j)$, $X_D(i, k)$, and $X_B(p, j)$ remained unchanged. The new decision variable of x_p , was limited by the following constraint:

$$x_p = \sum_j X_B(p, j) \quad 15.$$

The results indicated that this model, considering soil characteristic and borrow and landfill capacities, represented the earthwork allocation operations better than the mass-haul diagram and provided minimum construction cost using the optimization techniques.

Christian and Caldera (1988) introduced an operational research model to minimize earthmoving cost by optimizing the distribution of cut and fill quantities. This study assumed that the unit costs of excavation, haul, and embankment were non-constant and affected by locations of cut and fill sections. The earthmoving model was formulated as follows:

$$\text{Min } Z = \sum_i \sum_j X_{ij} [C_{ei} + K_{bi} d_{ij} C_{tj} + K_{ci} C_{fj}] \quad 16.$$

where X_{ij} was the quantity of material moved from location i , the cut section or borrow area, to destination j , the fill section or landfill area. C_{ei} , C_{tj} , and C_{fj} were the unit cost of excavation, haul, and embankment, respectively. The distance between location i and destination j was represented by d_{ij} . The difference in swell (K_{bi}) and shrinkage (K_{ci}) were taken into the account. The capacities of location i and destination j were also considered in the formulation of constraints as follows:

$$\begin{aligned} \sum_j X_{ij} &\leq a_i \\ \sum_i X_{ij} K_{ci} &\geq b_j \\ \sum_i a_i &\geq \sum_j b_j \end{aligned} \quad 17.$$

where a_i and b_j were the maximum quantity excavated at location i and the maximum quantity compacted at destination j , respectively. The formulation was completed with the non-negative restriction $X_{ij} \geq 0$.

Due to possible imbalance between the cut and fill quantities, dummy locations or destinations were generated to absorb the excess fill or cut. The model included machinery selection for excavation or embankment operation by multiplying the unit cost of haul by a factor to include the variation in the unit costs. Application of the model provided decision makers with an effective and easy method to minimize the total cost of the earthwork operation by optimizing the cut and fill distributions.

Forest Road Design Systems

The design of a forest road between two given locations on a surface is a complex engineering problem involving economic considerations and environmental requirements. For low traffic volume forest roads in mountainous terrain, the construction and maintenance costs are the major components of the on-road transportation cost. Forest roads are potentially the most problematic features of timber harvesting operations since inadequate road construction and poor maintenance can cause more stream sedimentation than any traditional forestry operation (Skaugset and Allen, 1998). Excessive sediment delivered to streams from a road section can have a dramatic effect on water supplies and aquatic life. Thus, forest roads must be carefully designed to minimize construction and maintenance costs, and minimize environmental damage.

A 3D forest road alignment optimization model, TRACER, was developed to help the forest road designer with a quick evaluation of alternatives in order to design a path with the lowest total cost considering construction and future maintenance and transportation costs, while conforming to design specifications and environmental requirements. This section discusses the current state of the available methods in the field of forest road design and construction and describes the TRACER 3D forest road alignment optimization model. The theory behind the model is not presented in detail here but is presented in other articles. The development of the model is still continuing and the graphical capabilities of the model are improving.

Current Methods

Traditional manual methods of road design analysis depend upon a designer's judgment and experience. There has been increasing interest in computer-aided analysis of route selection as it could lead to considerable savings of time in road design. Computers have been used in forest road design since the 1960's, but have largely been applied to automate the computational tasks of earthwork calculation and computer aided drafting. The mass diagram is employed to balance the required quantities of cut and fill. However, the usefulness of the mass diagram decreases when hauling costs are not linearly proportional to the hauling distance, soil characteristics vary along the roadway, and additional quantities of material are required to be borrowed from borrow areas or wasted at landfill areas.

The systems currently available for forest road design are not intended to make computer-aided design judgments such as automated generation of alternative

grade lines, best fitting vertical alignment for minimizing earthwork, minimizing the total cost of construction, maintenance, and transportation, and aiming for least environmental impact. They are generally used as a tool to make the mathematical calculations required to do basic manual road design. Since the manual method is “trial and error” and there are many possible alignments, it is highly conceivable that the manual design might not yield the best result. Also, data input might be cumbersome in current programs. The road designer must enter many set-up parameters and input traverse notes into the related modules.

After entering the survey data and design parameters, some programs manipulate geometric road design and earthwork balance calculations by allowing the designer to work in plan, profile or cross section view simultaneously, using a visual display screen (RoadEng, 2002 and Lumberjack, 1995). However, the designer has to make these manipulations while all the constraints of horizontal and vertical alignments are satisfied, which can be very time consuming. The designer has to examine a number of alternatives to be sure that the final route location is “reasonably” cost effective among the infinite number of alternative grade lines.

TRACER, a Decision Support System

The TRACER model is proposed as a decision support system for forest road design. It will automate many of the current mundane, time consuming tasks, while implementing a decision support framework. The theory behind the model is shown in Figure 2.5. First, the model reads input data files including digital elevation model (DEM) and attribute data. The model relies on a DEM to provide terrain data for

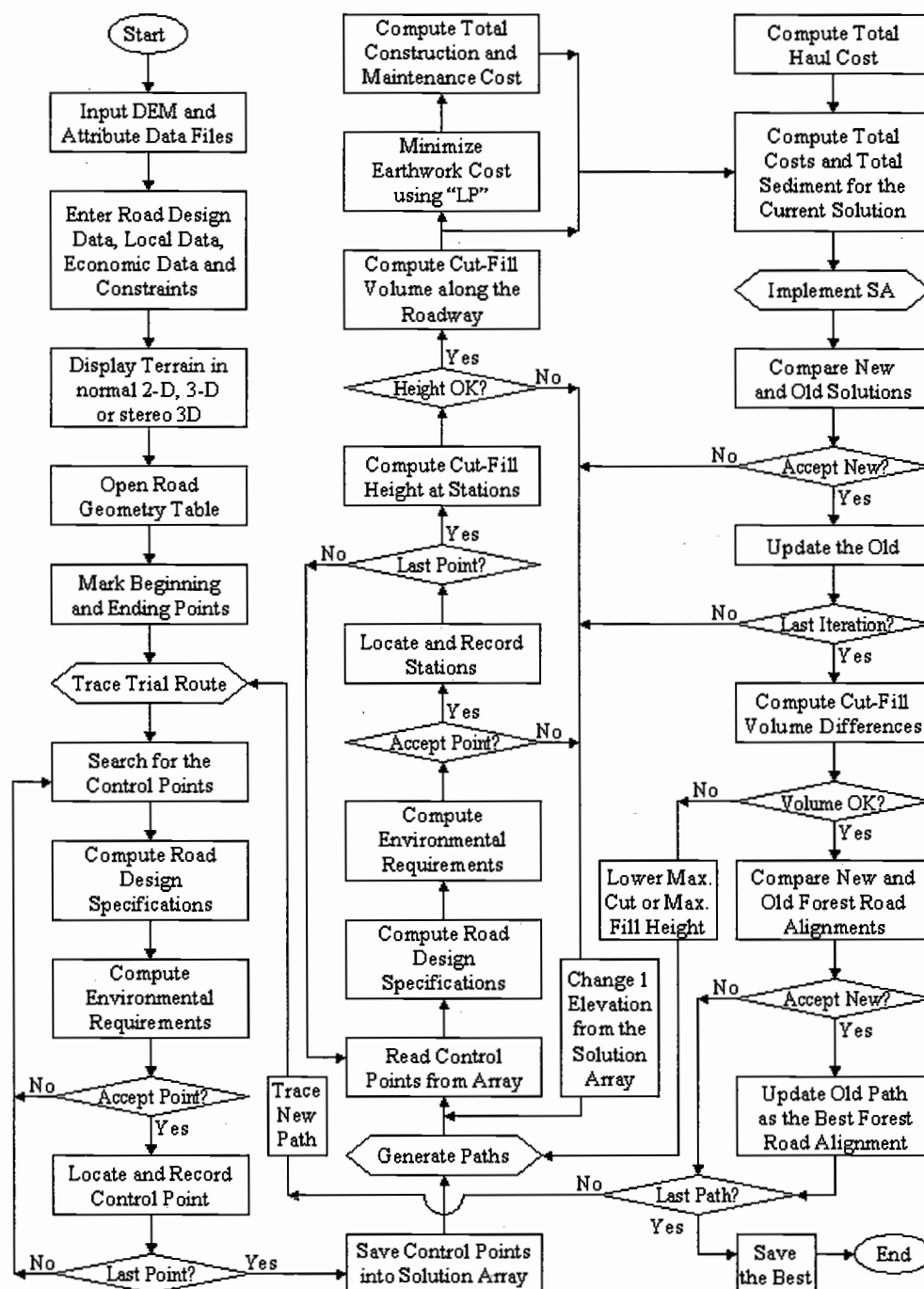


Figure 2.5. The Theory of the forest road alignment optimization model, TRACER.

supporting the analysis of road design features such as ground slope, topographic aspect, and other landform characteristics. LIDAR (Light Detection and Ranging) is one of the fastest growing systems that provides high-resolution and accurate DEM data. The spatial resolution of the DEM depends on the LIDAR scanning angle, pulse repetition rate, flying height and aircraft speed. After accounting for errors, the resulting accuracy of each point on the ground is approximately 15 cm in the vertical and 1 meter in the horizontal (Ahmed et al. 2000). According to Pereira and Janssen (1999), LIDAR systems achieve these accuracies in open areas with hard surface. However, in areas with very tall, dense canopy, the photogrammetric heights occasionally might have larger errors. Since LIDAR technology is one of the fastest growing systems, it is expected to provide even better accuracy in the near future, as the laser beam width is reduced, which is the key receiving reflections from the forest floor.

The DEM data file is a set of scattered metric data points (X, Y, Z), which represents the ground surface. In order to reduce the input data file size, the original DEM coordinate system can be converted into a simple Cartesian coordinate system in which X and Y values are both zero at the lower left origin. Table 2.1 indicates the data format of DEM data file. The attribute data file includes soil type and stream data, represented in the same format as the metric data points. The designer can input more attribute data if desired, using the same format.

After the input data files are read, the designer enters the road design data, economic data, local data, geometric specifications, and environmental requirements.

Table 2.1. The data format of the digital elevation model (DEM) data format.

X (row)	Y (column)	Z (elevation)
297434	172652	349.69
297435	172652	349.51
297436	172652	349.32
297437	172652	349.14

The road design data include road standard, road surface type, road template specifications, turnout dimensions, distance between road sections, design speed, vehicle specifications, and traffic volume. Local data include swell and shrinkage factors of soil types, ground cover type, geological data, vegetation (timber stand) data, and distance to local resources of required road construction materials.

Economic data consist of the unit costs of road construction and maintenance activities and machine rate components of specified vehicles.

The geometric specifications are maximum allowable road grade, minimum radius of the horizontal curves, minimum length of the vertical curves, minimum distance between curves, and minimum safe stopping distance for driver safety. It is also required that horizontal and vertical curves do not overlap each other. The environmental requirements include minimum allowable road grade and rolling road

grades to provide proper drainage, minimum distance from the riparian zones to protect the stream channels, minimum stream-crossing angle to reduce the damage on the riparian zones, and maximum height of cuts and fills at any section to decrease soil movement.

The display and interactive features of the model were provided by NewCyber3D (2002), using an improved 3D OpenGL accelerator. The model has the capacity of displaying and rendering high-resolution 3D images of the terrain in real-time, based on DEM and attribute data files. It also supports the real-time interactive stereo display, which requires liquid crystal glasses and an infrared emitter that connects the glasses to standard graphic card. Due to increased interest in high-resolution stereo image display on low-cost personal computers, the cost of this viewing system has fallen dramatically within recent years.

Displaying the image of the terrain on the computer screen (Figure 2.6), the designer first opens the Road Geometry Window and locates the beginning and ending points of the road section. This window shows road geometry information and attribute data in real time, helping the designer to locate control points satisfying the constraints. Road geometry information includes X and Y coordinates, elevation, road grade, horizontal and vertical deflection between two consecutive road segments, length of the current segment, and cumulative segment length. Miscellaneous attribute data include soil type and stream data. The stream data are used to identify the distance to the closest stream in real-time. Second, the designer selects a feasible trial route between the beginning and ending points by establishing a series of control

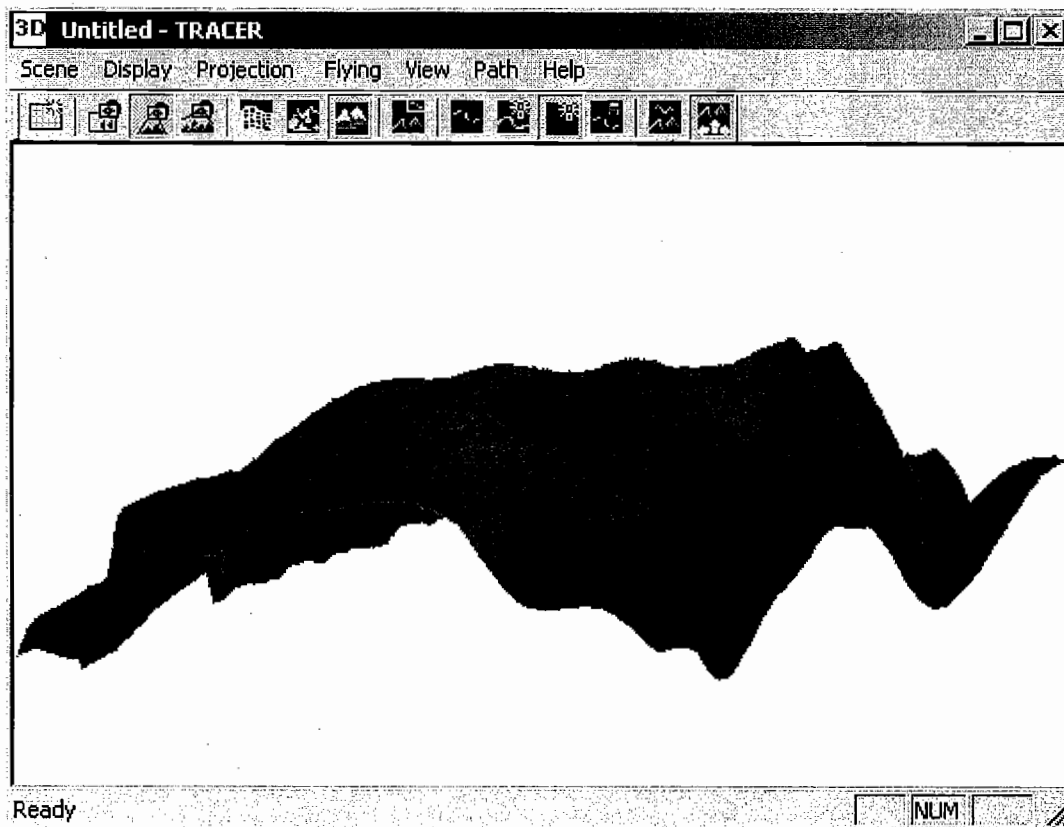


Figure 2.6. Graphical user interface of the model, displaying 3D image of the terrain.

points on the 3D image of the terrain, subject to geometric specifications and environmental requirements. Trial routes are generated by tracing the possible paths using the computer cursor on the 3D image of the terrain (Figure 2.7). The curves connecting the control points are not used to represent the final location of the route path, but for visualization purposes only. The designer can zoom, pan, rotate, and scale the area in order to search candidate control points around the terrain. If the designer chooses a candidate point, which is not acceptable by one or more constraints, the model warns the designer by changing the color of the line between

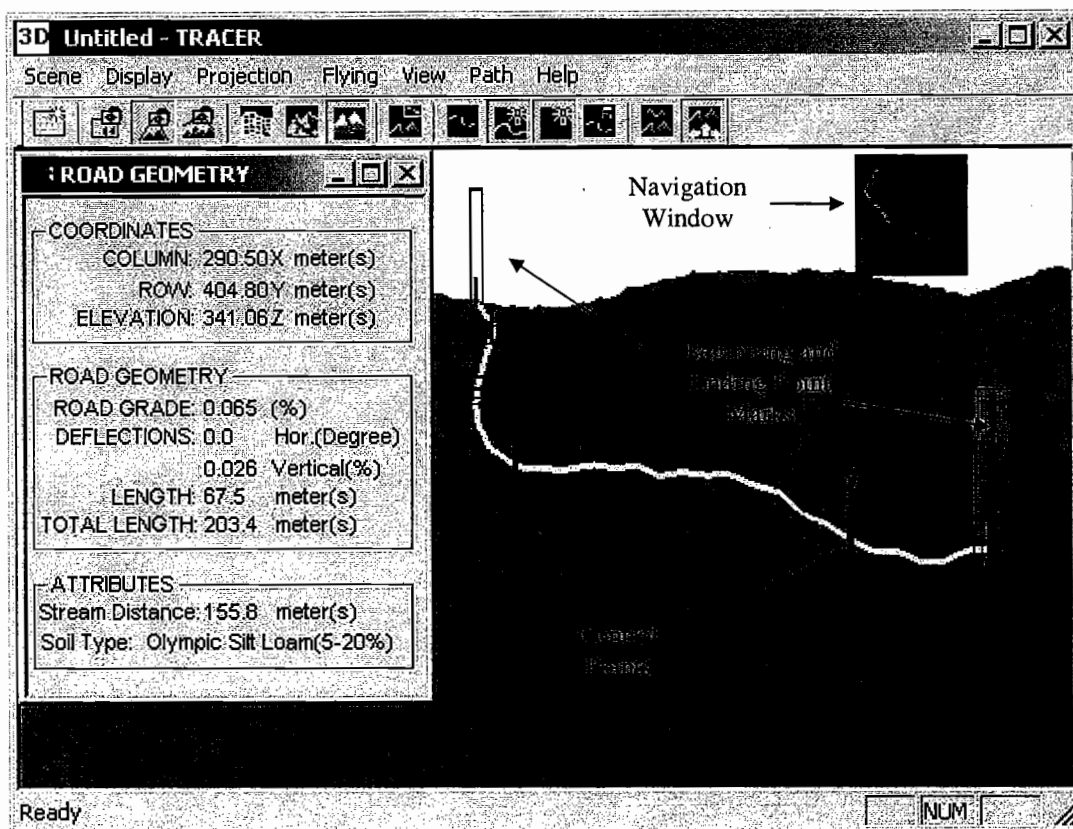


Figure 2.7. Locating a feasible trial route between two given points.

the previously selected control point and the candidate point. Thus, the designer does not select this candidate point and searches for other points. The data for the selected feasible trial route are stored in an array, which contains X, Y, and Z (elevation) data for a series of control points.

Using the trial route data as an initial alignment, the model automatically locates the horizontal and vertical curves and calculates the station points between the control points, obeying the constraints. Figure 2.8 shows the horizontal and vertical

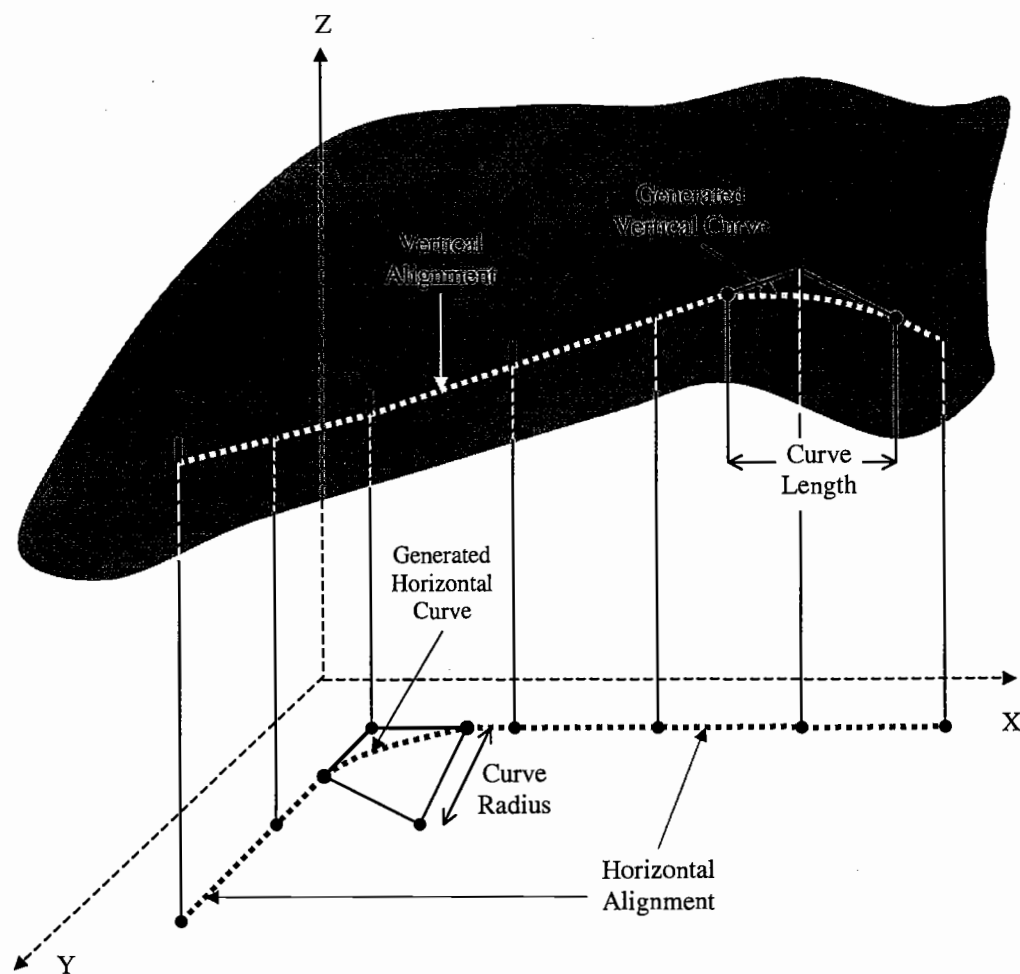


Figure 2.8. Generation of a vertical and horizontal alignment.

alignments simultaneously. If the cut or fill height at any station is not feasible, the model generates a new alignment by changing the elevation at a randomly selected control point by a specified value (e.g. 0.5 meters) within the elevation range of the control points. When cut-fill height and all the other constraints are satisfied, the

model computes the cross section areas and average end areas to compute earthwork volume for each road stage, which is a part of the road section between two consecutive stations.

The economic distribution of cut and fill quantities is determined using linear programming, considering possible borrow and landfill locations and various soil characteristics along the roadway. The model adopts the method of Mayer and Stark (1981) described previously. Then, the model computes the total cost of the road section including construction, future maintenance and future transportation costs.

The road construction cost is the total cost of the road construction activities: construction staking, clearing and grubbing, earthwork allocation, water supply and watering, drainage, rip rap, surfacing, and seeding and mulching. The maintenance activities involve rock replacement, grading, culvert and ditch maintenance, and brush cleaning. Design speed, entering and exit speed, acceleration and deceleration rates of truck traffic, and machine rate were analyzed as the effective factors of the forest transportation costs. Additional costs (accident costs, land usage costs, ecological penalties etc.) and constraints can be included into the model if they can be expressed quantitatively.

To help the designer identify road segments with a high potential for delivering sediment to streams in a watershed, the model estimates average annual volume of road sediment, using the method of a GIS based road erosion/delivery model, SEDMODL (Boise Cascade Corporation, 1999). SEDMODL is the slightly modified version of the Washington Department of Natural Resources surface erosion

module (WDNR, 1995). Road erosion factors considered in the model are geologic erosion rate, road surface type, traffic density, road width and length, average road slope, average precipitation factor, distance between road and stream, cut slope cover density, and cut slope height.

In the final stage, TRACER generates new road alignment alternatives by randomly adjusting the vertical alignment to find the best path with lowest total cost. A heuristic combinatorial optimization technique (Simulated Annealing) is used to select the best vertical alignment that minimizes the sum of construction, maintenance and transportation costs considering technically feasible grades within the specified elevation ranges of the intersection points of the vertical alignment. For each alternative vertical alignment, the model computes cross sections, earthwork volumes, sediment delivery, and minimizes earthwork costs using linear programming, subject to geometric specifications and environmental requirements. The capacities of borrow and landfill areas are assumed to be adequate to satisfy borrow or waste requirements.

In order to reduce the cost of hauling excessive cut or fill quantities, the difference between total cut and total fill are monitored. If it is positive and is greater than a specified volume that can be hauled from cut sections to the landfill area, the model discards this alignment, lowers the maximum cut height to reduce the amount of excessive cut volume, and generates new alignment alternatives. If the difference is negative and its absolute value is greater than a specified volume that can be hauled from a borrow area to the fill sections, the model discards this alignment, lowers the maximum fill height to reduce the amount of excessive fill volume, and generates

new alignment alternatives. When this last constraint is satisfied, the model records the current alignment.

To develop additional road alignments to connect the same beginning and ending points, the road designer traces out different feasible route paths. Then, for each selected route path, TRACER follows the same procedure to find the road alignment with minimum cost by using optimization techniques. Thus, the designer can rapidly develop and then choose among the alternative road locations in an efficient way. After developing the final vertical alignment, the designer determines the appropriate location for a turnout, considering on visibility, side slope, and road grade.

Applying TRACER to Forest Road Design

The model was applied to two examples to illustrate the differences between surface rock specifications (Table 2.2). The study area is approximately 55 hectares of predominantly forested land on the southern edge of the Capitol State Forest in western Washington. The site is mountainous with elevation varying from 270-355 meters and ground slope from 0-50 percent. The forest stand is primarily 50-70 year-old second-growth conifers. The DEM data (1m intervals) of the study area was from a LIDAR (Light Detection and Ranging) data set collected (Aerotec, 1999) in western Washington. Soil, hydrology, and geology data were obtained from Washington Department of Natural Resources and added into the attribute data set.

In Example A, a horizontal alignment was generated to connect two known end points of a road section. The vertical alignment with the minimum total cost was

Table 2.2. Specifications for the aggregate surfacing material.

Layers	Example A	Example B
Base Course	Good quality rock (7.5 cm)	Grade $\leq 10\%$: Pit run Grade $> 10\%$: Good quality rock (7.5cm)
Traction Surface	Grade $\leq 16\%$: Finer traction surface rock (2.5cm) Grade $> 16\%$: Traction surface rock (4cm)	Grade $\leq 10\%$: No Traction Surface Grade $> 10\%$: Traction surface rock (4cm)

found by using optimization techniques. The road section had a length of approximately 300 meters (Figure 2.9). The vertical road alignment that minimized the total cost located a 27m long vertical curve and a horizontal curve with a radius of 45m. The road gradient varied from 4% to 11%. Two hundred and two feasible solutions were identified during the search process. The lowest value of the objective function was obtained at iteration 188 with the unit cost of \$46.04/m. Surfacing cost (including riprap and watering costs) was the largest cost component (\$22/m), followed by rock replacement (\$7.5/m), and earthwork (\$5.7/m) costs. The annual sediment delivered to a stream from the road section was 0.29 ton.

In Example B, the same horizontal alignment from the first example was repeated with different specifications for surfacing material to investigate their effects on cost components, road gradient, and sediment production. The model located one

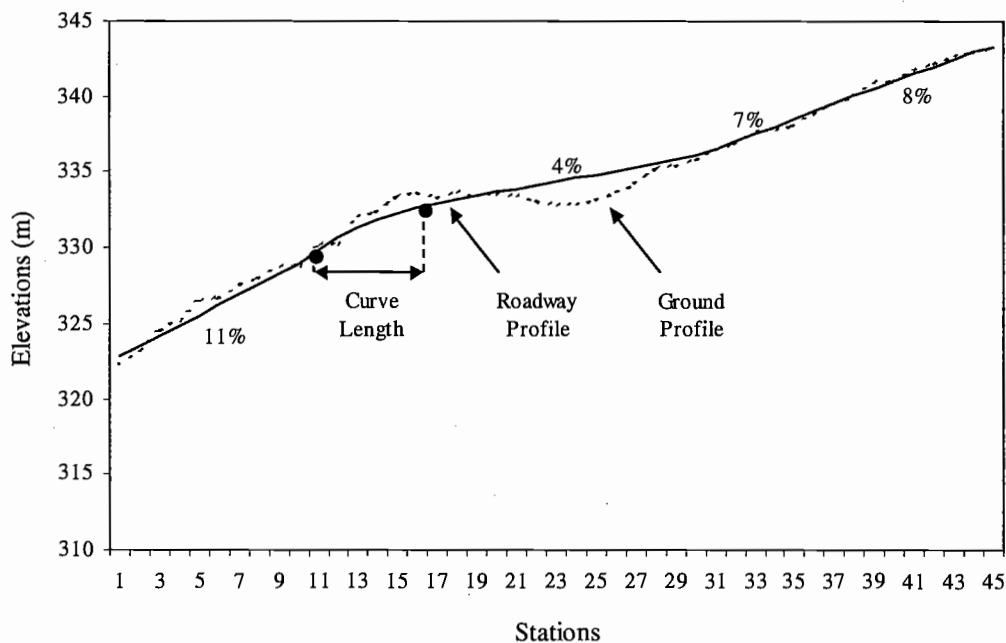


Figure 2.9. Road Profile indicating gradient and vertical alignment in Example A.

horizontal curve with a radius of 45m (Figure 2.10). The road gradient varied from 4% to 9% along the roadway. Two hundred and twelve feasible solutions were evaluated during the search process and the lowest value of the objective function was obtained at iteration 199 with the cost of \$27.5/m. Reducing the road gradient increased the earthwork costs (\$7/m), while using pit run for surfacing decreased the surfacing (\$8.8/m) and rock replacement (\$1/m) costs. The average annual volume of sediment delivered to a stream from the road decreased (0.17 ton) due to reduced road gradient.

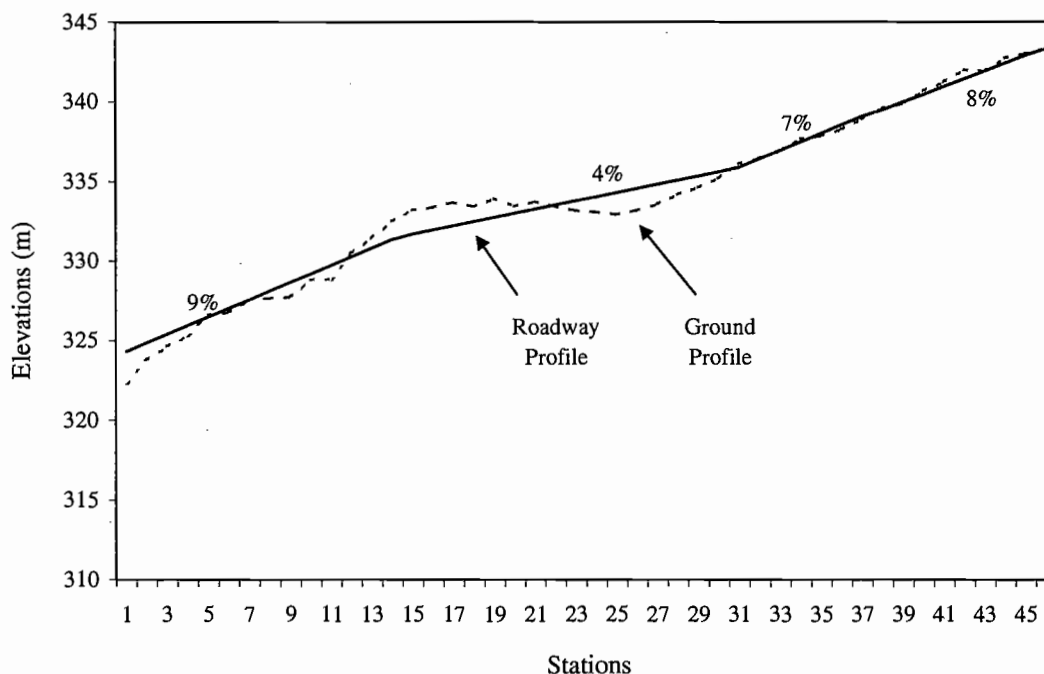


Figure 2.10. Road Profile indicating gradient and vertical alignment in Example B.

In both examples, total construction cost (Example A: \$9107 and Example B: \$5754) was the largest cost component, followed by maintenance (Example A: \$2918 and Example B: \$1112) and transportation costs (Example A: \$941 and Example B: \$929). In construction cost elements, earthwork allocation and surfacing costs were the largest cost components. The best solution involved adjusting the vertical alignment to keep grading below 10 percent in Example B. By reducing the road gradient, the solution did not require a vertical curve since the absolute value of the difference between grades was not more than 5%. Besides, the road length in Example B was slightly longer than in Example A. These factors increased earthwork allocation, construction staking, clearing and grubbing, seeding and mulching, and

blading costs, but decreased surfacing, rock replacement, transportation, maintaining culvert and ditches and removing brush, watering, drainage, and riprap costs.

The results indicated that the unit cost of sum of the construction, maintenance, and transportation costs in Example B was 40% percent less than in Example A. Sediment production was less in Example B. Even though the surfacing factors for good quality rock was less than that of pit run, the SEDMODL road slope factor assigned to road segments with more than 10% grade was 2.5 times greater than the road segments with less than or equal to 10% grade (Boise Cascade Corporation, 1999). Therefore, total annual sediment production in Example B was 41% less than the sediment production estimated in Example A.

Conclusions and Extensions

Current forest road design relies on manual procedures that have not changed in several decades. Meanwhile, developments in highway design have progressed toward the introduction of optimization methods to improve the search for better road designs. Highway design optimization algorithms have not been applied to the design of low volume roads in mountainous terrain with environmental considerations. The development of a design procedure that incorporates modern graphics capability, hardware, software languages, modern optimization techniques, and environmental considerations would improve the design process for forest roads.

In recent years, advances in generating digital elevation model of forested areas using LIDAR technology provides accurate terrain data for supporting the analysis of road design features such as ground slope, topographic aspect, and other

landform characteristics. A proposed approach has been described and implemented in the TRACER program, which provides the forest road designer with a decision support system for evaluating alternative horizontal alignments through finding efficient vertical alignments.

The contributions of the TRACER program are: (1) data input is enhanced through a 3D graphic interface, (2) user efficiency is enhanced through automated horizontal and vertical curve fitting routines, cross section generation, and cost routines for construction, maintenance, and vehicle use, (3) road feasibility is ensured by automatically considering geometric specifications, environmental impacts, and driver safety, (4) design time is reduced in the early stage of the forest road design by allowing the designer to quickly examine alternative routes, and (5) economic efficiency is enhanced by combining modern optimization techniques to minimize earthwork allocation cost using linear programming and to optimize vertical alignment using a heuristic technique (Simulated Annealing).

In the examples shown, the slightly longer road alignment using flatter grades and more earthwork yielded a lower total sediment load. The results from the two short examples should not be generalized. But, the examples are instructive in showing the tradeoffs that can occur. To evaluate the benefits and additional development requirements, TRACER must move out of the office and must focus on applications to real problems.

Although development efforts have sought to capture the basic elements facing the forest road designer, additional development will be required. Some of the

most important are discussed below. The model does not compute the total water discharge along the roadway. Therefore, it is not providing the designer with the most appropriate culvert locations or culvert size. TRACER assumes that the unit costs of earthwork do not change with the quantity of the material moved. When there is a case where the unit costs vary with the quantity of the cut and fill, the model can be enhanced using the available methods that consider such a case.

TRACER depends upon available GIS data coverage of attribute data to represent ground conditions. Available GIS data in many areas do not represent the actual ground condition with high accuracy; however, quality of the GIS data is improving as GIS technologies advance.

Future work could include refinements to the graphic interface, optimization of the horizontal alignment, and additional options for cut and waste areas within the road prism including more flexibility in the location of turnouts. Although TRACER is not intended to provide a final road location, this model can be enhanced by integrating it with GPS extensions to help the designer evaluate the model solutions on the ground.

Literature Cited

- Ahamed, K.M., S.E. Reutebuch, T.A. Curtis. 2000. Accuracy of high-resolution airborne laser data with varying forest vegetation cover. In Proceedings of the 2nd International Conference on Earth Observation and Environmental Information. 11-14, Cairo, Egypt.
- Aerotec, 1999. Airborne laser-scan and digital imagery. 560 Mitchell Field Road, Bessemer, AL 35022.
- Antoniotti P. 1969. APPOLLON: A new road design optimization procedure. PTRC Symposium on Cost Models and Optimization in Road Location, Design and Construction, London. 236-241.
- Boise Cascade Corporation, 1999. SEDMODL-Boise Cascade road erosion delivery model. Technical documentation. 19 p.
- Chew, E.P., Goh, C.J., and Fwa, T.F. 1989. Simultaneous optimization of horizontal and vertical alignment for highways. *Transportation Research*. 23B(5):315-329.
- Christian J. and H. Caldera. 1988. Earthmoving cost optimization by operational research. *Canadian Journal of Civil Engineering*. 51:679-684.
- Easa, S.M. 1987. Earthwork allocations with linear unit costs. *Journal of Construction Engineering and Management*. 114(4):641-655.
- Easa, S.M. 1988a. Selection of roadway grades that minimize earthwork cost using linear programming. *Transportation Research*. 22A(2):121-136.
- Easa, S.M. 1988b. Earthwork allocations with non-constant unit costs. *ASCE Journal of Construction Engineering and Management*, 113(1):34-50.
- Gladding, D.F. 1964. Automatic selection of horizontal alignments for highway location. Unpublished M.S. Thesis, Massachusetts Institute of Technology, Boston, Mass.
- Goh, C.J., Chew, E.P., and Fwa, T.F. 1988. Discrete and continuous models for computation of optimal vertical highway alignment. *Transportation Research*. 22B(6):399-409.
- Hickerson, T. 1964. Route location and design. McGraw-Hill, New York. 634 p.

- Hoffman, W. and R. Pavley. 1959. A method for the solution of the nth best path problem. *Journal of the Association for Computing Machinery*. 6(4):506-514.
- Howard, B.E., Bramnick, Z., and Shaw, J.F.B. 1968. Optimum curvature principle in Highway Routing. *Proc. Am. Soc. Civil Engrs.* (94):61-82.
- Lumberjack, 1995. A Road Design System, Version 5. Cheney, WA, 99004. 72 p.
- Mayer, R. and Stark, R. 1981. Earthmoving logistics. *Journal of Const. Div.* 107(CO2):297-312.
- Nandgaonkar, S. 1981. Earthwork transportation allocations: operation research. *Journal of Const. Div.* 107(CO2):373-392.
- NewCyber3D, 2002. GIS Solution Systems. 11 Tennessee St., Redlands, CA 92373.
- Nicholson, A.J. 1974. A variational approach to optimal route location. Civil Engineering Report 74-7, University of Canterbury, N.Z.
- O'Brien, W.T. and Bennett, D.W. 1969. A dynamic programming approach to optimal Route Location. *Proc Symposium on Cost Models and Optimization in Road Location, Design and Construction.* pp.175-199.
- Parker, N.A. 1977. Rural highway route corridor selection. *Transportation Planning Techniques.* (3):247-256.
- Pereira, L. and L. Janssen. 1999. Suitability of laser data for DTM generation: a case study in the context of road planning and design. *ISPRS Journal of Photogrammetry and Remote Sensing.* 54(1999): 244-253
- RoadEng, 2002. Forest road design using Softree 98, Forestry Edition. Technical Training Manual, Logging Engineering International, Inc., Eugene, Oregon, 97402. 124 p.
- Roberts, P.O. 1957. Using new methods in highway location. *Photogrammetric Engineering.* 23(3):563-569.
- Skaugset, Arne, and Marganne M. Allen. 1998. Forest road sediment and drainage monitoring project report for private and state lands in Western Oregon. Oregon Department of Forestry, Salem, Oregon, 97310. 20 pp.
- Trypia, M. 1979. Minimizing cut and fill costs in road making. *Computer-Aided Design.* (11):337-339.

- Turner, A.K. 1968. Computer-assisted procedures to generate and evaluate regional highway alternatives, Joint Highway Research Project report No.31, Purdue University, Lafayette, Indiana.
- WDNR, 1995. Standard methodology for conducting watershed analysis, Version 3.0. Washington Forest Practices Board.
- Whiting P.D. and J.A. Hillier. 1960. A method for finding the shortest route through a road network. Operational Research Quarterly. 11(1/2):37-40.
- Willenbrock J. 1972. Estimating costs of earthwork via simulation. Journal of Construction Division. 98(CO1):49-60.

Chapter 3

A Method for Minimizing Construction, Maintenance, and Transportation Costs with Computer-Aided Forest Road Design

Abdullah E. Akay
John Sessions

Department of Forest Engineering
Oregon State University
Corvallis, OR 97331

Abstract

Advances in the processing speed of microcomputers have increased interest in computer-aided design systems employing modern optimization techniques to provide rapid evaluation of road alignments in a more systematic manner. The current forest road design systems are not capable of making computer-aided design judgments such as automated generation of alternative grade lines, minimizing total costs, and aiming for least environmental impacts. A 3D forest road alignment model, TRACER Version 1.0, aided by an interactive computer system, was developed to help a designer with rapid evaluation of alternatives. The objective is to design a path with the lowest construction, maintenance, and transportation costs, while conforming to design specifications and environmental requirements, and providing driver safety. The model integrates two optimization techniques; a combination of linear programming for earthwork allocation and a heuristic approach (Simulated Annealing) for selection of vertical alignment. The average sediment delivered to a stream from the road section is also estimated using the method of a GIS-based road erosion/delivery model. It is anticipated that the development of a design procedure incorporating modern graphics capability, hardware, software languages, modern optimization techniques, and environmental considerations will improve the design process for forest roads.

Introduction

Forest roads connect forested lands to primary roads to provide access for timber extraction and management, fish and wildlife habitat improvement, fire control, and various recreational activities. The design of a forest road between two given locations on a surface is a complex engineering problem involving economic and environmental requirements. For low volume forest roads in mountainous terrain, construction and maintenance costs are the largest components in the total cost of producing timber for industrial uses. Forest roads are potentially the most problematic features of timber harvesting operations since inadequate road construction and poor maintenance can cause more stream sedimentation than any other operation (Skaugset and Allen, 1998). Excessive sediment delivered to streams from a road section can have a dramatic effect on water supplies, aquatic life, and wildlife populations. Thus, forest roads must be carefully designed to minimize construction and maintenance costs, and to minimize environmental damage.

There are an infinite number of possible combinations of grade lines to connect two given locations on a surface. In order to be confident that the designer's final route location is a cost effective one with low environmental damage, the designer has to examine a sufficient number of alternatives. Such a problem with many solutions can be solved using optimization techniques that systematically search for the solution with minimum cost among the acceptable solutions.

Several different optimization techniques have been considered for use in the field of highway design. The optimum curvature principle was employed by Howard

et al. (1968) to generate the curvature of an optimum highway location. Trypia (1979) developed a mixed integer programming formulation to determine the vertical alignment of the road that minimizes the earthwork cost. Dynamic Programming has been used for solving two-dimensional and three-dimensional alignment problems (Antoniotti 1969, O'Brien and Bennett 1969, Nicholson et al. 1976, Trietsch 1987, and Goh et al. 1988). The operations research model has been developed by Nandgaonkar (1981) and Christian et al. (1988) to optimize earthwork allocation cost. Linear Programming has also been used in several studies to plan the movement of earthwork during road construction (Mayer et al. 1981, Easa 1987, and Easa 1988b); to determine the optimal path (Parker, 1977); and to select the roadway grades that minimize the cost of earthwork (Easa, 1988a). Chew et al. (1989) proposed an alternative approach of solving a three-dimensional highway route selection problem where the optimal horizontal and vertical alignments are determined simultaneously. It was an extension from an earlier study (Goh et al., 1988) where optimal vertical highway alignment was determined for a preselected horizontal alignment.

The fundamental route location problem of finding the best or optimum path between two points, a function of physical, economical, and environmental factors, normally involves similar stages for both highway and forest roads. Computers have been used in forest road design since the 1960's, but have largely been applied to automate the computational tasks of earthwork calculation and computer aided drafting. The systems currently available for forest road design are not intended to make computer-aided design judgments such as automated generation of alternative

grade lines, best fitting vertical alignment for optimizing earthwork, minimizing the total cost of construction, maintenance, and transportation, and aiming for least environmental impact. They are generally used as a tool to make the mathematical calculations required to do basic manual road design. Since the manual method is “trial-and-error” and there are many possible alignments, it is highly conceivable that the manual design might not yield the best result. Also, data input is cumbersome in current programs. The road designer must enter many set-up parameters and input traverse notes into the related modules.

In current forest road design programs, the mass diagram is used to balance the required quantities of cut and fill. However, the capability of the mass diagram is decreased in some real life cases where soil characteristics vary along the roadway and additional quantities of material are required to be borrowed from borrow areas or wasted at landfill areas. After entering the survey data and design parameters, some programs manipulate geometric road design and earthwork balance calculations by allowing the designer to work in plan, profile or cross section view, using a visual display screen (RoadEng, 2002 and Lumberjack, 1995). However, the designer has to make these manipulations in such a way that all the constraints of horizontal and vertical alignments are satisfied. This can be very time consuming. The designer has to examine a number of alternatives to be sure that the final route location is “reasonably” cost effective and environmentally sound among the infinite number of alternative grade lines.

In recent years, advances in the processing speed and real-time rendering and viewing of high-resolution three dimensional (3D) graphics on microcomputers have made it possible to locate a route interactively on a 3D display of a ground surface generated by a high-resolution digital elevation model (DEM). LIDAR (Light Detection and Ranging) is one of the fastest growing systems that provide high-resolution and accurate DEM data. The accuracy of each point on the ground is approximately 15 cm in the vertical, and 1.0 meter in the horizontal (Ahmed et al. 2000).

A three-dimensional forest road alignment optimization model, TRACER Version 1.0, has been developed as a decision support system for forest road design. It automates many of the current mundane, time consuming tasks, while implementing a decision support framework. The purpose of this paper is to present the model, aided by an interactive computer system which helps a designer with a rapid evaluation of alternatives for the most economical path selection problem. The objective is to design a path between two given locations that minimizes the sum of construction, and future maintenance and transportation costs, while conforming to design specifications, environmental requirements, and driver safety.

The model has three main steps: (1) selecting a feasible trial route by establishing a series of intersection points on a 3D image of the terrain, subject to a wide range of geometric specifications and environmental requirements; (2) locating horizontal and preliminary vertical alignment, minimizing earthwork costs, calculating total cost including construction, maintenance and transportation costs,

and computing sediment delivery from the road section; and (3) selecting the vertical alignment with minimum total cost using a combinatorial optimization technique.

Initial trial routes are generated by “tracing” the possible paths using computer cursor on a 3D image of the terrain. For each alternative vertical alignment, the model calculates cross sections, earthwork volumes, and sediment delivery, and minimizes earthwork costs using linear programming, satisfying geometric specifications and environmental requirements. The model guaranties the optimum solution for earthwork allocation while providing a good quality/near optimum solution for the best path design problem.

Method

This section presents the model in detail. First, the data preparation is described along with the description of initial steps in the model. The formulation of the design constraints, the cost components, and the sediment model are then presented. Finally, an application of the model to a numerical example is illustrated. The theory behind the model is shown in Figure 3.1.

Data Preparation

The model reads input data files including digital elevation model (DEM) and attribute data. The model relies on a DEM to provide terrain data for supporting the analysis of road design features such as ground slope, topographic aspect, and other landform characteristics. The DEM data file is a set of scattered metric data points (X , Y , and Z), which represents the ground surface. In order to reduce the input data file

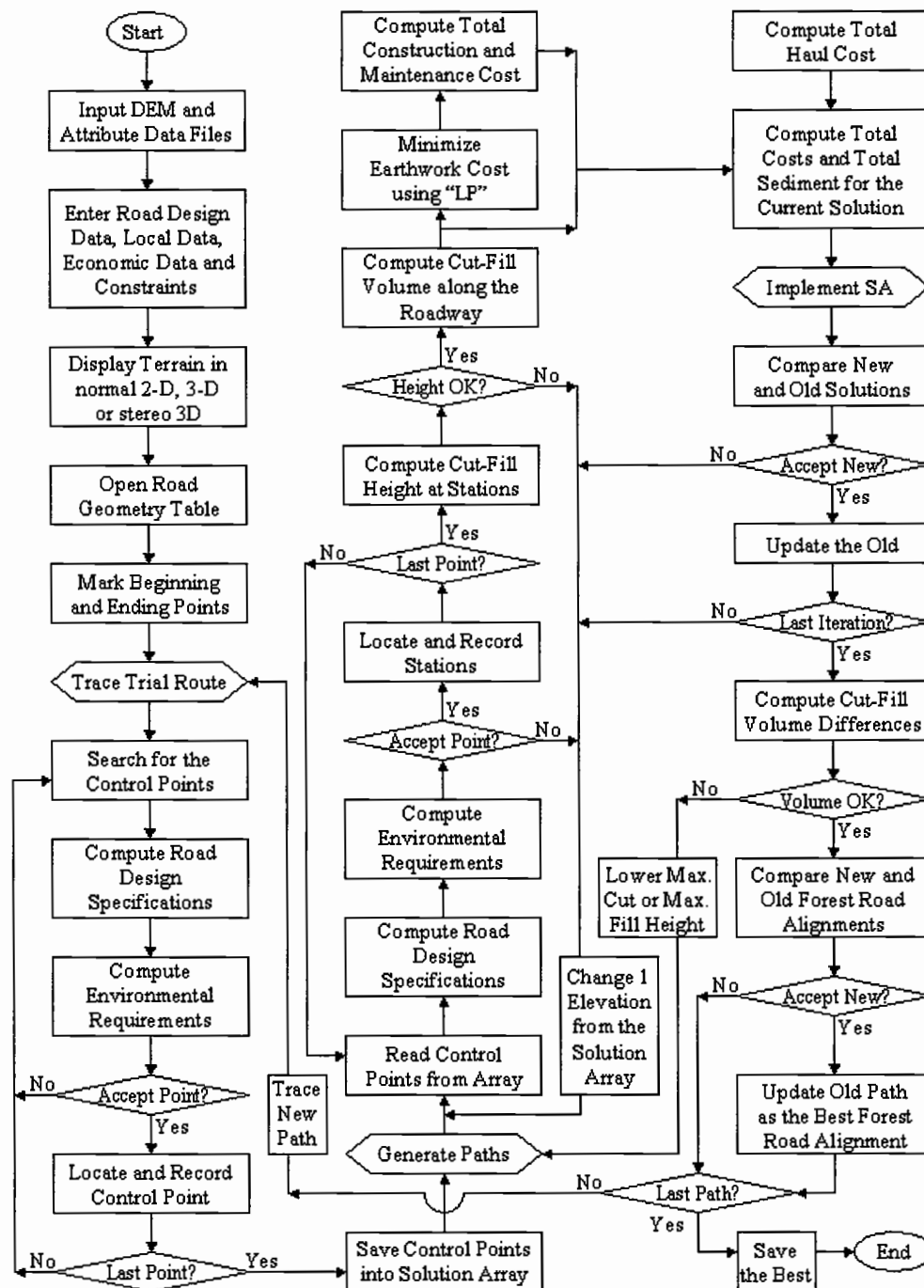


Figure 3.1. Theory of the forest road alignment optimization model, TRACER.

size, the original DEM coordinate system can be converted into a simple Cartesian Coordinate System in which X and Y values are both zero at the lower left origin. The attribute data file includes soil type and stream data, represented in the same format of metric data points. The designer can input more attribute data if desired, using the same format.

After the input data files are read, the designer enters the road design standards, economic data, local data, and road design constraints. The road design standards include road standard, road surface type, road template specifications, distance between road stations, design speed, vehicle specifications, and traffic volume. Economic data consist of the unit costs of road construction and maintenance activities and machine rate components of specified vehicles. Local data are soil swell and shrinkage factors, ground cover type, geological data, vegetation (timber stand) data, and distance to local resources of required road construction materials.

The road design constraints include geometric specifications and environmental requirements. The geometric specifications are maximum allowable road grade, minimum radius of the horizontal curves, minimum length of the vertical curves, minimum distance between curves, and minimum safe stopping distance for driver safety. It is also required that horizontal and vertical curves do not overlap each other. The environmental requirements are minimum allowable road grade and rolling road grades to get proper drainage, minimum distance from the riparian zones to protect the stream channels, minimum stream-crossing angle to reduce the damage on

the riparian zones, and maximum height of cuts and fills at any section to decrease soil movement.

The display and interactive features of the model are provided by NewCyber3D (2002), using an improved 3D OpenGL accelerator (Appendix 1). The model has a capacity of displaying and rendering high-resolution 2D and 3D image of the terrain in real-time, based on DEM and attribute data files. It also supports the real-time interactive stereo display, which requires liquid-crystal glasses and an infrared emitter that connects the glasses to standard graphic card. Due to increased interest in high-resolution stereo image display on low-cost personal computers, the cost of this viewing system has fallen dramatically in recent years.

Displaying the 3D image of the terrain on the screen, the designer opens the Road Geometry Window and locates the beginning and ending points of the road section. This window shows road geometry information and attribute data in real time, helping the designer to locate control points satisfying the constraints. Road geometry information includes *X*, *Y*, and *Z* coordinates, road grade, horizontal and vertical deflection between two consecutive road segments, length of the current segment, and cumulative segment length. Miscellaneous attribute data include soil type and stream data. The stream data are used to identify the distance to the closest stream in real-time.

The designer selects a feasible trial route between the beginning and ending points by establishing a series of control points on the 3D image of the terrain, subject to the road design constraints. Trial routes are generated by tracing the possible paths

using the computer cursor on the 3D image of the terrain (Figure 3.2). The curves connecting the control points are not used to represent the final location of the route path, but for visualization purposes only. The designer can zoom, pan, rotate, and scale the area in order to search for candidate control points around the terrain. If the designer chooses a candidate point, which is not acceptable by one or more constraints, the model warns the designer by changing the color of the line between the previously selected control point and the candidate point. Thus, the designer does not select this candidate point and searches for other points.

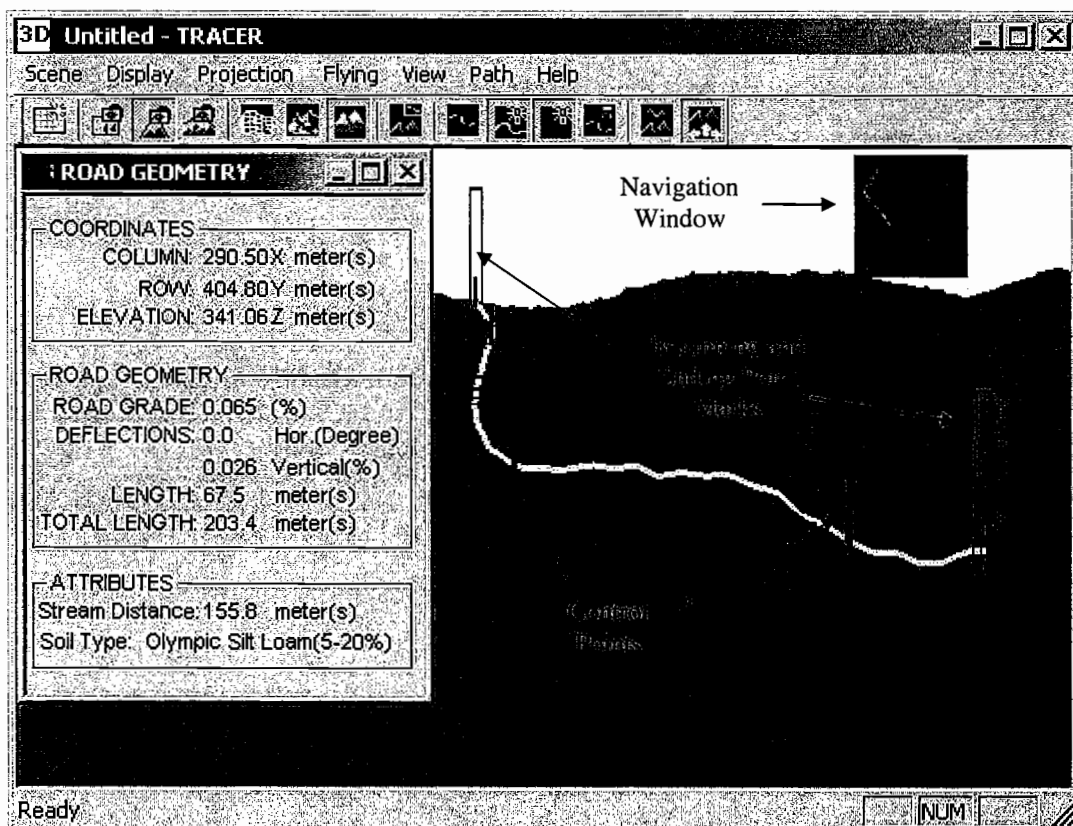


Figure 3.2. Locating a feasible trial route between two given points.

Design Constraints

The selected control points are stored so that the data for previously selected control points can be reached by the model in real-time to evaluate whether the candidate point selected by the designer will provide a feasible roadway transition that obeys the design constraints. The design variables selected for identification are as follows (Figure 3.3):

- i = the parameter for numbering the control points
- j = the parameter for numbering the roadway grades (tangents)
- X_i = centerline coordinate of X axis at control point i
- Y_i = centerline coordinate of Y axis at control point i
- Z_i = centerline elevation at control point i
- n = number of control points on some particular project
- Δ_i = horizontal deflection angle in degree at control point i
- G_j = road grade at tangent j in percent
- A_i = absolute value of the difference between G_j and G_{j+1} at control point i .

In Figure 3.3, i is the currently evaluated candidate point, while $i-1$ and $i-2$ refers to the previously selected and stored control points. The mathematical formulation is developed for each road design constraint with respect to specific geometric conditions in this figure.

Road Grade Constraints

The road grade is computed in Equation 1, using the vertical change of the road elevation and horizontal distance between two consecutive control points.

$$G_{j-1} = \frac{Z_i - Z_{i-1}}{\sqrt{(X_i - X_{i-1})^2 + (Y_i - Y_{i-1})^2}} \quad 1.$$

A negative road grade (favorable) in the direction of a unloaded log truck is limited by the maximum allowable road grade, G_f , considering the ability of a loaded log truck traveling on this grade uphill from the landing. A positive grade (adverse) in the direction of an unloaded log truck is limited by the maximum allowable road grade, G_a , considering the ability of an unloaded log truck to negotiate this uphill grade. The road grade is also limited by the minimum acceptable road grade, G_{\min} , to provide proper drainage. Therefore, the inequalities are formulated as follows:

$$\begin{aligned} -G_{\min} &\geq G_{j-1} \geq -G_f \\ G_{\min} &\leq G_{j-1} \leq G_a \end{aligned} \quad 2.$$

After locating the stations between the control points later in the model, these inequalities are also used to evaluate the grades between two consecutive station points along the roadway.

Curvature Constraints

At each control point, the model calculates the horizontal deflection angle and absolute value of the difference between two consecutive roadway grades to determine whether any type of curve is necessary. It is convenient to formulate the horizontal curve deflection angle in such a way that it will be also positive all the

time. Following equation indicates the formulation of A_{i-1} and Δ_{i-1} at control point $i-1$ with respect to specific geometric conditions in Figure 3.3:

$$A_{i-1} = |G_{j-1} - G_{j-2}|$$

$$\Delta_{i-1} = \arctan\left(\frac{|Y_{i-1} - Y_{i-2}|}{|X_{i-1} - X_{i-2}|}\right) - \arctan\left(\frac{|Y_i - Y_{i-1}|}{|X_i - X_{i-1}|}\right) \quad 3.$$

For low volume forest roads, it is assumed that it is not necessary to locate a vertical curve if A_{i-1} is less than or equal to a specified small percentage of difference in grades, A_{min} (e.g. $\leq 5\%$). If A_{i-1} is greater than A_{min} and Δ_{i-1} is zero, the model locates a vertical curve. If A_{i-1} is less than or equal to A_{min} and Δ_{i-1} is greater than zero, then the model locates a horizontal curve. Otherwise, a straight roadway (tangent) is located. If there is a case where A_{i-1} is greater than A_{min} and Δ_{i-1} is greater than zero, the model warns the designer to choose a different control point that avoids the overlapping of vertical and horizontal curves.

Vertical Curve Constraints

Vertical curves are used to connect roadway sections between two grades. Forest road engineers generally use symmetrical vertical curves, in which the horizontal projections of the intersecting tangents are equal. The primary challenge of locating vertical curves lies in generating a sufficient curve length that permits a log truck to pass a curve without bottoming out in the sag or breaching the crest and provides safe stopping distance, SSD . Thus, to ensure a safe roadway passage, the model locates a vertical curve that accommodates an adequate curve length. The minimum curve length (L_{vmin}) of a forest road suggested is about 15 meters (e.g. 50

feet) (USDA Forest Service, 1987). Three times the design speed is also used to define minimum curve length (AASHTO, 1990).

If the absolute value of the difference between grades is greater than A_{min} and the horizontal deflection angle is equal to zero, then the model locates a vertical curve. When the final tangent grade, G_{j-1} , is less than the initial tangent grade, G_{j-2} , a crest curve occurs, and when G_{j-1} is greater than G_{j-2} , a sag curve occurs. The tangent grades, G_{j-1} and G_{j-2} , can be positive or negative. Figure 3.4 illustrates the geometry of a vertical crest curve, generated based on three consecutive control points. In this figure, $L_{v_{i-1}}$ is the length of the curve, BVC_{i-1} is the beginning point of the curve, and EVC_{i-1} is the ending point of the curve.

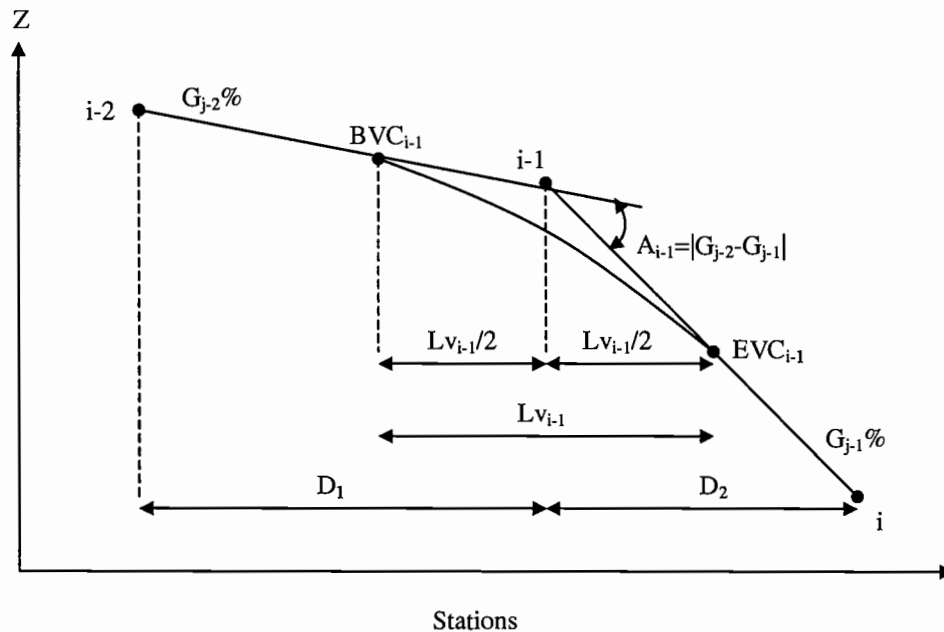


Figure 3.4. Geometry of a symmetrical vertical curve (crest) used in the model.

$D1$, the horizontal distance from control point $i-1$ to the previous control point $i-2$, and $D2$, the horizontal distance from control point $i-1$ to candidate control point i , are computed as follows:

$$D1 = \sqrt{(X_{i-1} - X_{i-2})^2 + (Y_{i-1} - Y_{i-2})^2}$$

$$D2 = \sqrt{(X_i - X_{i-1})^2 + (Y_i - Y_{i-1})^2} \quad 4.$$

In determining a feasible curve length, crest and sag vertical curves are considered separately based on whether the curve length is greater or less than the *SSD* (Appendix 2). Safe stopping distance is one of the primary elements in designing horizontal and vertical curves with an appropriate level of safety. The objective is to provide a sufficient sight distance for the drivers to safely stop their vehicles before reaching objects obstructing their forward motion. On two directional one-lane roads, stopping distance is approximately twice the stopping distance for a two-lane road, since for both drivers must safely stop their vehicles (AASHTO, 1990).

By using the coordinates of the previously selected control point, $i-2$ and $i-1$, the model searches for a third control point that generates a feasible vertical curve satisfying the geometric constraints, minimum curve length and required safe stopping distance. If the curve length is less than the user-defined minimum, the model warns the designer to select a different candidate point that provides the minimum curve length.

When the curve length is greater or equal to the minimum curve length, L_{vmin} , then the model tests the curve length, $L_{v_{i-1}}$, considering three different cases in which $L_{v_{i-1}}$ should be treated accordingly.

Case 1:

If there is no curve located on the previous control point ($i-2$), the model compares Lv_{i-1} with $D1$ and $D2$ (Equation 4). It investigates whether Lv_{i-1} is less than $D1$ and $D2$ to ensure that available sets of control points provide adequate space to locate the vertical curve.

Case 2:

If there is a horizontal curve located on the previous control point, the model first computes $D1_{new}$ as follows:

$$D1_{new} = D1 - T_{i-2} - \delta \quad 5.$$

where T_{i-2} is the tangent length of the previous horizontal curve and δ is the user-defined value of minimum distance between curves. Then, It investigates whether Lv_{i-1} is less than $D1_{new}$ and $D2$ to ensure that available sets of control points provide adequate space to locate the vertical curve.

Case 3:

If there is a vertical curve located on the previous control point, the model first computes $D1_{new}$ as follows:

$$D1_{new} = D1 - (Lv_{i-2}/2) - \delta \quad 6.$$

where $Lv_{i-2}/2$ is half length of the previous vertical curve (symmetrical). Then, it investigates whether Lv_{i-1} is less than $D1_{new}$ and $D2$ to ensure that available sets of control points provide adequate space to locate the vertical curve.

If all of the specified design constraints for the vertical curve are satisfied, the model defines the candidate control point as the third control point, i , and stores the

coordinates (X , Y , and Z) into the solution array. Otherwise, it warns the designer to choose a different control point that satisfies the design constraints.

Horizontal Curve Constraints

The critical aspect of horizontal alignment is the horizontal curve that changes the direction of the roadway left or right in a horizontal plane. On low volume forest roads, a simple circular horizontal curve is generally designed to provide a transition between two straight roadway sections. To design a feasible horizontal curve that provides safe continuous operation, the model considers geometric constraints such as minimum radius, acceptable road grade on horizontal curve, and minimum safe stopping distance.

If the absolute value of the difference between grades is less than or equal to A_{min} and the horizontal deflection angle is greater than zero, the model locates a horizontal curve. Figure 3.5 indicates the geometry of a simple horizontal circular curve, generated based on three consecutive control points. In this figure, PC_{i-1} is the beginning of curve, PT_{i-1} is the ending of curve, PI_{i-1} is the point of intersection at control point $i-1$, R_{i-1} is the radius measured from the centerline of the road, T_{i-1} is the tangent length, Lh_{i-1} is the length of curve, M_{i-1} is the middle ordinate, E_{i-1} is the external distance, and LC_{i-1} is the chord length from PC_{i-1} to PT_{i-1} .

The model searches for a feasible horizontal curve that meets the geometric constraints by adjusting the tangent lengths. The model first computes the maximum tangent length, T_{max} , that is generated by the current set of three control points. There are three different cases in which T_{max} should be treated accordingly.

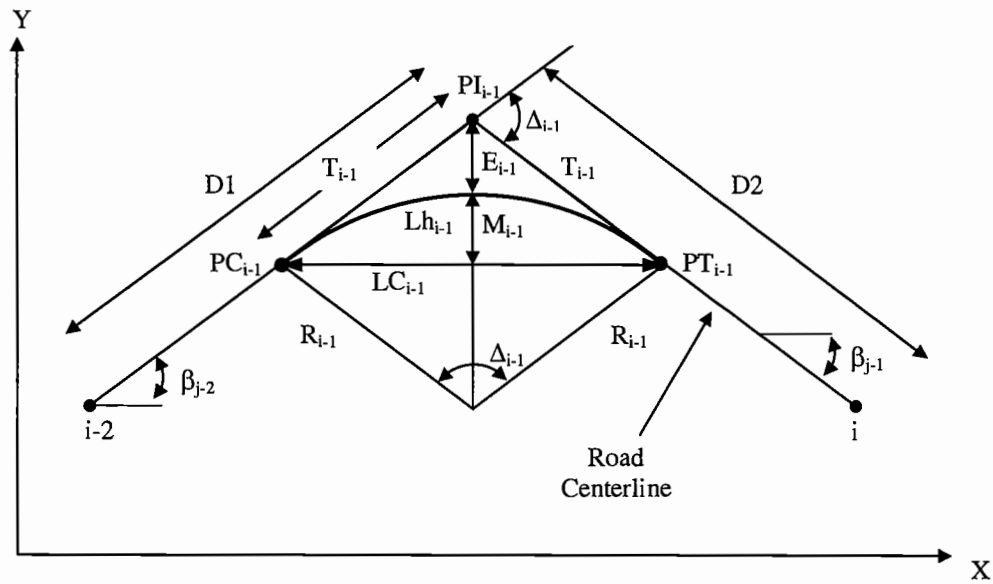


Figure 3.5. Geometry of a simple horizontal circular curve used in the model.

Case 1:

If there is no curve located on the previous control point ($i-2$), the model compares $D1$ and $D2$ (Equation 4), and assigns the shorter one as a maximum tangent length.

Case 2:

If there is a horizontal curve located on the previous control point, the model first computes $D1_{new}$ using Equation 5. Then, the model compares $D1_{new}$ and $D2$, and assigns the shorter one as a maximum tangent length.

Case 3:

If there is a vertical curve located on the previous control point, the model first computes $D1_{new}$ using Equation 6. Then, the model compares $D1_{new}$ and $D2$, and

assigns the shorter one as a maximum tangent length. After T_{max} is defined, the model computes the maximum radius, R_{max} , as follows (Anderson et al. 1985):

$$R_{max} = \frac{T_{max}}{\tan\left(\frac{\Delta_i - 1}{2}\right)} \quad 7.$$

If R_{max} is less than a user-defined value of the minimum curve radius, R_{min} , the model warns the designer to choose a different control point that provides the minimum turning radius. At the lowest speed of an off-road truck with trailer, the minimum radius is considered to be about 18 meters (about 60 feet) on forest roads.

If R_{max} is greater than or equal to R_{min} , the model searches for a feasible tangent length, between minimum tangent length, T_{min} , and maximum tangent length by incrementing T_{min} by a specified value (e.g. 1 meter). The minimum tangent length is computed based on horizontal deflection angle, Δ_{i-1} , and R_{min} as follows:

$$T_{min} = R_{min} \tan\left(\frac{\Delta_i - 1}{2}\right) \quad 8.$$

The tangent length, which satisfies the geometric constraints listed earlier, is assigned as a feasible tangent length, T_{i-J} . If a feasible tangent is not found, the designer is warned by the model to search for a different control point that provides a feasible tangent length.

In the process of determining the feasible tangent length, the model first computes the curve radius for each tangent length generated in the loop (Equation 9).

$$R_{i-1} = \frac{T_{i-1}}{\tan\left(\frac{\Delta_i - 1}{2}\right)} \quad 9.$$

When R_{i-1} is greater or equal to R_{min} , the chosen tangent length satisfies the minimum radius constraint, and the model moves to the next constraint, which is acceptable road grade in percent on horizontal curve $G_{C_{i-1}}$. A negative grade on a curve in the direction of a unloaded log truck is limited by the maximum allowable road grade, G_{C_f} , considering the ability of a loaded log truck traveling on this grade uphill from the landing. A positive grade on a curve in the direction of an unloaded log truck is limited by the maximum allowable road grade, G_{C_a} , considering the ability of an unloaded log truck to negotiate this uphill grade.

The grade on the curve should be kept lower than that on a tangent because: (a) off tracking of the vehicle creates a higher “effective” grade for both the truck and the trailer, (b) the truck incurs additional forces required to turn the tandem axles around the curve, and (c) the powered wheels may have unbalanced normal loads due to a combination of centrifugal force, superelevation, and angle of the trailer. All three factors reduce the gradeability of the vehicle. Since the effect of these factors is increased as the radius decreases, the model uses a threshold value for each radius. If the radius of the current horizontal curve is greater than this threshold, the model allows the designer to locate a horizontal curve whose grade is at least 2% less than the maximum allowable road grade on a tangent. However, if the curve is less than the threshold, the model warns the designer until the grade on the horizontal curve is at least 4% less than the maximum allowable road grade on a tangent. The threshold value for the radius can be defined by the designer based on road standards and vehicle specifications.

In order to compute road grade on the curve, the model first locates the beginning and ending point of the curve, using T_{i-1} and horizontal angle of initial tangent and final tangent, β_{j-2} and β_{j-1} , respectively. Equation 10 indicates the formulation of β_{j-2} and β_{j-1} .

$$\begin{aligned}\beta_{j-2} &= \arctan\left(\frac{|Y_{i-1} - Y_{i-2}|}{|X_{i-1} - X_{i-2}|}\right) \\ \beta_{j-1} &= \arctan\left(\frac{|Y_i - Y_{i-1}|}{|X_i - X_{i-1}|}\right)\end{aligned}\tag{10}$$

The coordinates of PC_{i-1} on X axis, PCx_{i-1} , and Y axis, PCy_{i-1} , are computed as follows:

$$\begin{aligned}PCx_{i-1} &= X_{i-1} - \cos(\beta_{j-2})T_{i-1} \\ PCy_{i-1} &= Y_{i-1} - \sin(\beta_{j-2})T_{i-1}\end{aligned}\tag{11}$$

The coordinates of PT_{i-1} can be computed in the same manner, using β_{j-1} .

After defining the X and Y coordinates of PC_{i-1} and PT_{i-1} , the model computes the elevation of these points, PCz_{i-1} and PTz_{i-1} , respectively. Using the elevation of the control point $i-1$ (Z_{i-1}) and grade of initial tangent (G_{j-2}) and final tangent (G_{j-1}), PCz_{i-1} and PTz_{i-1} are computed in Equation 12 with respect to specific geometric conditions in Figure 3.3.

$$\begin{aligned}PCz_{i-1} &= Z_{i-1} - G_{j-2}T_{i-1} \\ PTz_{i-1} &= Z_{i-1} + G_{j-1}T_{i-1}\end{aligned}\tag{12}$$

Then, the road grade on the horizontal curve (G_{Ci-1}) is computed as follows:

$$G_{Ci-1} = \frac{PTz_{i-1} - PCz_{i-1}}{Lh_{i-1}}\tag{13}$$

where the length of horizontal curve (Lh_{i-1}) is calculated from the following equation (Anderson et al. 1985):

$$Lh_{i-1} = \frac{\Delta_{i-1} \pi R_{i-1}}{180^\circ} \quad 14.$$

If Gc_{i-1} satisfies the requirements of road grade on a horizontal curve, the model investigates the next constraint, which is minimum safe stopping distance of a horizontal curve. In horizontal curve design, safe stopping distance is used as a limiting factor for the curve length (Appendix 3). If the curve length is less than the safe stopping distance of an operating vehicle traveling at or near the design speed, the model warns the designer to avoid locating this curve due to inadequate curve length.

If all of the specified design constraints (R_{i-1} , Gc_{i-1} , and SSD) are satisfied, the model defines the candidate control point as the third control point, i , and stores the coordinates (X , Y , and Z) into the solution array. Otherwise, it warns the designer to choose a different control point that satisfies the design constraints.

Stream Constraints

Since riparian forest buffers improve stream by reducing erosion, improving water quality, and enhancing fish and wildlife habitat, the road designer should demonstrate certain practices including providing a sufficient minimum distance between fill slope and streams and reducing connectivity to stream crossings (Burroughs et al. 1989). In the Road Geometry Window, TRACER provides the designer with the horizontal distance between any control point considered and the

closest stream point in real-time, using the attribute data file in which X and Y coordinates of the stream points are stored. The stream distance (D_s) from the candidate control point i is computed in Equation 15, in which s is the parameter for numbering the stream points, and X_s and Y_s are the coordinates of the stream point.

$$D_s = \sqrt{(X_s - X_i)^2 + (Y_s - Y_i)^2} \quad 15.$$

The stream-crossing angle is also considered in the model since connectivity to stream crossing is recognized as a significant contributor of the sediment associated with timber harvesting. To minimize or eliminate the sediment delivery and create the least amount of disturbance to the stream, the designer should construct the crossing at or close to a 90-degree angle to the stream (Appendix 4).

If the currently selected control point, i , satisfies the stream constraints including minimum stream distance and stream-crossing angle, it is defined as the new control point, i , and the model stores the coordinates (X , Y , and Z) into the solution array. Otherwise, it warns the designer to choose a different control point that satisfies the design constraints.

Cut and Fill Height Constraints

After connecting the two end points of the road by selecting feasible control points that satisfy the design constraints, TRACER stores the data for this path. Using the trial route data as an initial solution, the model automatically locates the station points between the control points along the horizontal curve, vertical curve and straight roadways (Appendix 5).

After locating the station points along the road section, the model stores the coordinates of the station points, X_p , Y_p , and Z_p , into an array. Then, it determines whether there is a cut, fill or neither by computing the difference between ground elevation, Z_{g_p} , and road elevation, Z_p , at each station point. If Z_p is less than Z_{g_p} there is cut and if Z_p is greater than Z_{g_p} there is fill. Otherwise, there is no cut or fill at the station. The ground elevation, as a function of X_p and Y_p coordinates, is obtained from the DEM data file (Appendix 6).

For each station point, the model computes the associated cut and fill heights using Equations 16 and 17, in which HC_p and HF_p are the cut and fill heights at station point p , respectively.

$$HC_p = Z_{g_p} - Z_p \quad 16.$$

when there is cut, or:

$$HF_p = Z_p - Z_{g_p} \quad 17.$$

when there is fill.

If the cut or fill height at any station is greater than the user-defined values of maximum cut height, HC_{max} , or maximum fill height, HF_{max} , then the model generates a new solution (alignment) by changing the elevation in a randomly selected control point by a specified value (e.g. 0.5 meters) within the elevation range of the control points. The alternative alignment generation will be explained later in detail. When cut and fill heights and other specified constraints are satisfied, the model moves to the next step.

Cross Sections

Cross sections show the ground slope and angle of topography at each station point. They are located perpendicular to the road section. The model first determines the type of the cross section (Appendix 7) and calculates cut and fill areas (Appendix 8). Figure 3.6 indicates the terminology of a forest road on a cut and fill type cross section, which generally applies to most road types. The model employs inslope and crowned type forest road surfaces.

The cross sections are used to compute earthwork volume (Appendix 9) and major cost elements for each road stage between two consecutive stations. The length of the road stage must be carefully determined by the designer to compute the earthwork volume more accurately, particularly in rough and mountainous terrain

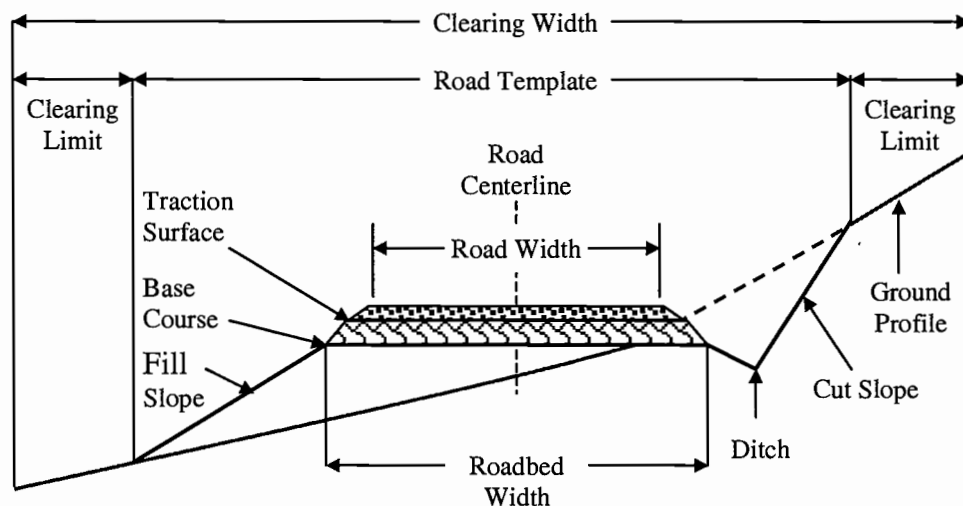


Figure 3.6. Road elements on the cross section.

where rapid changes occur in ground elevation. The cut and fill slopes should be constructed in such a way that slope failure and erosion of the cut and fill banks are minimized. In the model, cut and fill slope angles and maximum cut and fill slope heights are defined depending on the soil type data stored in the attribute data file (Appendix 8). For the road stages located on a horizontal curve, the model considers the curve widening due to providing sufficient vehicle offtracking (Appendix 10) and clearing the middle ordinate distance for safe stopping distance (Appendix 11).

Total Cost

As mentioned earlier, the total cost of a road section consists of the construction cost, maintenance cost, and transportation cost. In order to compare the total costs for various routes, the present value of the future maintenance and transportation costs are computed using a terminating periodic series approach. The objective function that minimizes the total cost, TC , takes the following form:

$$\text{Min } TC = C + M_0 + T_0 \quad 18.$$

where C is the construction cost, M_0 is the present value of the maintenance cost, and T_0 is the present value of the transportation cost.

The road construction cost is the total cost of the road construction activities: construction staking, clearing and grubbing, earthwork allocation, drainage and riprap, surfacing, water supply and watering, and seeding and mulching. The maintenance activities involve rock replacement, grading, culvert and ditch maintenance, and brush cleaning. Design speed, entering and exit speed, acceleration and deceleration rates of truck traffic, and machine rate are analyzed as the effective

factors of the forest transportation costs. Additional costs (accident costs, land costs, ecological penalties etc.) can be included into the model if they can be expressed quantitatively.

Construction Costs

The cost elements of road construction and maintenance are determined based on “Cost Estimate Guide For Road Construction Region 6” prepared by the USDA Forest Service (1999). The cost guide provides standard methods for estimating road construction in the Pacific Northwest Region. The basic unit costs (profit, risk, overhead, materials, equipment, transportation, and labor costs) of the construction activities and related adjustment factors can be obtained from the data tables. Wage rates are also adjusted based on the wage ratio and labor range tables in this cost guide.

Construction Staking Cost

Construction staking cost is estimated by multiplying the basic unit costs per kilometer by specified adjustment factors and total road length in kilometers. These include ground cover, terrain, section, and travel factors. The formulation of the construction staking cost, C_{cs} , in a road stage r is:

$$C_{cs} = u_{cs}(1 + f)L_r \quad 19.$$

where u_{cs} is the basic unit cost, f is the sum of adjustment factors, and L_r is the length of the road stage. The ground cover factor varies depending on stand and brush density. The model computes the sideslope at each road station point to estimate the

terrain factor. If the sideslope is greater than 30% or the road stage is close to the stream channel (e.g. <10 meters), the model considers staking both sides by increasing the basic unit cost by 25%. The basic unit cost is also increased by 10% considering the average daily round trip travel. The section factor increases as the number of station points per kilometer increase along the roadway.

Clearing and Grubbing Cost

The model first estimates the area to be cleared between two consecutive stations (Appendix 12). Then, clearing and grubbing costs are estimated by multiplying the basic unit costs per hectare by adjustment factors and clearing area in hectares. The adjustment factors are clearing classifications, slash factor, sideslope factor, and clearing width factor (USDA Forest Service, 1999). The formulation of the clearing and grubbing cost, C_{cg} , in a road stage r is:

$$C_{cg} = u_{cg}(1 + f)CA_r \quad 20.$$

where u_{cg} is the basic unit cost, f is the sum of adjustment factors, and CA_r is the clearing area of the road stage. Clearing classifications increase as the density of the ground cover increases. The slash factor varies depending on type of the slash treatment method selected by the designer. The model computes the sideslope of two consecutive cross sections, and takes their average to define the sideslope factor. Average clearing width is also computed based on the clearing widths at these sections (Appendix 12).

Earthwork Allocation Cost

The economic distribution of cut and fill quantities is determined using the linear programming method of Mayer and Stark (1981), considering possible borrow and landfill locations and various soil characteristics along the roadway. This method is used to overcome the limitation of the mass diagram on roadway sections with various soil characteristics. Besides, it represents the earthwork allocation better than the other methods and provides the optimal solution to the problem. In order to incorporate this method into the model, a linear programming code, using the idea of the simplex algorithm (Bowman and Fetter, 1967), is developed.

In the method, it is assumed that the unit costs do not vary with the amount of material moved. It is also assumed that the unit cost of hauling is linearly proportional to the hauling distance. The specific unit costs for earthwork activities including excavation, haul, and embankment are defined based on the soil type data for each road stage. Swell factor of the material moved from cut section i , and shrinkage factor of the material compacted into fill section j , are considered to determine haul and fill quantities. Therefore, the objective function is stated as follows:

$$\begin{aligned} \text{Min } Z = & \sum_i \sum_j C(i, j) X(i, j) + \sum_i \sum_k C_D(i, k) X_D(i, k) + \\ & \sum_p \sum_j C_B(p, j) X_B(p, j) \end{aligned} \quad 21.$$

subject to the following constraints:

$$(1) \sum_j X(i, j) + \sum_k X_D(i, k) = Q_c(i) \quad 22.$$

where $X(i,j)$ (the amount of cut moved from cut section i to fill section j) plus $X_D(i,k)$ (the amount of cut moved from cut section i to landfill area k) are equal to the available amount of cut, $Q_c(i)$, at cut section i .

$$(2) \sum_i s_{ij}^f X(i,j) + \sum_p s_{pj}^f X_B(p,j) = Q_f(j) \quad 23.$$

where $s_{ij}^f X(i,j)$ (the adjusted amount of cut moved from cut section i to fill section j) plus $s_{pj}^f X_B(p,j)$ (the adjusted amount of material moved from borrow area p to fill section j) are equal to the amount of fill required, $Q_f(j)$, at fill section j . The shrinkage factors for material moved from cut section i and borrow area p are defined as s_{ij}^f and s_{pj}^f , respectively.

$$(3) \sum_i s_{ik}^f X_D(i,k) \leq Q_D(k) \quad 24.$$

where $s_{ik}^f X_D(i,k)$ (the adjusted amount of cut moved from cut section i to landfill area k) is equal to or less than the capacity of the landfill k , $Q_D(k)$. s_{ik}^f is the swell factor for material moved from cut section i and wasted in landfill area k .

$$(4) \sum_j X_B(p,j) \leq Q_B(p) \quad 25.$$

where $X_B(p,j)$ (the amount of material moved from borrow area p to fill section j) is equal to or less than the material available in borrow area p , $Q_B(p)$.

$$(5) X(i,j), X_D(i,k), \text{ and } X_B(p,j) \geq 0 \quad 26.$$

where non-negative conditions are represented.

The unit cost of moving and compacting the material from cut section i to fill section j , $C(i,j)$, is estimated based on unit cost of each operation including excavation

(u_e), hauling (u_h), and compacting (u_c), assuming that the costs are linearly proportional to the quantities. The formulation for adjusted quantities is:

$$C(i,j) = u_e + s_i^h (u_h d_{ij} + u_c) \quad 27.$$

where d_{ij} is the distance between the center of cut section i and the fill section j . For each road stage, the model computes the distance between the beginning of the road section and the middle point of this road stage. The distance between the beginning of the road section and the middle point of cut section i and fill section j are denoted by Lb_i and Lb_j , respectively. Then, d_{ij} is equal to $|Lb_i - Lb_j|$. The unit cost of borrow, $C_B(p,j)$, and disposal, $C_D(i,k)$, are determined similarly.

Drainage and Riprap Costs

To intercept road surface drainage, crowned or insloped surface templates with ditches are used in the model. The ditches carry road surface runoff, overland surface runoff, and subsurface water away from the road through ditch relief culverts. Drainage cost is estimated by multiplying the basic unit costs (material, installation, elongation, treatment, and special item costs) per lineal meter of the culvert by the culvert length in meters. The basic unit cost varies with the type and dimensions of the culvert being installed. The formulation of the drainage cost, C_d , is:

$$C_d = u_d L_c \quad 28.$$

where u_d is the basic unit costs and L_c is the length of the culvert.

The procedure for locating culverts involves collecting field data, computing the surface drainage and estimating the flood flow for a chosen frequency. Since engineer's interpretation of field data and hydrology data is affected by personal

judgment, it is very often that two engineers arrive at two different answers. The model is not equipped to compute the total water discharge along the roadway, therefore, it is not intended to provide the designer with the final culvert locations and dimensions along the road section. Instead, the model first estimates the number of required culverts using the guidelines of maximum culvert spacing by soil erosion classes and average road grade (Pearce, 1974). Second, the ditch relief culverts (skewed) are located on the low point of vertical curves and at intervals on the road grade (Appendix 13). If the number of culverts located by the model is less than the number of culverts estimated by the guidelines, the model computes the cost of the additional culverts with average size and length, and adds this into the total drainage cost. If the model estimates more culverts than the guidelines, then the cost of overestimated culverts is subtracted from the total drainage costs.

To minimize ground disturbance due to surface runoff and falling water on the downspout, the model considers placing adequate amounts of riprap material. In forest roads, 15-20 centimeters size rocks are commonly used as riprap material. The riprap cost in a specific road stage is computed by multiplying the basic unit cost of riprap per cubic meter by required volume of rock used as riprap material in cubic meters. The basic unit cost varies depending on material, equipment, transportation, and labor costs. Based the cross section type and amount of the rock required, the model uses hand-placed or machine-placed riprap techniques (Appendix 13). The formulation of the riprap cost, C_{rr} , at road stage r is:

$$C_{rr} = u_{rr}V_{rr}$$

where u_{rr} is the basic unit cost and V_{rr} is the volume of the riprap material required at the site.

Surfacing Cost

Native-soil surfacing can be used when harvest operations are conducted during the dry season. However, logging in the wet season requires aggregate surfacing (crushed rock) to increase the strength of the forest road surface to support vehicle traffic. Aggregate surfacing also provides increased wheel traction and relatively smooth traveling surface that reduces the subsequent road maintenance, and extends the life of the subgrade by reducing road surface ruts and erosion.

The surfacing cost varies depending on the type and required quantity of the surfacing material and haul distance. In the model, the rock size and the depth of the aggregate surfacing are determined based on the type of the subgrade soil along the roadway. The quantity of the surfacing material is computed using the length and width of the road section, and surfacing depth. The surfacing cost includes rock purchasing or production cost, hauling cost, processing costs (compacting, mixing, and placing) and testing cost. The formulation of the surfacing cost is presented in Appendix 14.

The model considers multiple layers of surfacing including base course and traction surface (Figure 3.6). Large size base rocks are used to support vehicle wheels and to retard moisture penetration into the subgrade. A traction surface is then placed over the base rock to increase traction and to provide a smooth durable traveling surface of low rolling resistance for rubber-tired traffic. The depth of the base course

is determined based on the bearing strength of the subgrade soil. The California Bearing Ratio (CBR) is used to estimate the bearing strength of the soil along the roadway (Pearce, 1974). In forest roads, 15 cm to 7.5 cm size rock is commonly used to build up the base course with 25 cm depth (Kramer, 2001). The rock size and depth of the traction surface is mostly defined depending on the road grade. On grades less than 16%, 4 cm rocks are used to build up the traction surface with 8 cm depth. If grade is greater than or equal to 16%, 2.5 cm rocks are used to build up the traction surface with 10 cm depth (Kramer, 2001).

Water Supply and Watering Cost

Watering cost is estimated based on the amount of water required for excavation and surfacing operations. After estimating total quantity of the excavation (Q_e) and the surfacing material of the project ($Q_s = Q_{ts} + Q_{bc}$), the model computes the total amount of water based on the amount of water in liters per cubic meter of excavation (w_e) and surfacing material (w_s).

$$Q_w = Q_e w_e + Q_s w_s \quad 30.$$

where w_e and w_s are defined by the cost guide (USDA Forest Service, 1999). The components of the watering cost include purchasing cost and hauling cost. In the model, it is assumed that the required amount of water is purchased from local sources and that the water truck is equipped with a water pump. The purchasing cost, C_p (including loading cost), can be defined by the designer based on the local economic data. The hauling cost, C_h , is divided into fixed and variable hauling costs. The fixed cost per liter (u_{fw}) is defined by the cost guide depending on truck size,

approximate legal load limit, and delay time. The variable cost (u_{vw}) per liter per kilometer, based on round trip haul distance and average truck speed (loaded and empty), is also provided by the cost guide. The formulation of the total hauling cost is:

$$C_h = (Q_w)(u_{fw} + u_{vw}D_{wr}) \quad 31.$$

where D_{wr} is the distance (in kilometers) to the local water resources. Then, the formulation of the total watering cost is developed as follows:

$$C_w = C_p + C_h \quad 32.$$

Seeding and Mulching Cost

Bare cut and fill slopes, resulting from road construction on sloping terrain, increase soil erosion and stream sedimentation. Since natural re-vegetation is extremely slow, seeding, fertilizing, and mulching are recommended to provide quick stabilization and enhance the beauty of the area. In the model, it is assumed that a user-defined amount of grass seed mixture and fertilizer per hectare is uniformly distributed over the area. The use of mulch is also considered to prevent erosion, keep seed and fertilizer on steeper slopes, reduce seedling mortality and preserve soil moisture. Seed, fertilizer and mulch can be applied using various methods. The basic unit costs of material per kilogram and the application cost (includes overhead, equipment, transportation, and labor costs) per hectare can be obtained from local economic data.

The model first estimates the area (A_{sfm} in hectare) to be seeded and mulched between two consecutive stations (Appendix 15). Then, the total amount of seeding

(Q_{seed}), fertilizing (Q_{fert}) and mulching (Q_{mul}) material used for a road stage is computed as follows:

$$\begin{aligned} Q_{seed} &= A_{sfm} q_{seed} \\ Q_{fert} &= A_{sfm} q_{fert} \\ Q_{mul} &= A_{sfm} q_{mul} \end{aligned} \quad 33.$$

where q_{seed} , q_{fert} , q_{mul} are the minimum amount of material used in kilograms per hectare for seeding, fertilizing, and mulching, respectively. The total cost of material (C_m) is estimated by multiplying the basic unit costs of seeding (u_{seed}), fertilizing (u_{fert}), and mulching (u_{mul}) material per kilogram by the total amount of materials used in area:

$$C_m = u_{seed}Q_{seed} + u_{fert}Q_{fert} + u_{mul}Q_{mul} \quad 34.$$

The cost of application (C_a) is computed based on the basic unit costs of application (u_{apl}) per hectare and the total area of seeding, fertilizing and mulching:

$$C_a = u_{apl}A_{sfm} \quad 35.$$

then, the formulation of the total cost, C_{sfm} , is developed as follows:

$$C_{sfm} = C_m + C_a \quad 36.$$

Maintenance Costs

It is important to know as much as possible about the future performance of roads so that adequate roads can be designed and built at minimum expense. The lack of a long-term prediction for road performance makes it difficult to estimate future maintenance expenditures (Christian and Newton, 1999). Road maintenance generally consists of replacing the aggregate to preserve structural integrity and travel quality,

performing blade maintenance activities, maintaining culverts, and cleaning ditches. Removing brush from both cut and fill slopes is also considered to maintain visibility. If forest roads are planned for use during spring thaw conditions, road designers should follow procedures of aggregate placement, compaction, and blade maintenance that will reduce the deformation of the road (Sigurdsson, 1993).

Rock replacement cost is often computed depending on the timber volume transported over the road stage. If the road stage is part of a horizontal curve, the loss of the surfacing material is greater than the loss on a straight road section due to increased traction requirements to oppose centrifugal forces. On forest roads, rock displacement occurs from truck traffic. The amount of rock replacement material is computed based on the rock displacement in depth, road width, and length of the road stage (Appendix 14). The future value of rock replacement cost (C_{fr}) is formulated as follows:

$$C_{fr} = C_s \frac{V_{timber}}{4500} \quad 37.$$

where C_s is the cost of surface replacement material, C_s (Appendix 14) and V_{timber} is the timber volume (cubic meters) transported over the road stage.

The blading cost is also computed depending on the timber volume transported over the road section and average volume of haul that requires at least one blade maintenance operation. The following equation is used to compute the future value of blading cost (C_{fb}):

$$C_{fb} = u_b L_r \frac{V_{timber}}{9000} \quad 38.$$

where u_b is the basic unit cost of blading per kilometer and L_r is the length of the road stage in kilometers.

The cost of maintaining ditches (Cf_d) and cleaning brush (Cf_{cb}) is calculated depending on their basic unit costs per kilometer and length of the road stage to be maintained. The cost of maintaining culverts (Cf_c) is computed by multiplying the basic unit cost of maintaining a culvert by the number of culverts installed along the roadway. The unit cost of these activities can be obtained from local economic data. The culvert and ditch maintenance, and brush cleaning takes place in time intervals, t_m .

Finally, the present value of future maintenance costs, M_0 , are computed using a terminating periodic series approach (Klemperer, 1996):

$$M_0 \approx (Cf_r + Cf_b) \left[\frac{1 - (1 + r)^{-n}}{(1 + r)^t - 1} \right] + (Cf_d + Cf_{cb} + Cf_c) \left[\frac{1 - (1 + r)^{-n}}{(1 + r)^{t_m} - 1} \right] \quad 39.$$

where r is annual interest rate, t is harvesting periods in years, and n is estimated total service time of the road in years or the time when last harvesting occurs.

Transportation Costs

Designing forest roads with the lowest construction and transportation costs is highly desirable. Transportation costs mainly vary with truck performance and the hourly cost of the truck with operator (machine rate). In the model, vehicle performance is calculated in terms of design speed, entering and exit speed, and acceleration and deceleration rates of truck traffic. The effect of gradient and curvature on truck travel time is considered for each road section. The machine rate is

divided into ownership, operating, and labor costs, assuming equipment and production elements are not rented (Sessions, 1992). The fuel and tire costs are computed separately and then added into the total transportation cost.

After determining the truck speed based on the vehicle performance, gradient, and curvature (Appendix 16), the total truck travel time (t_{trv} in hour) is computed as follows:

$$t_{trv} = L_r \left(\frac{V_L + V_{UL}}{V_L V_{UL}} \right) (1 + t_d) \quad 40.$$

where L_r is the length of the road stage in kilometers, V_L and V_{UL} are loaded and unloaded truck speeds in kilometers per hour, respectively, and t_d is the estimated delay time during the travel in percent.

The future cost of the transportation is computed using the following equation:

$$Tf = t_{trv} \left(\frac{V_{timber}}{Load} \right) MR + C_{fuel} + C_{tire} \quad 41.$$

where $Load$ is the average load capacity of the truck in cubic meters, V_{timber} is the timber volume transported over the road stage, and MR is the machine rate. The straight-line method is used to compute the machine rate (Appendix 17). The fuel cost (C_{fuel}) and tire cost (C_{tire}) are computed based on fuel consumption rate and tire wear rate, respectively (Appendix 17). The present value of the future transportation costs are computed using a terminating periodic series approach (Klemperer, 1996).

Sediment Production

The model estimates average annual volume of sediment delivered to a stream from the road segments, using the method of a GIS based road erosion/delivery model, SEDMODL (Boise Cascade Corporation, 1999). SEDMODL is a slightly modified version of the Washington Department of Natural Resources surface erosion module (WDNR, 1995). Road erosion factors considered are geologic erosion rate, road surface type, traffic density, road width and length, average road slope, average precipitation factor, distance between road and stream, cut slope cover density, and cut slope height (Appendix 18). For general use, the equations are developed based on the road erosion surveys in six watersheds in Washington, Oregon, and Idaho. SEDMODL reasonably predicts the sediment delivery at the time of developing the road design model (Boise Cascade Corporation, 1999). It provides the designer with the advantage of identifying the road segments with a high potential for delivering sediment to streams and it is easy to incorporate in computer programming. The limitations and the assumptions of the model are described in Appendix 18.

Vertical Alignment Optimization

In the final stage, the model generates new road alignment alternatives by randomly adjusting the vertical alignment to find the best path with the lowest total cost. A heuristic combinatorial optimization technique (Simulated Annealing) is used to guide the search for the best vertical alignment that minimizes the sum of construction, maintenance and transportation costs considering technically feasible grades within the specified elevation ranges of the intersection points of the vertical

alignment (Appendix 19). For each alternative vertical alignment, the model calculates cross sections, earthwork volumes, sediment delivery, and minimizes earthwork costs using linear programming, subject to geometric specifications and environmental requirements. The capacities of borrow and landfill areas are assumed to be adequate to satisfy borrow and waste requirements.

In order to reduce the cost of hauling excessive cut or fill quantities, the difference between total cut and total fill are monitored. If it is positive and is greater than a specified volume that can be hauled from cut sections to the landfill area, the model discards this alignment, lowers the maximum cut height to reduce the amount of excessive cut volume, and generates new alignment alternatives. If the difference is negative and its absolute value is greater than a specified volume that can be hauled from a borrow area to the fill sections, the model discards this alignment, lowers the maximum fill height to reduce the amount of excessive fill volume, and generates new alignment alternatives. When this last constraint is satisfied, the model records the current alignment.

To develop additional road alignments to connect the same beginning and ending points, the road designer traces out different feasible route paths. Then, for each selected route path, the model follows the same procedure to find the road alignment with minimum cost by using optimization techniques. Thus, the designer can rapidly develop and then choose among the alternative road locations in an efficient way. After developing the final vertical alignment, the designer determines

the appropriate location for a turnout, considering on visibility, side slope, and road grade (Appendix 20).

Model Application

The model was applied to two examples to illustrate the differences between surface rock specifications (Table 3.1). The study area is approximately 55 hectares of predominantly forested land on the southern edge of the Capitol State Forest in western Washington. The site is mountainous with elevation varying from 270-355 meters and ground slope from 0-50 percent. The forest stand is primarily 50-70 year-old second-growth conifers. The DEM data (1m intervals) of the study area was from a LIDAR (Light Detection and Ranging) data set collected (Aerotec, 1999) in western Washington. Soil, hydrology, and geology data were obtained from Washington Department of Natural Resources and added into the attribute data set.

Table 3.1. Road specifications for the surfacing material used in design examples.

Layers	Example A	Example B
Base Course	Good quality rock (7.5 cm)	Grade \leq 10%: Pit run Grade $>$ 10%: Good quality rock (7.5cm)
Traction Surface	Grade \leq 16%: Finer traction surface rock (2.5cm) Grade $>$ 16%: Traction surface rock (4cm)	Grade \leq 10%: No Traction Surface Grade $>$ 10%: Traction surface rock (4cm)

In Example A, a horizontal alignment was generated to connect two known end points of a road section. The vertical alignment with the minimum total cost was found by using optimization techniques. The road section had a length of approximately 300 meters (Figure 3.7). The vertical road alignment that minimized the total cost located a 27m long vertical curve and a horizontal curve with a radius of 45m. The road gradient varied from 4% to 11%. Two hundred and two feasible solutions were identified during the search process. The lowest value of the objective function was obtained at iteration 188 with the unit cost of \$46.04/m. Surfacing cost (including riprap and watering costs) was the largest cost component (\$22/m), followed by rock replacement (\$7.5/m), and earthwork (\$5.7/m) costs. The annual sediment delivered to a stream from the road section was 0.29 ton.

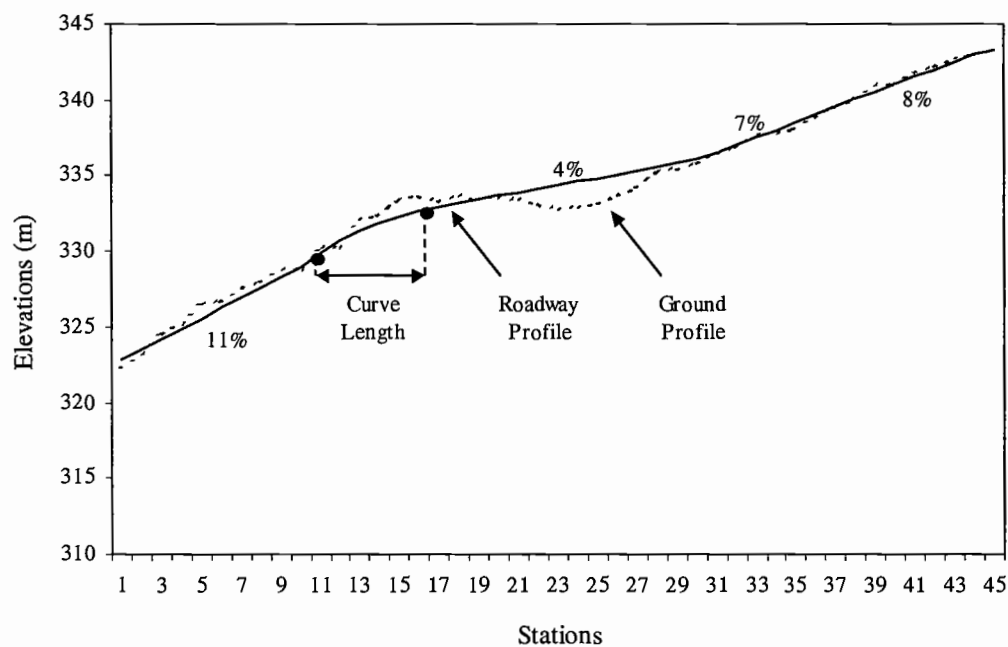


Figure 3.7. Profile view showing road gradient and vertical alignment in Example A.

In Example B, the same horizontal alignment from the first example was repeated with different specifications for surfacing material to investigate their effects on cost components, road gradient, and sediment production. The model located one horizontal curve with a radius of 45m (Figure 3.8). The road gradient varied from 4% to 9% along the roadway. Two hundred and twelve feasible solutions were evaluated during the search process and the lowest value of the objective function was obtained at iteration 199 with the cost of \$27.5/m. Reducing the road gradient increased the earthwork costs (\$7/m), while using pit run for surfacing decreased the surfacing (\$8.8/m) and rock replacement (\$1/m) costs. The average annual volume of sediment delivered to a stream from the road decreased (0.17 ton) due to reduced road gradient.

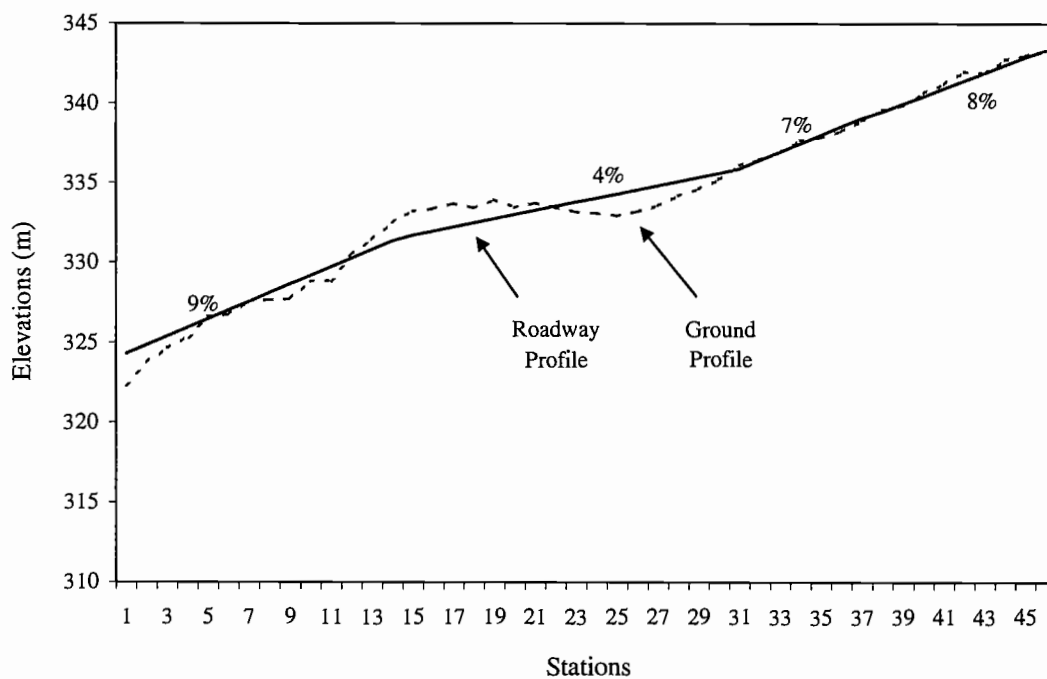


Figure 3.8. Profile view showing road gradient and vertical alignment in Example B.

In both examples, total construction cost (Example A: \$9107 and Example B: \$5754) was the largest cost component, followed by maintenance (Example A: \$2918 and Example B: \$1112) and transportation costs (Example A: \$941 and Example B: \$929). In construction cost elements, earthwork allocation and surfacing costs were the largest cost components. The best solution involved adjusting the vertical alignment to keep grading below 10 percent in Example B. By reducing the road gradient, the solution did not require a vertical curve since the absolute value of the difference between grades was not more than 5%. Besides, the road length in Example B was slightly longer than in Example A. These factors increased earthwork allocation, construction staking, clearing and grubbing, seeding and mulching, and blading costs, but decreased surfacing, rock replacement, transportation, maintaining culvert and ditches and removing brush, watering, drainage, and riprap costs.

The results indicated that the unit cost of sum of the construction, maintenance, and transportation costs in Example B was 40% percent less than in Example A. Sediment production was less in Example B. Even though the surfacing factors for good quality rock was less than that of pit run, the SEDMODL road slope factor assigned to road segments with more than 10% grade was 2.5 times greater than the road segments with less than or equal to 10% grade (Boise Cascade Corporation, 1999). Therefore, total annual sediment production in Example B was 41% less than the sediment production estimated in Example A.

Conclusions and Extensions

The 3D forest road alignment model, TRACER, aided by an interactive computer system, has been presented. The model provides the forest road designer with a decision support system for evaluating alternative horizontal alignments through finding efficient vertical alignments. Road feasibility is ensured by automatically considering geometric specifications, environmental impacts, and driver safety. The designer generates the initial road alignment by tracing the possible paths using computer cursor on 3D image of the terrain. Allowing the designer to quickly examine various feasible route paths, design time is reduced in the early stage of the forest road design.

The model generates alternative vertical alignments by randomly adjusting the elevation of the initial road alignment, considering technically feasible grades within the specified elevation ranges of the intersection points. A combinatorial optimization technique, Simulated Annealing (SA), is used to determine the best vertical alignment that minimizes the sum of construction, maintenance and transportation costs. The model employed SA since it is easy to implement and usually provides a good quality/near optimal solution to a combinatorial optimization problem.

For each alternative vertical alignment, the model calculates cross sections, earthwork volumes, and sediment delivery, and minimizes earthwork costs. User efficiency is enhanced through automated horizontal and vertical curve fitting routines, cross section generation, and cost routines for construction, maintenance, and vehicle use. To determine the economic distribution of cut and fill quantities, the

model uses the Linear Programming (LP) to avoid the limitation of the mass diagram on roadway sections with different soil characteristics. The global minimum cost of earthwork allocation can be reached using LP. Economic efficiency is enhanced by combining modern optimization techniques to minimize earthwork allocation cost using linear programming and to optimize vertical alignment using a heuristic technique (SA). To identify road segments with a high potential for delivering sediment to streams in a watershed, the model estimates average annual volume of sediment delivered to a stream from the road segments.

The two road examples illustrate the complexities involved with designing even a short section of road. Conventional wisdom suggests that reducing earthwork through rolling the grades to fit the terrain is often the best way to reduce environmental effects. In the examples shown, the slightly longer road alignment using flatter grades and more earthwork yielded a lower total sediment load. The results from the two short examples should not be generalized. But, the examples are instructive in showing the tradeoffs that can occur.

The model has several limitations and opportunities for further development. It is assumed that the unit costs of earthwork are constant. When there is a case where the unit costs vary with the quantity of the cut and fill, the model can be enhanced using available methods that consider such a case (Easa 1988b. and Christian et al. 1988). The cross sections used to set the road on the ground profile are cut and fill, through cut, and through fill sections. The current state of the model does not allow the designer to generate a full bench type cross section since the horizontal alignment

is fixed once the station points are located along the roadway. One model improvement to be considered is to optimize horizontal alignment automatically allowing the use of a full bench type cross section. The model considers total costs of construction, maintenance, and transportation. Additional costs that can be expressed quantitatively can be included in the model.

Most of the computation time in the process is spent on earthwork allocation using linear programming. However, since many of the vertical alignment alternatives are eliminated due to one or more constraints, the model only evaluates the earthwork for feasible routes.

The model depends upon available GIS coverages of attribute data to represent ground conditions. Available GIS data in forested areas do not represent the actual ground condition with high accuracy; however, quality of GIS data is improving as GIS technologies advance. LIDAR (Light Detection and Ranging), one of the fastest growing systems in the field, can provide a high-resolution and accurate DEM. It is expected to provide even better accuracy in the near future, as the laser beam width is reduced, which is the key receiving reflections from the forest floor.

The model is not intended to compute the total water discharge along the roadway; therefore, it is not providing the designer with the most appropriate culvert locations or culvert size. Future work could also provide refinements to the graphic interface, optimization of the horizontal alignment, and additional options for cut and waste areas within the road prism including more flexibility in the location of turnouts.

Literature Cited

- AASHTO, 1990. American association of safe highway and transportation officials. A policy on geometric design of highway s and streets, Washington, D.C.
- Aerotec, 1999. Airborne laser-scan and digital imagery. 560 Mitchell Field Road, Bessemer, AL 35022
- Ahamed, K.M., S.E. Reutebuch, and T.A. Curtis. 2000. Accuracy of high-resolution airborne laser data with varying forest vegetation cover. In Proceedings of the 2nd International Conference on Earth Observation and Environmental Information.11-14, Cairo, Egypt.
- Antoniotti P. 1969. APPOLLON: A new road design optimization procedure. PTRC symposium on cost models and optimization in road location. Design and Construction, London. 236-241.
- Boise Cascade Corporation, 1999. SEDMODL-Boise Cascade road erosion delivery model. Technical documentation. 19 p.
- Bowman, E.H. and R.B. Fetter. 1967. Analysis for production and operations management. Irwin Series in Quantitative Analysis for Business. Yale University. 870 p.
- Burroughs, Edward R. Jr. and John G. King. 1989. Reduction of soil erosion on forest roads. Gen. Tech. Rep. INT-264. Ogden, UT: US Department of Agriculture, Forest Service, Intermountain Research Station. 21 p.
- Chew, E.P., Goh, C.J., and Fwa, T.F. 1989. Simultaneous optimization of horizontal and vertical alignment for highways. Transportation Research. 23B(5):315-329.
- Christian J. and H. Caldera. 1988. Earthmoving cost optimization by operational research. Canadian Journal of Civil Engineering. 51:679-684.
- Christian J. and L. Newton. 1999. Highway construction and maintenance costs. Canadian Journal of Civil Engineering. 26:445-452.
- Easa, S.M. 1987. Earthwork allocations with linear unit costs. Journal of Construction Engineering and Management. 114(4):641-655.
- Easa, S.M. 1988a. Selection of roadway grades that minimize earthwork cost using linear programming. Transportation Research. 22A(2):121-136.

- Easa, S.M. 1988b. Earthwork allocations with non-constant unit costs. *ASCE Journal of Construction Engineering and Management*, 113(1):34-50.
- Goh, C.J., Chew, E.P., and Fwa, T.F. 1988. Discrete and continuous models for computation of optimal vertical highway alignment. *Transportation Research*. 22B(6):399-409.
- Howard, B.E., Bramnick, Z., and Shaw, J.F.B. 1968. Optimum curvature principle in highway routing. *Proc. Am. Soc. Civil Engrs.* (94):61-82.
- Klemperer, D. 1996. *Forest Resource economics and finance*. Virginia Polytechnic Institute and State University, College of Forest and Wildlife Resources, Virginia. 551 p.
- Kramer, B.W. 2001. *Forest road contracting, construction, and maintenance for small forest woodland owners*. Oregon State University, College of Forestry, Forest Research Laboratory, Research Contribution 35. 79 p.
- Lumberjack, 1995. *A Road Design System, Version 5*. Cheney, WA, 99004. 72 p.
- Mannering F. and W.Kilareski. 1990. *Principles of highway engineering and traffic analysis*. John Wiley and Sons, New York, New York. 251 p.
- Mayer, R. and Stark, R. 1981. Earthmoving logistics. *Journal of Const. Div.* 107(CO2):297-312.
- Nandgaonkar, S. 1981. Earthwork transportation allocations: operation research. *Journal of Const. Div.* 107(CO2):373-392.
- NewCyber3D, 2002. *GIS Solution Systems*. 11 Tennessee St., Redlands, CA 92373.
- Nicholson, A.J. 1974. *A variational approach to optimal route location*. Civil Engineering Report 74-7, University of Canterbury, N.Z.
- O'Brien, W.T. and Bennett, D.W. 1969. A dynamic programming approach to optimal route location. *Proc symposium on cost models and optimization in road location. Design and Construction*. pp.175-199.
- Parker, N.A. 1977. Rural highway route corridor selection. *Transportation Planning Techniques*. (3):247-256.
- Pearce, J.K. 1974. *A Guide for logging planning forest road engineering*, Forest Engineering Handbook. Bureau of Land Management, Oregon State Office, US Department of The Interior. Divisions 100-800. 219 p.

- RoadEng, 2002. Forest road design using Softree 98, Forestry Edition. Technical Training Manual, Logging Engineering International, Inc., Eugene, Oregon, 97402. 124 p.
- Sigurdsson, O. 1993. Effects of variable tire pressure on road surfacing. Volume II: Analysis of test results. US Army Corps of Engineers, Waterways Experiment Station. Prepared for the USDA Forest Service. Technical Report GL-93-20. 84p.
- Skaugset, Arne, and Marganne M. Allen. 1998. Forest road sediment and drainage monitoring project report for private and state lands in Western Oregon. Oregon Department of Forestry, Salem, Oregon, 97310. 20 pp.
- Trietsch, D. 1987. A family of methods for preliminary highway alignment. *Transportation Science*. (21):17-25.
- Trypia, M. 1979. Minimizing cut and fill costs in road making. *Computer-Aided Design*. (11):337-339.
- USDA Forest Service, 1987. Forest service handbook No. 7700.56 - Road Preconstruction handbook.
- USDA Forest Service, 1999. Cost estimate guide for road construction Region 6. Cost Guide Zone 5, Davis-Bacon Area 5, Oregon.
- WDNR, 1995. Standard methodology for conducting watershed analysis, Version 3.0. Washington Forest Practices Board.

Chapter 4

Applying The Decision Support System, TRACER, to Forest Road Design

Abdullah E. Akay
John Sessions

Department of Forest Engineering
Oregon State University
Corvallis, OR 97331

Abstract

A 3D forest road alignment optimization model, TRACER Version 1.0, was developed to assist a forest road designer to design a route with the lowest total cost considering construction and future maintenance and transportation costs, while conforming to design specifications and environmental requirements, and providing driver safety. The model enhanced user efficiency through automated horizontal and vertical curve fitting routines, cross section generation, and cost routines for construction, maintenance, and vehicle use. Linear programming for earthwork allocation and a heuristic approach (Simulated Annealing) for selection of vertical alignment were integrated to minimize the total cost. The average sediment, delivered to a stream from the road section, is also estimated using the method of a GIS-based road erosion delivery model. This paper describes the features of TRACER and presents an application of the model to a road location problem.

Introduction

The design of a forest road between two given locations on a surface is a complex engineering problem involving economic considerations and environmental requirements. The objective is to determine a route with the lowest sum of construction, future maintenance, and future transportation costs while protecting soil and water resources, and providing driver safety. The sediment delivered to streams from a road section can adversely impact water quality and aquatic life. Thus, forest roads must be carefully designed to minimize construction and maintenance costs, and minimize environmental damage.

Several different optimization techniques have been considered for use in the field of highway design (Parker 1977, Trypia 1979, Mayer et al. 1981, Easa 1987, Easa 1988, Goh et al. 1988, and Chew et al. 1989). However, the systems currently available for forest road design are not intended to make computer-aided design judgments such as automated generation of alternative grade lines, best fitting vertical alignment for optimizing earthwork, minimizing the total cost of construction, maintenance, and transportation, and aiming for least environmental impact. They are generally used as a tool to make the mathematical calculations required to do basic manual road design. The mass diagram is used to balance the required quantities of cut and fill. After entering the survey data and design parameters, some forest road programs manipulate geometric road design and earthwork balance calculations by allowing the designer to work in plan, profile or cross section view, using a visual display screen (RoadEng, 2002 and Lumberjack, 1995). However, the designer has to

make these manipulations in a trial-and-error way to assure that the constraints of horizontal and vertical alignments are satisfied, which can be very time consuming.

A three-dimensional forest road alignment optimization model, TRACER Version 1.0, was developed as a decision support system for forest road design. It automates many of the current mundane, time consuming tasks, while implementing a decision support framework. The TRACER program, aided by an interactive computer system, helps a designer with a rapid evaluation of alternatives to design a path between two identified locations. The objective is to minimize the total cost of construction, and future maintenance and transportation costs, while conforming to design specifications, environmental requirements, and driver safety. Initial trial routes are generated by “tracing” the possible paths using computer cursor on a 3D image of the terrain. The trial route is then evaluated with respect to a wide range of geometric specifications and environmental requirements. User efficiency is enhanced through automated horizontal and vertical curve fitting routines, cross-section generation, and cost routines for construction, maintenance, and vehicle use.

To determine the economic distribution of cut and fill quantities, the model uses linear programming (LP) to overcome the limitation of the mass diagram on roadway sections with different soil characteristics. The model adjusts the vertical alignment using a heuristic combinatorial optimization technique (Simulated Annealing) and selects the path with lowest total cost. The average sediment, delivered to a stream from the road section, is also estimated using the method of a GIS-based road erosion delivery model. This paper describes the features of the

TRACER program and presents an application of the model to an actual road location problem. The theory of the model is not presented here but can be found in Akay and Sessions (2003).

Program Features

The model reads input data files including digital elevation model (DEM) and attribute data. The model relies on a DEM to provide terrain data for ground slope, topographic aspect, and other landform characteristics. The DEM data file is a set of scattered metric data points (X, Y, Z), which represent the ground surface. The attribute data file includes soil type and stream data, represented in the same format as the metric data points.

After the input data files are read, the designer enters the road design, economic, and local site data, geometric specifications, and environmental requirements. The road design data include road standard, road surface type, road template specifications, turnout dimensions, distance between road sections, design speed, vehicle specifications, and traffic volume. Local site data include swell and shrinkage factors for each soil type, ground cover type, geological data, vegetation (timber stand) data, and distance to local resources of road construction materials. Economic data consist of the unit costs of road construction and maintenance activities and machine costs of transport vehicles.

The geometric specifications are maximum allowable road grade, minimum radius of horizontal curves, minimum length of vertical curves, minimum distance between curves, and minimum safe stopping distance for driver safety. It is also

assumed that the designer does not want overlapping horizontal and vertical curves. The environmental requirements include minimum allowable road grade and rolling road grades to provide proper drainage, minimum distance from the riparian zones to protect the stream channels, minimum stream-crossing angle to reduce the damage on the riparian zones, and maximum height of cuts and fills at any section to decrease potential soil movement.

The model has the capability to display and render high-resolution 3D images of the terrain in real-time (NewCyber3D, 2002). Displaying the image of the terrain on the computer screen, the designer first opens the Road Geometry Window and locates the beginning and ending points of the road section. This window displays road geometry information and attribute data in real time, helping the designer to locate control points satisfying the constraints. Road geometry information include X and Y coordinates, elevation, road grade, horizontal and vertical deflection between two consecutive road segments, length of the current segment, and cumulative segment length. Miscellaneous attribute data include soil type and stream data. The stream data are used to identify the distance to the closest stream in real-time. Then, the designer selects a feasible trial route by establishing a series of control points on the 3D image of the terrain, subject to design constraints (Figure 4.1).

The curves connecting the control points are not used to represent the final location of the route path, but are for visualization purposes only. If the designer chooses a candidate point which is not acceptable by one or more constraints, the model warns the designer by changing the color of the line between the previously

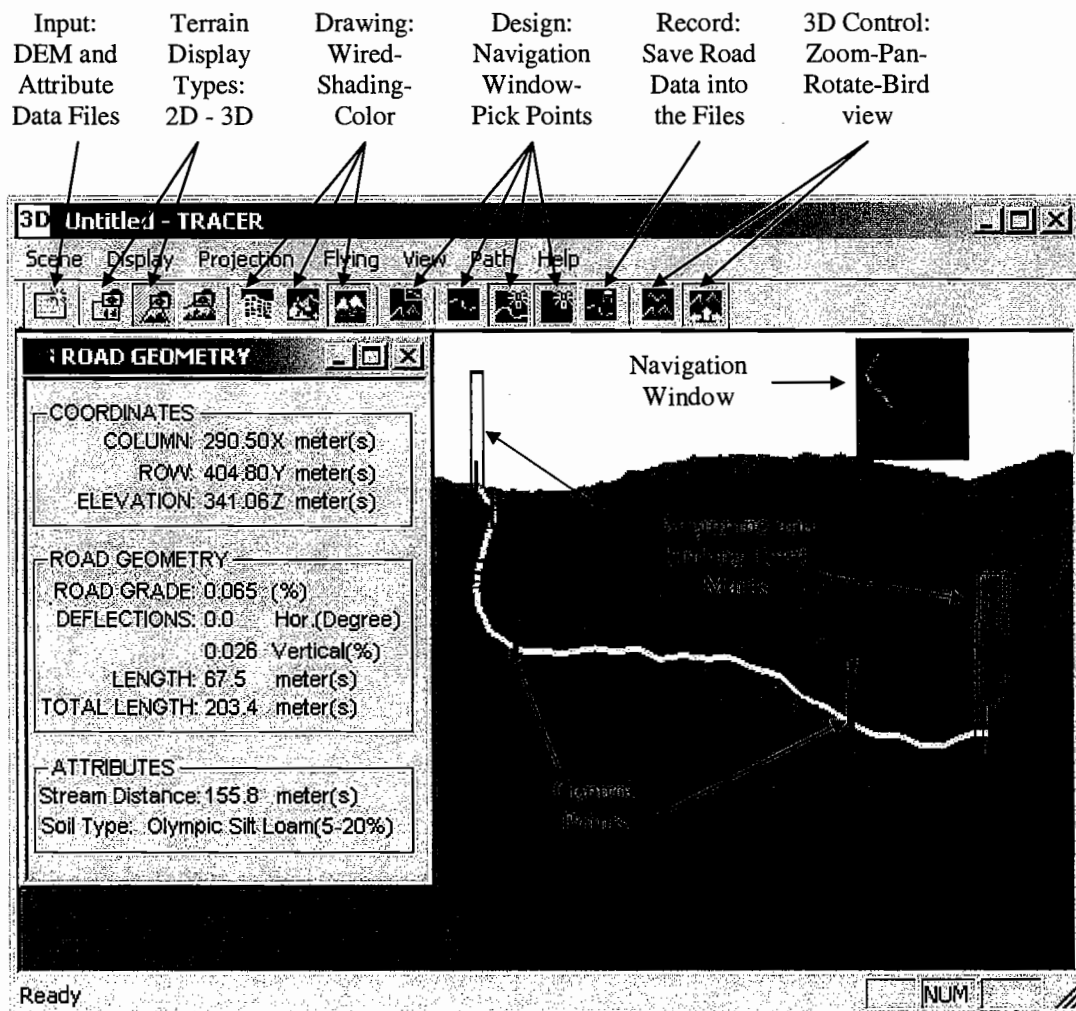


Figure 4.1. Locating a feasible trial route between two given points.

selected control point and the candidate point. Thus, the designer does not select this candidate point and searches for other points. The designer can zoom, pan, rotate, and scale the area in order to search for candidate control points around the terrain.

The model automatically locates the horizontal and vertical curves and calculates the station points between the control points, satisfying the constraints. If

cut-fill height and all the other constraints are satisfied, the model computes the cross-section areas and average end areas to compute earthwork volume for each road stage between two consecutive stations.

The economic distribution of cut and fill quantities is determined using linear programming, considering possible borrow and landfill locations and various soil characteristics along the roadway. The model uses the method of Mayer and Stark (1981) to overcome the limitation of the mass diagram on roadway sections with different soil characteristics. Linear programming provides the optimal solution to the earthwork allocation problem. Then, the model computes the total cost of the road section including construction, future maintenance and future transportation costs. In order to compare the total costs for different routes, the present value of the future maintenance and transportation costs are computed.

The road construction cost is the total cost of the road construction activities: construction staking, clearing and grubbing, earthwork allocation, drainage and riprap, surfacing, water supply and watering, and seeding and mulching. The maintenance activities involve rock replacement, grading, culvert and ditch maintenance, and brush cleaning. Design speed, entering and exit speed, acceleration and deceleration rates of truck traffic, and machine rate are analyzed as the effective factors of the forest transportation costs. Additional costs (accident costs, land costs, ecological penalties etc.) can be included into the model if they can be expressed quantitatively.

The model estimates average annual volume of sediment delivered to a stream from the road segments, using the method of a GIS based road erosion/delivery model, SEDMODL (Boise Cascade Corporation, 1999). Road erosion factors considered in this model are geologic erosion rate, road surface type, traffic density, road width and length, average road slope, average precipitation factor, distance between road and stream, cut slope cover density, and cut slope height. SEDMODL is one of the models that reasonably predict the sediment delivery from a road section and it is easy to implement in a computer program (Boise Cascade Corporation, 1999).

To find the path with the lowest total cost, the model generates alternative road paths by adjusting the vertical alignment. A heuristic combinatorial optimization technique (Simulated Annealing) is used to select the best vertical alignment that minimizes the sum of construction, maintenance and transportation costs considering technically feasible grades within the specified elevation ranges of the intersection points of the vertical alignment (Figure 4.2). For each alternative vertical alignment, the model computes cross-sections, earthwork volumes, sediment delivery, and minimizes earthwork costs using linear programming.

In order to reduce the cost of hauling excessive cut or fill quantities, the difference between total cut and total fill are monitored. If it is positive and greater than a specified volume that can be hauled from cut sections to the landfill area, the model discards this alignment, lowers the maximum cut height, and generates new alignment alternatives. If the difference is negative and its absolute value is greater

than a specified volume that can be hauled from a borrow area to the fill sections, the model discards this alignment, lowers the maximum fill height, and generates new alignment alternatives. To find the best road alignment, the designer can quickly generate many paths. After developing the final vertical alignment, the designer determines the appropriate location for a turnout, considering visibility, side slope, and road grade.

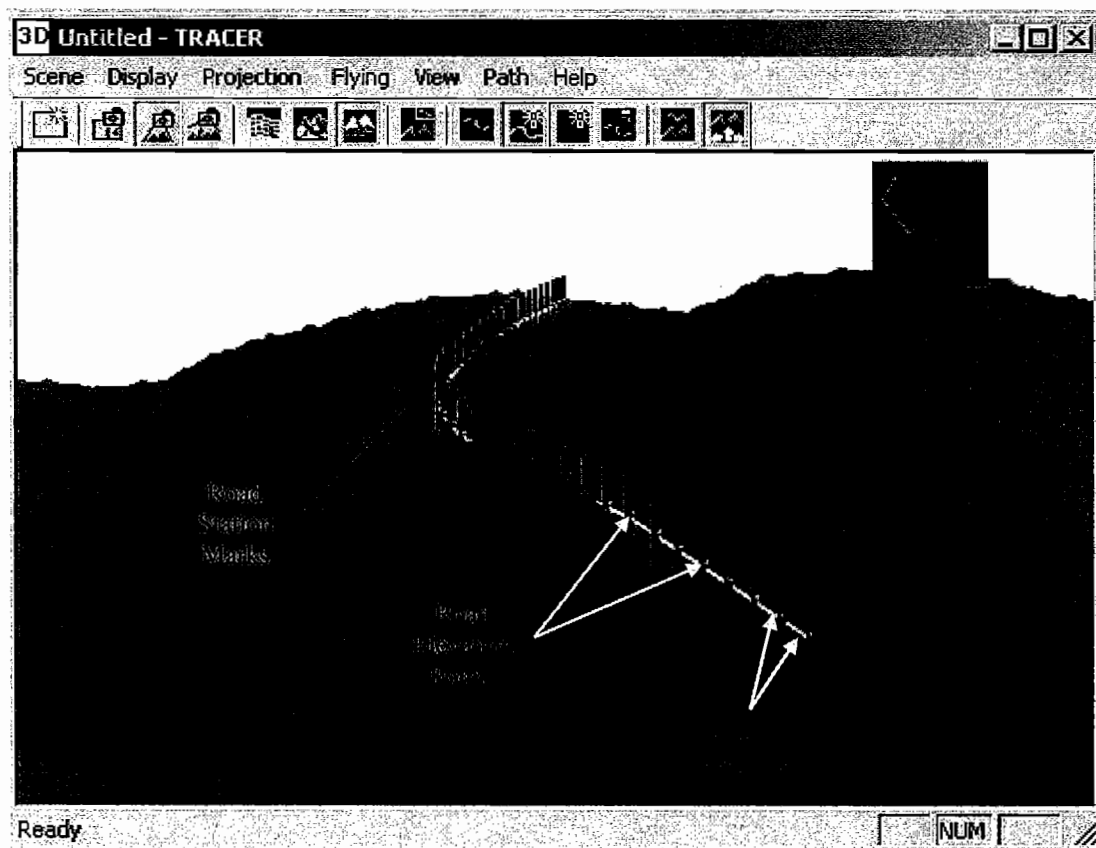


Figure 4.2. Optimized vertical alignment.

Model Application

The model has been applied to design a single lane forest road with ditches. The objective is to design a road alignment with the lowest total cost considering construction and future maintenance and transportation costs, while conforming to design specifications and environmental requirements. The study area is approximately 55 hectares of predominantly forested land on the southern edge of the Capitol State Forest in western Washington. The site is mountainous with elevation varying from 270-355 meters and ground slope from 0-50 percent. The forest stand is primarily 50-70 year-old second-growth conifers.

Data Preparation

The DEM data of the study area was from a LIDAR (Light Detection and Ranging) data set collected (Aerotec, 1999) in western Washington. The random points of LIDAR data were converted to a DEM data set by first filtering out all the points from the ground points and then creating a triangulated irregular network (TIN) from which the software (TerraScan, 1998) evaluates elevations at 1.0 meter intervals. The elevation data are then used to represent the surface (Figure 4.3). Airborne LIDAR is designed to measure variations in surface features and 3D coordinates (X, Y, and elevation) of a passive target by using pulsed light. The LIDAR system can separate and record different reflections from the ground. The first pulse gives information on the top object while last pulse gives information on

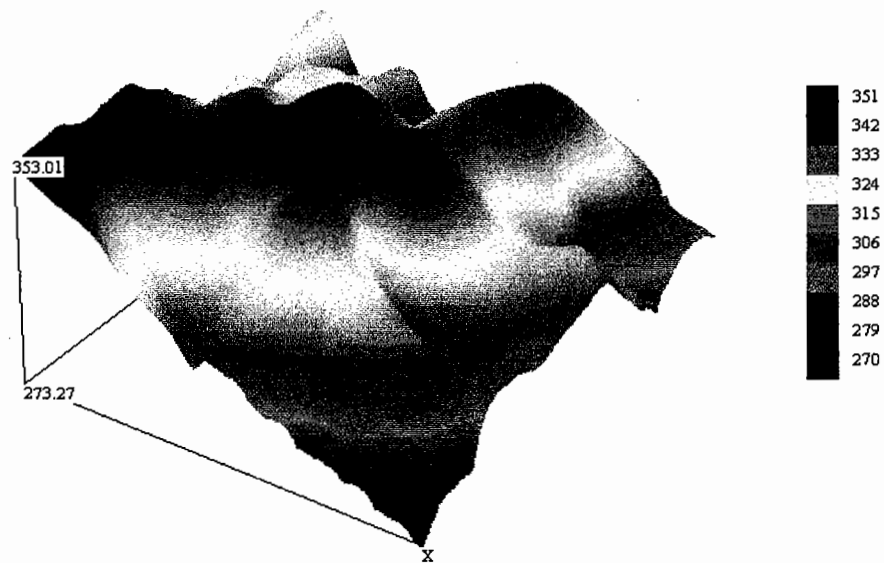


Figure 4.3. 3D image of the terrain.

the lowest object. The accuracy of each point on the ground is approximately 15 cm in the vertical and 1.0 meter in the horizontal (Ahmed et al. 2000). Soil and hydrology data were obtained from Washington Department of Natural Resources and added into the attribute data set. Information for the soil layers was derived from the Private Forest Land Grading system (PFLG, 1980) and subsequent soil surveys. PFLG was a five-year mapping procedure completed in 1980 for the purpose of forestland taxation. In order to register the soil type data onto the original data set in metric data format, the original soil coverage data was rasterized using GIS tools (ERDAS Imagine 1997 and ArcInfo 1998).

According to the soil survey map compiled by the U.S. Department of Agriculture, Soil Conservation Service, and cooperating agencies (USDA, 1990), there are four different soil types: (1) Olympic silt loam (5 to 20 percent slopes), (2) Olympic silt loam (20 to 40 percent slopes), (3) Raught silt loam (30 to 65 percent slopes), and (4) Eld loam. The hydrology layer of the study area, obtained from WDNR, was compiled and processed by the GIS, Cartography and Photogrammetry unit from 1992 through 1996 (WDNR, 1996). For sediment delivery predictions, a digital geology map of Washington State was obtained from the Washington Department of Natural Resources (Harris, 1998).

Road Design Specifications

The model was applied to two examples to illustrate the differences between surface rock specifications. In Example A, a horizontal alignment is generated to connect two known end points of a road section. Then, the vertical alignment with the minimum total cost is found by using optimization techniques. In Example B, the same horizontal alignment from the first example is repeated with different specifications for surfacing material to investigate their effects on cost components, road gradient, and sediment production. The specifications of the surfacing material used in the model is illustrated in Table 4.1.

The road specifications common to both examples include road width, side slopes, distance between road stations, elevations of beginning and ending point of the road section, minimum horizontal curve radius, minimum length of vertical curve, minimum value of the difference between grades for vertical curve requirement,

Table 4.1. Specifications for surfacing material used in the model application.

Layers	Example A	Example B
Base Course	Good quality rock (7.5 cm)	Grade \leq 10%: Pit run Grade $>$ 10%: Good quality rock (7.5cm)
Traction Surface	Grade \leq 16%: Finer traction surface rock (2.5cm) Grade $>$ 16%: Traction surface rock (4cm)	Grade \leq 10%: No Traction Surface Grade $>$ 10%: Traction surface rock (4cm)

minimum distance between curves, minimum and maximum road grades, minimum distance between fill slope and stream channel, maximum cut and fill height, and design speed (Table 4.2). The cost elements of road construction and maintenance are determined based on the "Cost Estimate Guide For Road Construction Region 6" prepared by the USDA Forest Service (1999). Wage rates are adjusted based on the wage ratio and labor range tables in this cost guide.

Construction staking cost is computed based on the unit cost (\$778/km) and total road length in kilometers. The clearing and grubbing cost is estimated by multiplying its unit cost (\$3700/ha) by adjustment factors and clearing area in hectares. Excavation, haul, embankment (placement and compaction) and disposal costs are \$1.61/m³, \$1.3/m³-km, \$0.58/m³, and \$0.1/m³, respectively. For borrow material, these costs are \$1.81/m³, \$1.3/m³-km, \$0.58/m³, and \$0.1/m³, respectively.

Table 4.2. Road design specifications for elements other than road surfacing.

Elements	Value
Width of road	4 m
Side Slopes in common material	Cut slope: 1:1 Fill slope: 1.5:1
Average length of each road stage	6 m
Elevation at the beginning point	322.31 m
Elevation at the ending point	343.33 m
Minimum curve radius	18 m
Minimum length of a vertical curve	15 m
Minimum value of differences between grades	5%
Minimum distance between curves	10 m
Minimum road grade	$\pm 2\%$
Maximum uphill road grade	16%
Maximum downhill road grade	-12%
Minimum distance between fill slope and a stream	10 m
Maximum cut and fill height at centerline	2 m
Design speed	55 km/hr

The earthwork allocation is determined considering a borrow and a landfill area located at the beginning of the road section. It is assumed that the capacities of borrow and landfill areas are more than sufficient to satisfy any cut or fill requirements. The estimated swell factor in haul and shrinkage factor in embankment for the soil along the roadway are 1.4 and 0.75, respectively. For borrow material, these factors are 1.2 and 0.9, respectively.

The earthwork volume is estimated using the average end-area method (Hickerson, 1964). This method is generally used in the field of forest road design due to its simplicity. The average end-area method tends to overestimate the volume (Hickerson, 1964). The length of the road stage between two consecutive cross sections is kept adequately short to compute the earthwork volume more accurately, particularly in rough and mountainous terrain where the type of the cross-sections change rapidly along the roadway. The model locates the cross-sections at more frequent intervals (about 6 meters) to reduce this error.

The surfacing cost is estimated considering the type and required quantity of the surfacing material and haul distance (10km). In the model, the rock size and the depth of the aggregate surfacing (base course is 25cm and traction surface is 7-10 cm) are determined based on the type of the subgrade soil along the roadway (Pearce, 1974). The quantity of surfacing material is computed using the length and width of the road section, and surfacing depth. The unit cost (including purchasing, hauling, processing, and testing costs) for various rock types is estimated as: pit run is \$3.92/m³, good quality base course rock (7.5cm) is \$7.85/m³, traction surface rock

(4cm) is \$11.77/m³, and finer traction surface rock (2.5cm) is \$15.69/m³. The riprap cost is computed by multiplying the unit cost of riprap (\$10/m³) by the required volume (m³) of rock used in riprap material.

Drainage cost is estimated by multiplying the estimated unit cost (material, installation, elongation, treatment, and special item costs) per lineal meter of the culvert (\$25/lm) by the total culvert length used in the road section. The number of required culverts is estimated using the guidelines of maximum culvert spacing by soil erosion classes and average road grade (Pearce, 1974). Watering cost (including purchasing and hauling) is computed based on the estimated unit cost of water (\$3/kilo liter), the amount of water required for excavation (26 liter/m³) and surfacing operations (114 liter/m³), and haul distance (30km). The minimum amount of material used for seeding, fertilizing, and mulching are 30kg/ha, 150kg/ha, and 3000kr/ha, respectively. The total cost is estimated by multiplying the basic unit costs of seeding (\$.33/kg), fertilizing (\$0.08/kg), and mulching (\$0.08/kg) by the amount of materials used per hectare, the total project area (hectare), and the application cost (\$550/ha).

Rock replacement is often computed depending on the timber volume transported over the road (i.e. 2.5cm rock displacement for every 4500m³ timber haul), road width, and length of the road stage. If the road stage is part of a horizontal curve, the loss of the surfacing material is greater than the loss on a straight road section due to increased traction requirements to provide cornering forces. The blading cost is also computed depending on the average volume of haul (9000m³) that

requires at least one blade maintenance operation, the unit cost of blading (\$.3/m), and the road length. The cost of maintaining culverts is computed by multiplying the basic unit cost of maintaining a culvert (\$15 per culvert) by the number of culverts installed along the roadway. The cost of maintaining ditches and cleaning brush is calculated depending on their basic unit costs, \$.2/m and \$25/m, respectively, and length of the road stage to be maintained.

Vehicle performance is calculated in terms of travel speed, and average acceleration and deceleration rates of a stinger type logging truck traffic. The effect of gradient and curvature on truck travel time is considered for each road section. The machine rate is divided into ownership, operating, and labor costs, assuming equipment and production elements are not rented (Sessions, 1992). The fuel and tire costs are computed separately and then added into the total transportation cost. In order to compare the total costs for various routes, the present value of the future maintenance and transportation costs are computed using a terminating periodic series approach. It is assumed that approximately 2500 m³ of timber is hauled every five years for 30 years.

The model estimates average annual volume of sediment delivered to a stream from the road segments, using the method of a GIS based road erosion/delivery model, SEDMODL (Boise Cascade Corporation, 1999). Road erosion factors considered are geologic erosion rate, road surface type, traffic density, road width and length, average road slope, average precipitation factor, distance between road and stream, cut slope cover density, and cut slope height. The model investigates how

sediment production responds to different surfacing materials and various road gradients.

Example A

The road section has a length of approximately 300 meters with 44 stages. The vertical road alignment that minimized the total cost located a 27m long vertical curve and a horizontal curve with a radius of 45m (Figure 4.4). The road gradient varied from 4% to 11%. Good quality base course rock (7.5cm) was used to build up the base course. On grades less than 16%, traction surface rock (4cm) was used to build up the traction surface to a 8 cm depth. If the grade was greater than or equal to

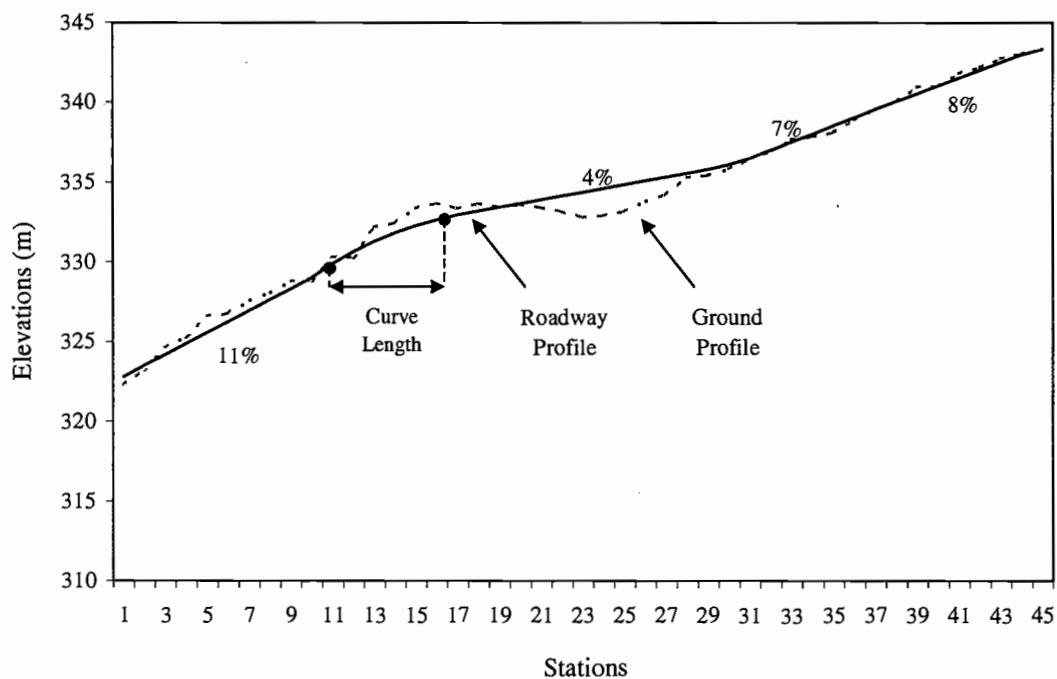


Figure 4.4. Example A: Profile view showing road gradient and vertical alignment.

16%, finer traction surface rock (2.5cm) was used to build up the traction surface to a 10 cm depth. Two hundred and two feasible solutions were identified during the search process of the optimization technique (Figure 4.5). The lowest value of the objective function was obtained at iteration 188 with the cost of \$46.04/m. Surfacing cost (including riprap and watering costs) was the largest cost component (\$22/m), followed by rock replacement (\$7.5/m) and earthwork (\$5.7/m) costs (Figure 4.6). The average annual volume of sediment delivered to a stream from the road section was estimated as 0.29 ton.

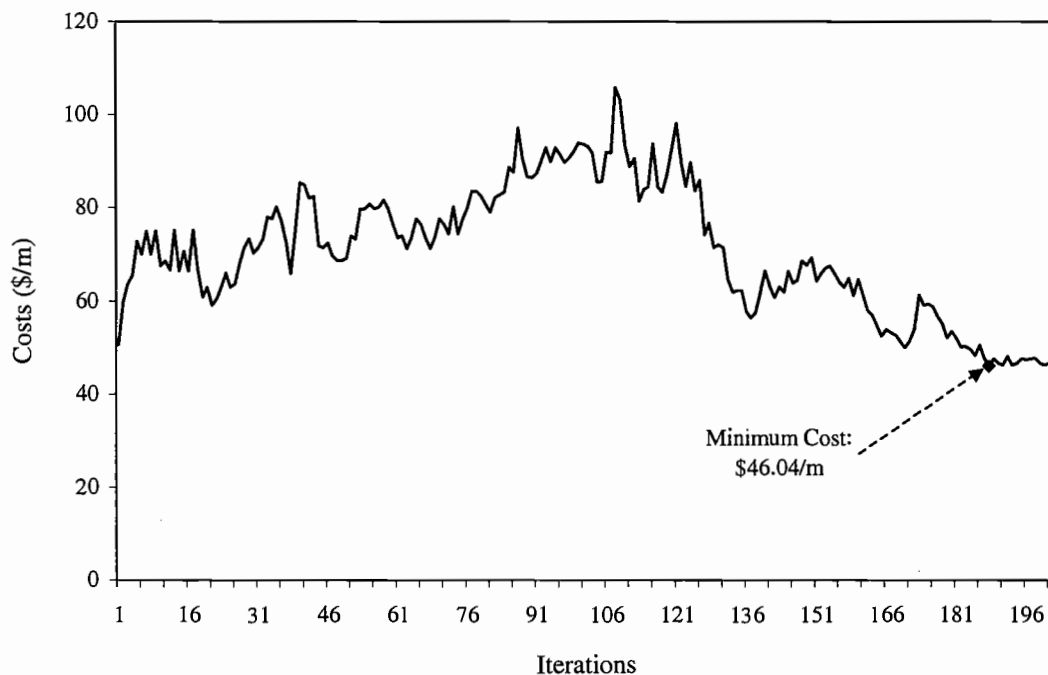
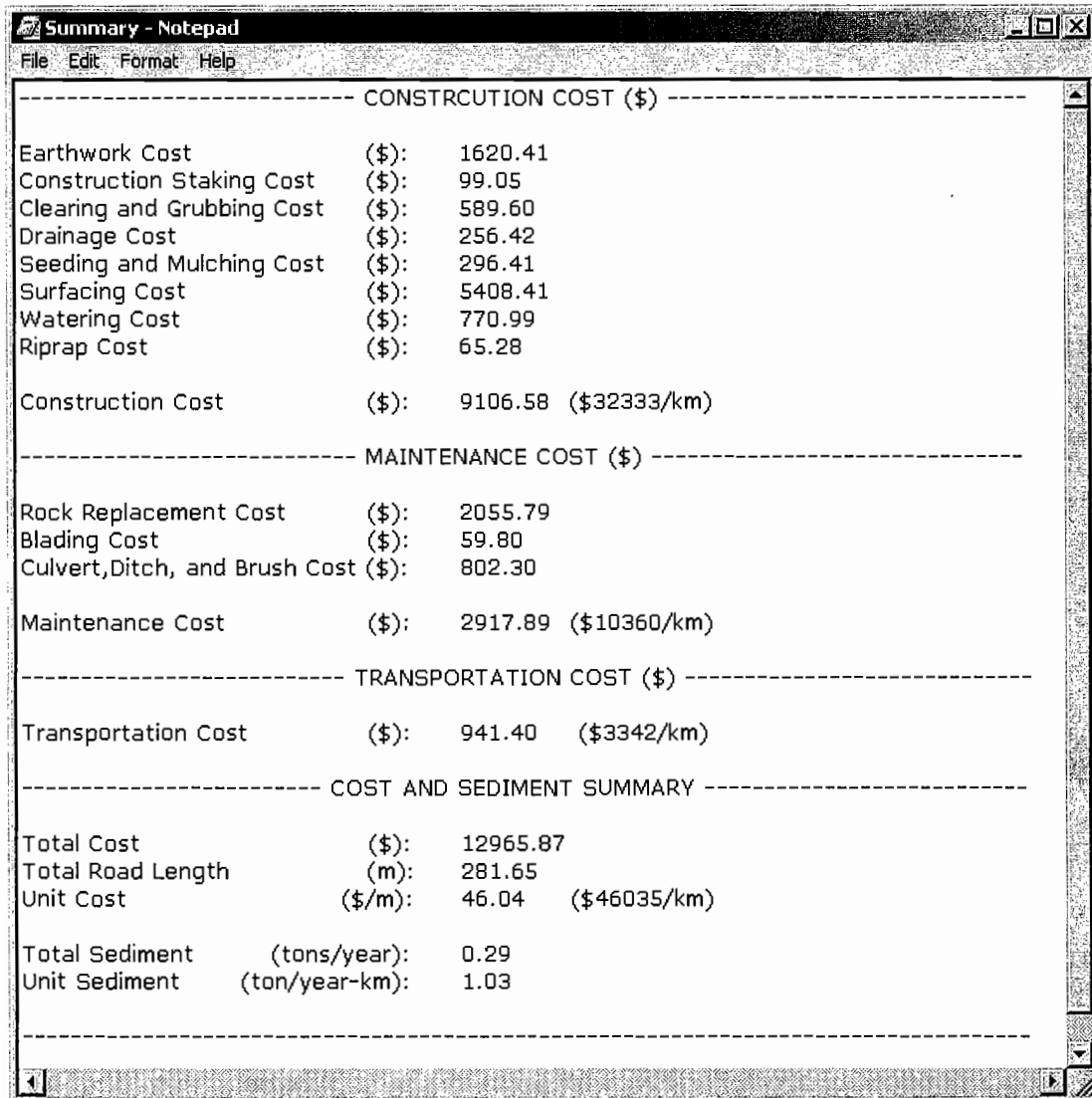


Figure 4.5. Example A: Feasible solutions during the search to identify the best vertical alignment.



----- CONSTRUCTION COST (\$) -----			
Earthwork Cost	(\$):	1620.41	
Construction Staking Cost	(\$):	99.05	
Clearing and Grubbing Cost	(\$):	589.60	
Drainage Cost	(\$):	256.42	
Seeding and Mulching Cost	(\$):	296.41	
Surfacing Cost	(\$):	5408.41	
Watering Cost	(\$):	770.99	
Riprap Cost	(\$):	65.28	
Construction Cost	(\$):	9106.58	(\$32333/km)
----- MAINTENANCE COST (\$) -----			
Rock Replacement Cost	(\$):	2055.79	
Blading Cost	(\$):	59.80	
Culvert, Ditch, and Brush Cost	(\$):	802.30	
Maintenance Cost	(\$):	2917.89	(\$10360/km)
----- TRANSPORTATION COST (\$) -----			
Transportation Cost	(\$):	941.40	(\$3342/km)
----- COST AND SEDIMENT SUMMARY -----			
Total Cost	(\$):	12965.87	
Total Road Length	(m):	281.65	
Unit Cost	(\$/m):	46.04	(\$46035/km)
Total Sediment	(tons/year):	0.29	
Unit Sediment	(ton/year-km):	1.03	

Figure 4.6. Example A: The summary table indicating cost components and sediment.

Example B

The same horizontal alignment from Example A was repeated with different specifications for surfacing material. The best vertical alignment that minimized the total costs of construction, maintenance, and transportation was shown in Figure 4.7.

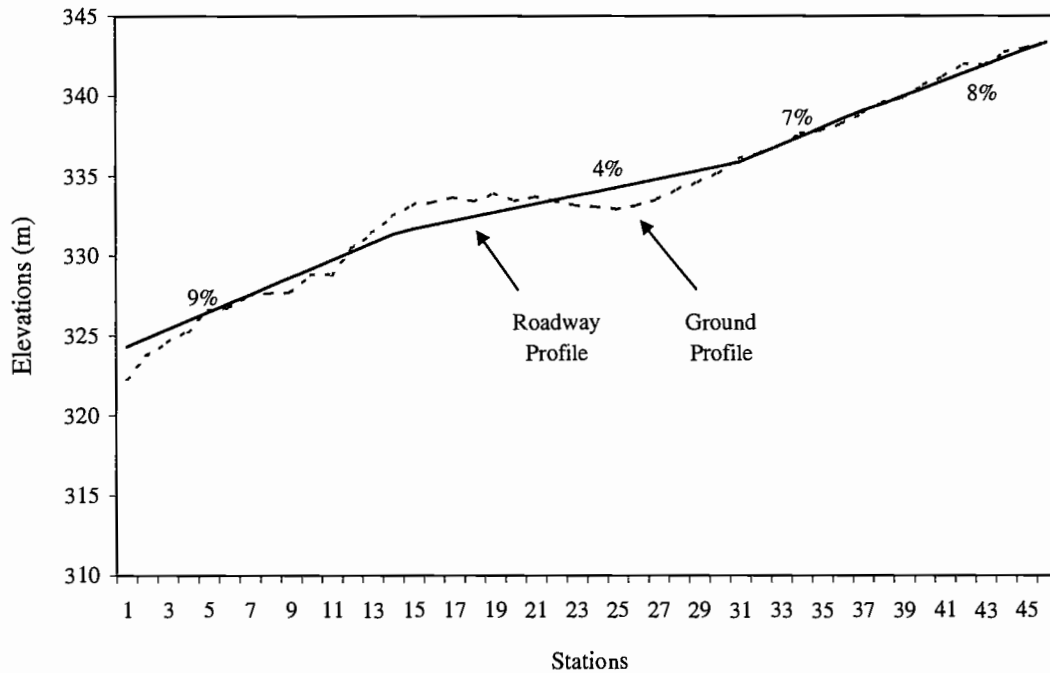


Figure 4.7. Example B: Profile view showing road gradient and vertical alignment.

The model located one horizontal curve with a radius of 45m. The road gradient varied from 4% to 9% along the roadway. If the road grade was greater than or equal to 10%, good quality base course rock (7.5cm) was used to build up the base course. If grade was less than 10%, pit run was used for base course. On grades greater than or equal to 10%, traction surface rock (4cm) was used to build up the traction surface to a 8 cm depth. If grade was less than 10%, a traction surface was not used. Two hundred and twelve feasible solutions were evaluated during the search process and the lowest value of the objective function was obtained at iteration 199 with the cost of \$27.5/m (Figure 4.8). Reducing the road gradient increased the

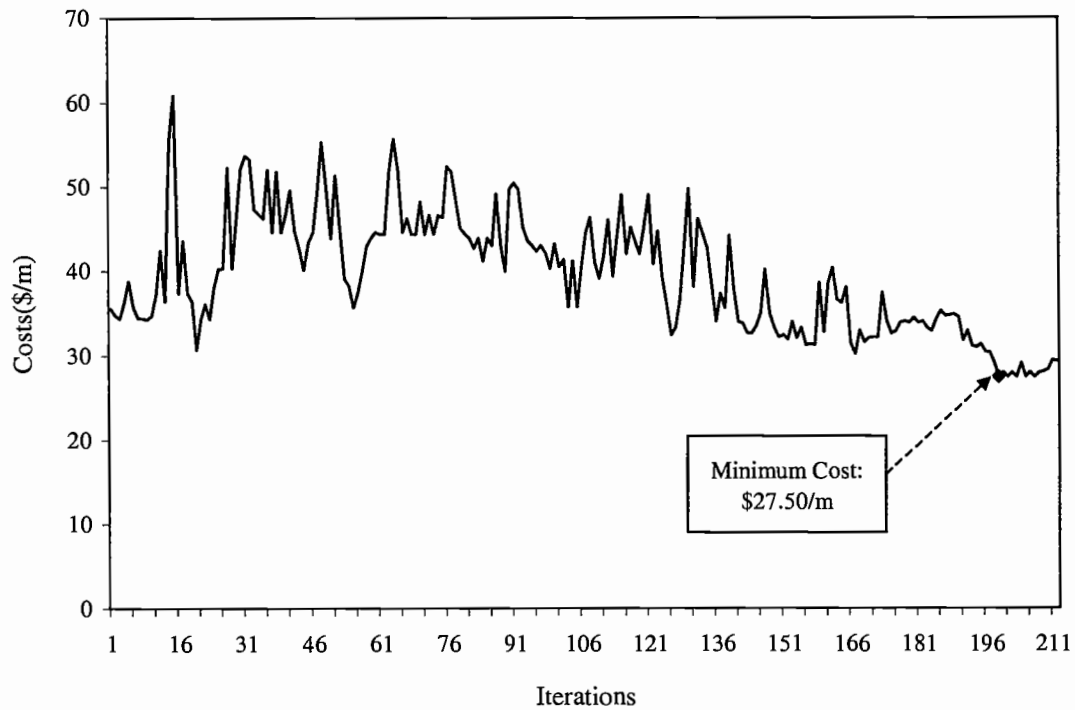


Figure 4.8. Example B: Feasible solutions during the search to identify the best vertical alignment.

earthwork costs (\$7/m), while using pit run for surfacing decreased the surfacing (\$8.8/m) and rock replacement (\$1/m) costs (Figure 4.9). The average annual volume of sediment delivered to a stream from the road section decreased to 0.17 ton due to reduced road gradient.

Results and Discussion

The unit costs for Example A and Example B were \$46.04/m and \$27.5/m, respectively. Total construction cost (Example A: \$9107 and Example B: \$5754) was the largest cost component, followed by maintenance (Example A: \$2918 and

CONSTRUCTION COST (\$)			
Earthwork Cost	(\$):	2004.83	
Construction Staking Cost	(\$):	100.10	
Clearing and Grubbing Cost	(\$):	599.74	
Drainage Cost	(\$):	225.57	
Seeding and Mulching Cost	(\$):	307.63	
Surfacing Cost	(\$):	1796.79	
Watering Cost	(\$):	663.28	
Riprap Cost	(\$):	55.87	
Construction Cost	(\$):	5753.81	(\$20300/km)
MAINTENANCE COST (\$)			
Rock Replacement Cost	(\$):	269.42	
Blading Cost	(\$):	60.17	
Culvert, Ditch, and Brush Cost	(\$):	781.99	
Maintenance Cost	(\$):	1111.58	(\$3922/km)
TRANSPORTATION COST (\$)			
Transportation Cost	(\$):	929.13	(\$3278/km)
COST AND SEDIMENT SUMMARY			
Total Cost	(\$):	7794.52	
Total Road Length	(m):	283.43	
Unit Cost	(\$/m):	27.50	(\$27500/km)
Total Sediment	(ton/year):	0.17	
Unit Sediment	(ton/year-km):	0.61	

Figure 4.9. Example B: The summary table indicating cost components and sediment.

Example B: \$1112) and transportation costs (Example A: \$941 and Example B: \$929). In construction cost elements, earthwork allocation and surfacing costs were the largest cost components. In Example A, surfacing cost (including riprap and watering costs) was approximately 69 % of the total construction cost due to

specifications for the surfacing material. In this example, good quality rock (7.5cm) for base course and traction surface material (4cm) was chosen for every road stage because of the road specifications. Surfacing cost was followed by earthwork allocation cost, clearing and grubbing, seeding and mulching, drainage, and construction staking costs (Figure 4.6). In Example B, where surface rock requirements were more flexible, earthwork allocation cost increased to 35 % of the total construction cost because the model reduced the road grade from 11% to 9% on the initial road stages (i.e., from 1 to 14) to take advantage of pit run rock for the base course. Traction surface was not employed since the road grade was less than 10% along the roadway. The surfacing cost decreased to 44% of the total road cost (69% in Example A). It was followed by clearing and grubbing, seeding and mulching, drainage, and construction staking costs (Figure 4.9).

Rock replacement (71%) was the largest cost component of the total maintenance cost in Example A. It was followed by the total cost of maintaining culverts and ditches and removing brush, and blading cost (Figure 4.6). In Example B, rock replacement cost decreased to 24% due to specifications for the surfacing material. The total cost of maintaining culverts and ditches and removing brush (70.5%) was the largest component of the total maintenance cost, followed by blading cost (Figure 4.9). The total transportation costs for Example A and Example B were \$941 and \$929, respectively. In Example B, reducing the road grade from 11% to 9% (i.e., from road stage 1 to stage 14) increased the travel speed, therefore, the total transportation cost in Example B was slightly less than that of Example A.

The best solution involved adjusting the vertical alignment to keep grading below 10 percent in Example B. By reducing the road gradient, the solution did not require a vertical curve since the absolute value of the difference between grades was not more than 5%. Besides, the road length in Example B was slightly longer than in Example A. These factors increased earthwork allocation, construction staking, clearing and grubbing, seeding and mulching, and blading costs, but decreased surfacing, rock replacement, transportation, maintaining culvert and ditches and removing brush, watering, drainage, and riprap costs. The results indicated that the unit cost of sum of the construction, maintenance, and transportation costs in Example B was 40% percent less than in Example A.

Sediment production was less in Example B. Even though the surfacing factors for good quality rock were less than for pit run, the SEDMODL road slope factor assigned to road segments with more than 10% grade was 2.5 times greater than the road segments with a grade less than or equal to 10% (Boise Cascade Corporation, 1999). Therefore, total annual sediment production in Example B was 41% less than the sediment production estimated in Example A.

Conclusions and Extensions

Forest road design involves simultaneous consideration of and tradeoffs between construction costs, vehicle performance, road maintenance, and environmental effects. The tradeoffs are not always obvious and vary depending upon local availability of construction materials, road standards, and topography. The decision support system, TRACER Version 1.0, has been developed to assist the road

designer in developing a preliminary road design. The two road examples illustrate the complexities involved with designing even a short section of road. Conventional wisdom suggests that reducing earthwork through rolling the grades to fit the terrain is often the best way to reduce environmental effects. In the examples shown, the slightly longer road alignment using flatter grades and more earthwork yielded a lower total sediment load. The results from the two short examples should not be generalized. But, the examples are instructive in showing the tradeoffs that can occur.

To evaluate the benefits and additional development requirements, TRACER must move out of the office and must focus on applications to real problems. Although development efforts have sought to capture the basic elements facing the forest road designer, additional development will be required. For example, the current version of TRACER allows optimization of the vertical alignment, but future versions will need to consider shifts the horizontal alignment in steep terrain where full bench construction is necessary.

TRACER is a prototype. Its strengths are that it can simultaneously consider tradeoffs that are difficult for the designer to do manually. Its optimization algorithm is flexible enough to accommodate other objective functions, technical relationships between design variables and environmental factors, and different cost relationships. Advancements in computer hardware, remote sensing technologies, and optimization algorithms have created the technical base, which may make a decision support system for forest road design feasible.

Literature Cited

- Aerotec, 1999. Airborne laser-scan and digital imagery. 560 Mitchell Field Road, Bessemer, AL 35022.
- Ahamed, K.M., S.E. Reutebuch, T.A. Curtis. 2000. Accuracy of high-resolution airborne laser data with varying forest vegetation cover. In Proceedings of the 2nd International Conference on Earth Observation and Environmental Information. 11-14, Cairo, Egypt.
- Akay, A.E. Minimizing Total Cost of Construction, Maintenance, and Transportation Costs with Computer-Aided Forest Road Design. Ph.D. Thesis. Forest Engineering Department, Oregon State University, Corvallis, Oregon. 229 p.
- ArcInfo, 1998. ArcInfo Version 7.0. ESRI Headquarters, Redlands, CA.
- Boise Cascade Corporation, 1999. SEDMODL-Boise Cascade road erosion delivery model. Technical documentation. 19 p.
- Chew, E.P., Goh, C.J., and Fwa, T.F. 1989. Simultaneous optimization of horizontal and vertical alignment for highways. *Transportation Research*. 23B(5):315-329.
- Easa, S.M. 1987. Earthwork allocations with linear unit costs. *Journal of Construction Engineering and Management*. 114(4):641-655.
- Easa, S.M. 1988. Selection of roadway grades that minimize earthwork cost using linear programming. *Transportation Research*. 22A(2):121-136.
- ERDAS Imagine, 1997. ERDAS Imagine, Version 8.3.1, Leica Geosystems GIS& Mapping, LLC, Worldwide Headquarters, Atlanta, GA.
- Goh, C.J., Chew, E.P., and Fwa, T.F. 1988. Discrete and continuous models for computation of optimal vertical highway alignment. *Transportation Research*. 22B(6):399-409.
- Harris, C.F.T. 1998. 1-100,000-Scale Digital Geology of Washington State. WDNr Division of Geology and Earth Resources, Washington.
- Hickerson, T. 1964. Route location and design. McGraw-Hill, New York. 634 p.
- Lumberjack, 1995. A Road Design System, Version 5. Cheney, WA, 99004. 72 p.

- Mayer, R. and Stark, R. 1981. Earthmoving logistics. *Journal of Const. Div.* 107(CO2):297-312.
- NewCyber3D, 2002. GIS Solution Systems. 11 Tennessee St., Redlands, CA 92373.
- Parker, N.A. 1977. Rural highway route corridor selection. *Transportation Planning Techniques.* (3):247-256.
- Pearce, J.K. 1974. A Guide for logging planning forest road engineering, *Forest Engineering Handbook*. Bureau of Land Management, Oregon State Office, US Department of The Interior. Divisions 100-800. 219 p.
- PFLG, 1980. Private Forest Land Grading system and subsequent soil Surveys. Washington State Department of Revenue with the WDNR, Soil Conservation Service, USDA Forest Service and Washington State University, Washington.
- RoadEng, 2002. Forest road design using Softree 98, Forestry Edition. Technical Training Manual, Logging Engineering International, Inc., Eugene, Oregon, 97402. 124 p.
- Sessions, J. 1992. Cost Control in Logging and Road Construction. Food and Agriculture Organization of the United Nations, Forest papers 99.
- TerraScan, 1998. TerraScan County Government Systems. TerraScan Inc. Lincoln, Nebraska.
- Trypia, M. 1979. Minimizing cut and fill costs in road making. *Computer-Aided Design.* (11):337-339.
- USDA, 1990. Soil Survey of Thurston County. USDA Soil Conservation Service with WDNR, Washington State University, and Agricultural Research Center, Washington.
- USDA Forest Service, 1999. Cost estimate guide for road construction Region 6. Cost Guide Zone 5, Davis-Bacon Area 5, Oregon.
- WDNR, 1996. Washington State Department of Natural Resources, Geographic Information System, Cartography and Photogrammetry, Washington.

Chapter 5

Conclusions

The design of a road between two end points of known locations and elevations is a function of physical, economical, and environmental factors. The solution of this problem normally involves similar stages for both highway and forest roads. A synthesis of the existing optimal route location systems has been presented, and then a 3D forest road alignment optimization model, TRACER, has been described. Finally, application of the model is illustrated by a numerical example.

The early automated vertical alignment selection models were based on generating a smoothed elevation using various techniques. In these models, design controls such as maximum gradient were not addressed. The optimum curvature principle has been used to generate the curvature of an optimum highway location. Dynamic programming (DP) has also been used for solving two-dimensional and three-dimensional alignment problems. This allows the designer to use more complex cost functions to determine optimum alignment. In a three-dimensional DP highway route selection model, both the optimal horizontal and vertical alignments are determined simultaneously. However, for large problems with an infinite number of alignment solutions, there is little chance of selecting the best path that minimizes the total costs due to possible excessive data storage space and computer processing time.

The mass diagram has been commonly used in highway design, as well as in forest road design, to balance the quantities of cut and fill. However, its performance

is limited where: 1) hauling costs are not linearly proportional to the hauling distance, 2) soil characteristics vary along the roadway, 3) and additional quantities of material are required to be borrowed from borrow areas or wasted at landfill areas. Various optimization models have been developed for the earthwork allocation problem to overcome the limitations of the mass diagram and improve the accuracy of the estimates. Linear programming has been used in several studies to plan the movement of earthwork and to select the roadway grades that minimize the cost of earthwork. This method provides the designer with a global minimum cost for earthwork allocation.

Many systems using optimization techniques have been developed for optimal route location and earthwork allocation problems in the field of highway design. However, the systems currently available for forest road design are not intended to make computer-aided design judgments such as: 1) automated generation of alternative grade lines, 2) best fitting vertical alignment for minimizing earthwork, 3) minimizing the total cost of construction, maintenance, and transportation, and 4) aiming for least environmental impact. They are generally used as a tool to make the mathematical calculations required to do basic manual road design.

In recent years, advances in the processing speed and real-time rendering and viewing of high-resolution three dimensional (3D) graphics on microcomputers have made it possible to locate a route interactively on a 3D display of a ground surface generated by a high-resolution digital elevation model (DEM). LIDAR (Light Detection and Ranging) is one of the fastest growing systems that provide high-

resolution and accurate DEM data. The accuracy of each point on the ground is approximately 15 cm in the vertical, and 1.0 meter in the horizontal (Ahmed et al. 2000).

In this thesis, a three-dimensional forest road alignment optimization model, TRACER Version 1.0, aided by an interactive computer system, has been developed to help the designer with a rapid evaluation of alternatives for the most economical path selection problem. The objective is to design a path with the lowest sum of construction, and future maintenance and transportation costs, while conforming to design specifications, environmental requirements, and driver safety. The model considers costs of construction, maintenance, and transportation. Additional costs that can be expressed quantitatively can be included in the model.

Although optimization methods have been used in highway design, this model is not developed to be used in highway design for several reasons. The design parameters for forest roads such as allowable road grade, horizontal and vertical curve constraints, design speed, vehicle type, traffic density, pavement requirements, and environmental concerns are defined differently in highway design (Layton, 2000). Also, according to public and private highway design engineers (Crossler 2001, and Bauman and Luebers 2001), unlike forest road projects limited primarily by the total construction cost, recent highway projects are limited by political, socioeconomic, and environmental constraints. Therefore, using the optimization techniques to minimize total cost is less important in modern day highway designs.

The designer generates the initial road alignment by tracing the possible paths using a computer cursor on the 3D image of the terrain, satisfying the constraints. The model generates alternative road alignments by a neighborhood search, adjusting the vertical alignment to find the best alignment that minimizes the sum of construction, maintenance and transportation costs. It potentially considers all technically feasible grades within the specified elevation ranges of the intersection points of the vertical alignment. This is done using a combinatorial optimization technique (Simulated Annealing), which is easy to implement and usually provides reasonable solutions to many combinatorial optimization problems after calibrating the algorithm parameters.

For each alternative vertical alignment, the model calculates cross-sections, earthwork volumes, and sediment delivery, and minimizes earthwork costs. Linear programming (LP) is used to determine the economic distribution of cut and fill quantities. The model considers possible borrow and landfill areas and various soil characteristics with different swell and shrinkage factors. The global minimum cost of earthwork allocation can be reached using LP. This model assumes that the unit costs of earthwork are constant.

To identify road segments with a high potential for delivering sediment to streams, the model estimates average annual volume of sediment using the methodology of a GIS based road erosion/delivery system, SEDMODL (Boise Cascade Corporation, 1999). When the designer interprets the results of annual sediment predictions, there are a number of limitations of the model that should be kept in mind. It is assumed that all roads are in-slope with ditch, and the roads are

over two years old. The model is highly sensitive to accuracy of the attribute data (stream, soil etc.) and road template information (road length, cut slope, etc.).

The majority of the computation time in the process is spent on earthwork allocation using linear programming. The computation is mainly affected by the number of cut and fill sections. However, many of the vertical alignment alternatives are eliminated due to one or more constraints. Therefore, the model has a reasonable computation time for each run.

The model relies on DEM and attribute data (soil, stream etc.) to display and render terrain information, using GIS technologies. Resolution and accuracy of the data directly affects the performance of the model. LIDAR (Light Detection and Ranging), one of the fastest growing systems in the field, can provide high-resolution and accurate DEM data. Available GIS data in forested areas do not represent the actual ground condition with high accuracy; however, the quality of GIS data showed improve as GIS technologies advance.

The model was applied to an actual road location problem in the Capitol State Forest in western Washington. The verification of the model is limited since no other techniques have been applied to the same problem. To improve the performance of the model in the future, the solution obtained from the model should be further tested by comparing it with current forest road design systems for the same area.

The model has several limitations and opportunities for further development. It is assumed that the unit costs of earthwork are constant. When there is a case where the unit costs vary with the quantity of the cut and fill, the model can be enhanced

using the available methods that consider such a case (Easa 1988b. and Christian et al. 1988). The cross-sections used to set the road on the ground profile are cut and fill, through cut, and through fill sections. The current state of the model does not allow the designer to generate full bench type cross-section since the horizontal alignment is fixed, once the station points are located along the roadway. Future work to optimize horizontal alignment automatically that allow using the full bench type cross-section should be considered.

The model is not intended to compute the total water discharge along the roadway, therefore, it is not providing the designer with the most appropriate culvert locations or culvert size. TRACER is not intended to provide a final road location, but this model can be enhanced by integrating it with GPS extensions to help the designer evaluate the model solutions on the ground. Future work could also provide refinements to the graphic interface, optimization of the horizontal alignment, and additional options for cut and waste areas within the road prism including more flexibility in the location of turnouts.

TRACER is not intended to provide a designer with a decision tool that locates the final route alignment, but a decision support tool that helps a designer with quick evaluation of alternatives. It is anticipated that this decision support tool networked with following features can contribute to better road design in terms of minimizing costs and environmental damage: 1) advanced features of sophisticated computer software languages to display and render high-resolution 3D images of the terrain in real-time on personal computers (PCs), 2) Geographic Information System

(GIS) techniques to store, analyze and display spatial data, 3) modern optimization techniques to minimize earthwork allocation cost using linear programming and to optimize vertical alignment using a heuristic technique, and 4) improved data sources for generating high-resolution digital elevation model (DEM) using the latest technology of Light Detection and Ranging (LIDAR).

BIBLIOGRAPHY

- AASHTO, 1990. American association of safe highway and transportation officials. A policy on geometric design of highway s and streets, Washington, D.C.
- Aerotec, 1999. Airborne laser-scan and digital imagery. 560 Mitchell Field Road, Bessemer, AL 35022.
- Ahamed, K.M., S.E. Reutebuch, and T.A. Curtis. 2000. Accuracy of high-resolution airborne laser data with varying forest vegetation cover. In Proceedings of the 2nd International Conference on Earth Observation and Environmental Information. 11-14, Cairo, Egypt.
- Akay, A.E. Minimizing Total Cost of Construction, Maintenance, and Transportation Costs with Computer-Aided Forest Road Design. Thesis. Forest Engineering Department, Oregon State University, Corvallis, Oregon.
- Antoniotti P. 1969. APPOLLON: A new road design optimization procedure. PTRC Symposium on Cost Models and Optimization in Road Location, Design and Construction, London. 236-241.
- ArcInfo, 1998. ArcInfo Version 7.0. ESRI Headquarters, Redlands, CA.
- Bauman and Luebers, 2001. Personal Interview. Highway and Bridge Services, CH2MHILL Transportation Services, Portland, Oregon.
- Beschta, R.L., 1978. Long-term patterns of sediment production following road construction and logging in the Oregon Coast Range. Water Resources Research. 14:1011-1016.
- Boise Cascade Corporation, 1999. SEDMODL-Boise Cascade road erosion delivery model. Technical documentation. 19 p.
- Bond, J.G. and C.H. Wood, 1978. Geological Map of Idaho. Idaho Department of Lands, Bureau of Mines and Geology. 1:500,000 scale.
- Botha, J.L., J.M. Follette, Sullivan, E.C., and D.J. Van Deventer. 1977. Link investment strategy model-user-guide. Institute of Transportation Studies, Research Report, UCB-ITS-RR-77-4.

- Bowman, E.H. and R.B. Fetter. 1967. Analysis for production and operations management. Irwin Series in Quantitative Analysis for Business. Yale University. 870 p.
- Burroughs, Edward R. Jr. and John G. King. 1989. Reduction of soil erosion on forest roads. Gen. Tech. Rep. INT-264. Ogden, UT: US Department of Agriculture, Forest Service, Intermountain Research Station. 21 p.
- Cain, C., and Langdon, J.A. 1982. A guide for determining minimum road width on curves for single-lane forest roads. Engineering Field Notes, Volume 14, USDA Forest Service.
- Chew, E.P., Goh, C.J., and Fwa, T.F. 1989. Simultaneous optimization of horizontal and vertical alignment for highways. Transportation Research. 23B(5):315-329.
- Christian J. and H. Caldera. 1988. Earthmoving cost optimization by operational research. Canadian Journal of Civil Engineering. 51:679-684.
- Christian J. and L. Newton. 1999. Highway construction and maintenance costs. Canadian Journal of Civil Engineering. 26:445-452.
- Crossler, R.B. 2001. Personal Interview. Roadway Engineering Section, Department of Transportation, Salem, Oregon.
- Easa, S.M. 1987. Earthwork allocations with linear unit costs. Journal of Construction Engineering and Management. 114(4):641-655.
- Easa, S.M. 1988a. Selection of roadway grades that minimize earthwork cost using linear programming. Transportation Research. 22A(2):121-136.
- Easa, S.M. 1988b. Earthwork allocations with non-constant unit costs. ASCE Journal of Construction Engineering and Management, 113(1):34-50.
- ERDAS Imagine, 1997. ERDAS Imagine, Version 8.3.1, Leica Geosystems GIS& Mapping, LLC, Worldwide Headquarters, Atlanta, GA.
- Gladding, D.F. 1964. Automatic selection of horizontal alignments for highway location. Unpublished M.S. Thesis, Massachusetts Institute of Technology, Boston, Mass.
- Goh, C.J., Chew, E.P., and Fwa, T.F. 1988. Discrete and continuous models for computation of optimal vertical highway alignment. Transportation Research. 22B(6):399-409.

- Harris, C.F.T. 1998. 1-100,000-Scale Digital Geology of Washington State. WDNR Division of Geology and Earth Resources, Washington.
- Hickerson, T. 1964. Route location and design. McGraw-Hill, New York. 634 p.
- Hoffman, W. and R. Pavley. 1959. A method for the solution of the nth best path problem. Journal of the Association for Computing Machinery. 6(4):506-514.
- Howard, B.E., Bramnick, Z., and Shaw, J.F.B. 1968. Optimum curvature principle in Highway Routing. Proc. Am. Soc. Civil Engrs. (94):61-82.
- Hunting, M.T., W.A. Bennett, V.E. Livingston Jr., and W.S. Moen, 1961. Geologic Map of Washington Department of Conservation, Division of Mine and Geology, 1:500,000 scale.
- Klemperer, D. 1996. Forest Resource economics and finance. Virginia Polytechnic Institute and State University, College of Forest and Wildlife Resources, Virginia. 551 p.
- Kramer, B.W. 1993. A road design process for low volume recreation and resource development roads. Oregon State University, Corvallis. 98 p.
- Kramer, B.W. 1997. Classnotes for FE551. Oregon State University Book Stores Inc. Corvallis, Oregon.
- Kramer, B.W. 2001. Forest road contracting, construction, and maintenance for small forest woodland owners. Oregon State University, Forest Research Laboratory, Research Contribution 35. 79 p.
- Layton, R.D. 2000. Personal Interview. Civil Engineering Department, Oregon State University, Corvallis, Oregon.
- Lecklider, R.G. and J.W. Lund. 1971. Road design handbook for USDA Forest Service in design of forest roads. Oregon State University, Corvallis, Oregon. 122 p.
- Lipton, L. and L. Meyer, 1984. A flicker-free field-sequential stereoscopic video system, SMPTE Journal. November: 1047.
- Lumberjack, 1995. A Road Design System, Version 5. Cheney, WA, 99004.
- Mannering F. and W.Kilaeski. 1990. Principles of highway engineering and traffic analysis. John Wiley and Sons, New York, New York. 251 p.

- Mayer, R. and Stark, R. 1981. Earthmoving logistics. *Journal of Const. Div.* 107(CO2):297-312.
- Nandgaonkar, S. 1981. Earthwork transportation allocations: operation research. *Journal of Const. Div.* 107(CO2):373-392.
- NewCyber3D, 2002. GIS Solution Systems. 11 Temiessee St., Redlands, CA 92373.
- Nicholson, A.J. 1974. A Variational Approach to Optimal Route Location. Civil Engineering Report 74-7, University of Canterbury, N.Z.
- O'Brien, W.T. and Bennett, D.W. 1969. A dynamic programming approach to optimal route location. *Proc Symposium on Cost Models and Optimization in Road Location, Design and Construction.* pp.175-199.
- Parker, N.A. 1977. rural highway route corridor selection. *Transportation Planning Techniques.* (3):247-256.
- Pearce, J.K. 1974. A Guide For Logging Planning Forest Road Engineering, Forest Engineering Handbook. Bureau of Land Management, Oregon State Office, US Department of The Interior. Divisions 100-800.
- Pereira, L. and L. Janssen. 1999. Suitability of laser data for DTM generation: a case study in the context of road planning and design. *ISPRS Journal of Photogrammetry and Remote Sensing.* 54(1999): 244-253.
- PFLG, 1980. Private Forest Land Grading system and subsequent soil Surveys. Washington State Department of Revenue with the WDNR, Soil Conservation Service, USDA Forest Service and Washington Sate University, Washington.
- Reeves, C. 1993. Modern heuristic techniques for combinatorial problems. Department of Statistic and Operational Research School of Mathematical and Information Sciences, Coventry University. 320 p.
- Reid, L.M. 1981. Sediment production from gravel-surfaced forest roads, Clearwater Basin, Washington. M.S. Thesis, University of Washington.
- Reid, L.M. and T. Dunne, 1984. Sediment production from forest road surfaces. *Water Resources Research.* 20(11):1753-1761.
- Reinig, L., R.L. Beveridge, J.P. Potyondy, and F.M. Hernandez, 1991. BOISED user's guide and program documentation. USDA Forest Service, Boise National Forest.

- RoadEng, 2002. Forestry Edition, Forest Road Design Using Softree 98, Technical Training Manual, Logging Engineering International, Inc., Eugene, Oregon, 97402.
- Roberts, P.O. 1957. Using New Methods in Highway Location. *Photogrammetric Engineering*. 23(3):563-569.
- Sessions, J., R. Stewart, P. Anderson, and B. Tuor. 1986. Calculating the Maximum Grade a Log Truck can Climb. *Western Journal of Applied Forestry* 1(2):43-45.
- Sessions, J. 1992. Cost Control in Logging and Road Construction. Food and Agriculture Organization of the United Nations, Forest papers 99.
- Sigurdsson, O. 1993. Effects of variable tire pressure on road surfacing. Volume II: Analysis of test results. US Army Corps of Engineers, Waterways Experiment Station. Prepared for USDA Forest Service. Technical Report GL-93-20. 84p.
- Skaugset, Arne, and Marganne M. Allen. 1998. Forest road sediment and drainage monitoring project report for private and state lands in Western Oregon. Oregon Department of Forestry, Salem, Oregon, 97310. 20 pp.
- TerraScan, 1998. TerraScan County Government Systems. TerraScan Inc. Lincoln, Nebraska.
- Trietsch, D. 1987. A family of methods for preliminary highway alignment. *Transportation Science*. (21):17-25.
- Trypia, M. 1979. Minimizing cut and fill costs in road making. *Computer-Aided Design*. (11):337-339.
- Turner, A.K. 1968. Computer-assisted procedures to generate and evaluate regional highway alternatives, Joint Highway Research Project report No.31, Purdue University, Lafayette, Indiana.
- USDA Forest Service, 1987. Forest service handbook No. 7700.56 - Road Preconstruction handbook.
- USDA, 1990. Soil Survey of Thurston County. USDA Soil Conservation Service with WDNr, Washington State University, and Agricultural Research Center, Washington.
- USDA Forest Service, 1999. Cost estimate guide for road construction Region 6. Cost Guide Zone 5, Davis-Bacon Area 5, Oregon.

- Walker, G.W. and N.S. MacLeod. 1991. Geologic Map of Oregon. U.S. Geological Survey. 1:500,000 scale.
- WDNR, 1995. Standard methodology for conducting watershed analysis, Version 3.0. Washington Forest Practices Board.
- WDNR, 1996. Washington State Department of Natural Resources, Geographic Information System, Cartography and Photogrammetry, Washington.
- Willenbrock J. 1972. Estimating costs of earthwork via simulation. Journal of Construction Division. 98(CO1):49-60.

APPENDICES

APPENDIX 1. Displaying and Rendering 2D and 3D Image of the Terrain

TRACER uses graphics routines from NewCyber3D (2002) to display high-resolution 2D (Figure A1-1) and 3D (Figure A1-2) images of the terrain in real-time, based on DEM and attribute data files. It computes 3D coordinates of points picked by mouse interactively on the scene for 3D route design. The model has various display features such as navigation control, birdview, and real-time flythrough/walkthrough.

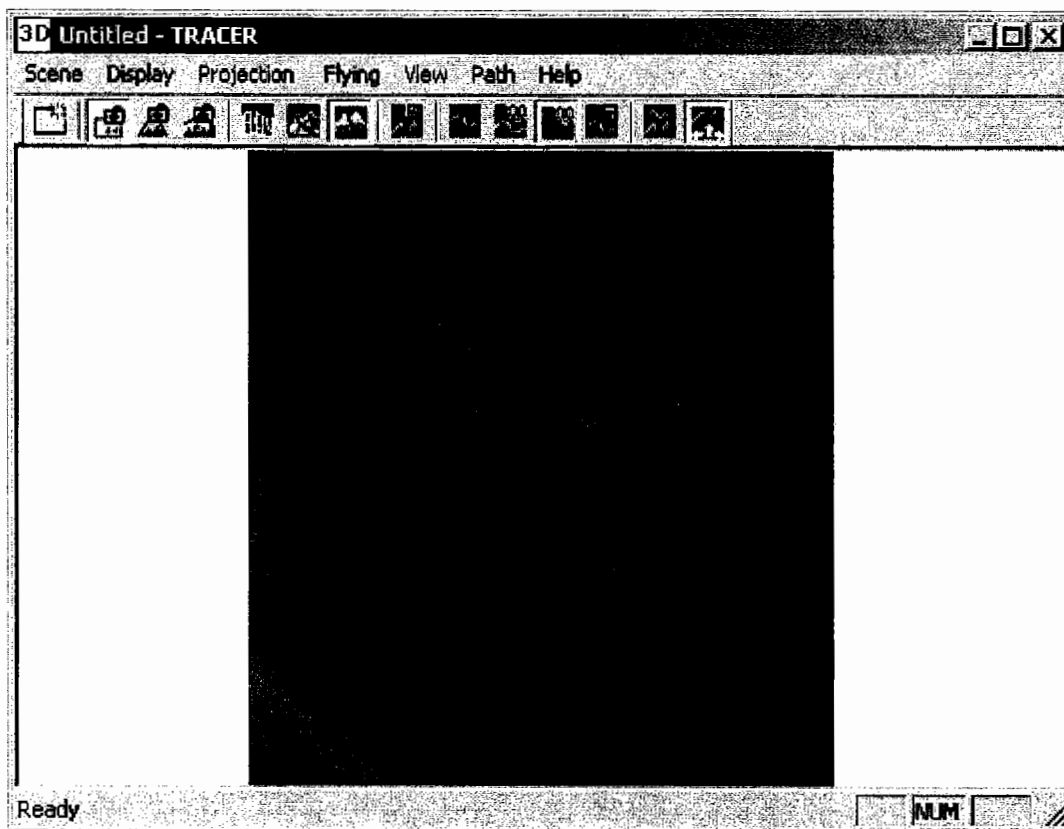


Figure A1-1. 2D image of the terrain.

The model also supports real-time 3D stereo display and stereo image composition. To generate stereo scenes, the model has used above-below stereo display format, which requires liquid-crystal glasses and an infrared emitter that connects the glasses to standard graphic card. In order to be compatible with this format, graphic programming must run full-screen. In this format, above and below images are squeezed top to bottom by a factor of two (Figure A1-3).

At the standard 60 fields per second, scanning each image takes half the duration of an entire field. Using a monitor operating at 120 fields per second, each

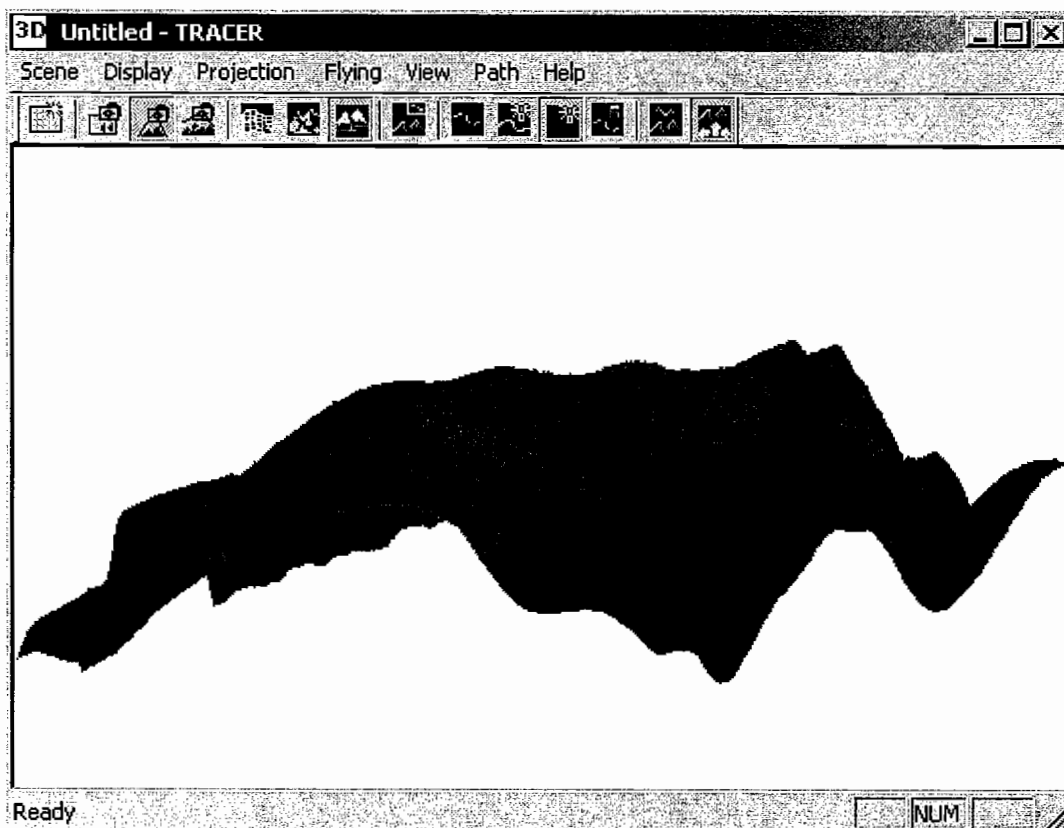


Figure A1-2. 3D image of the terrain.

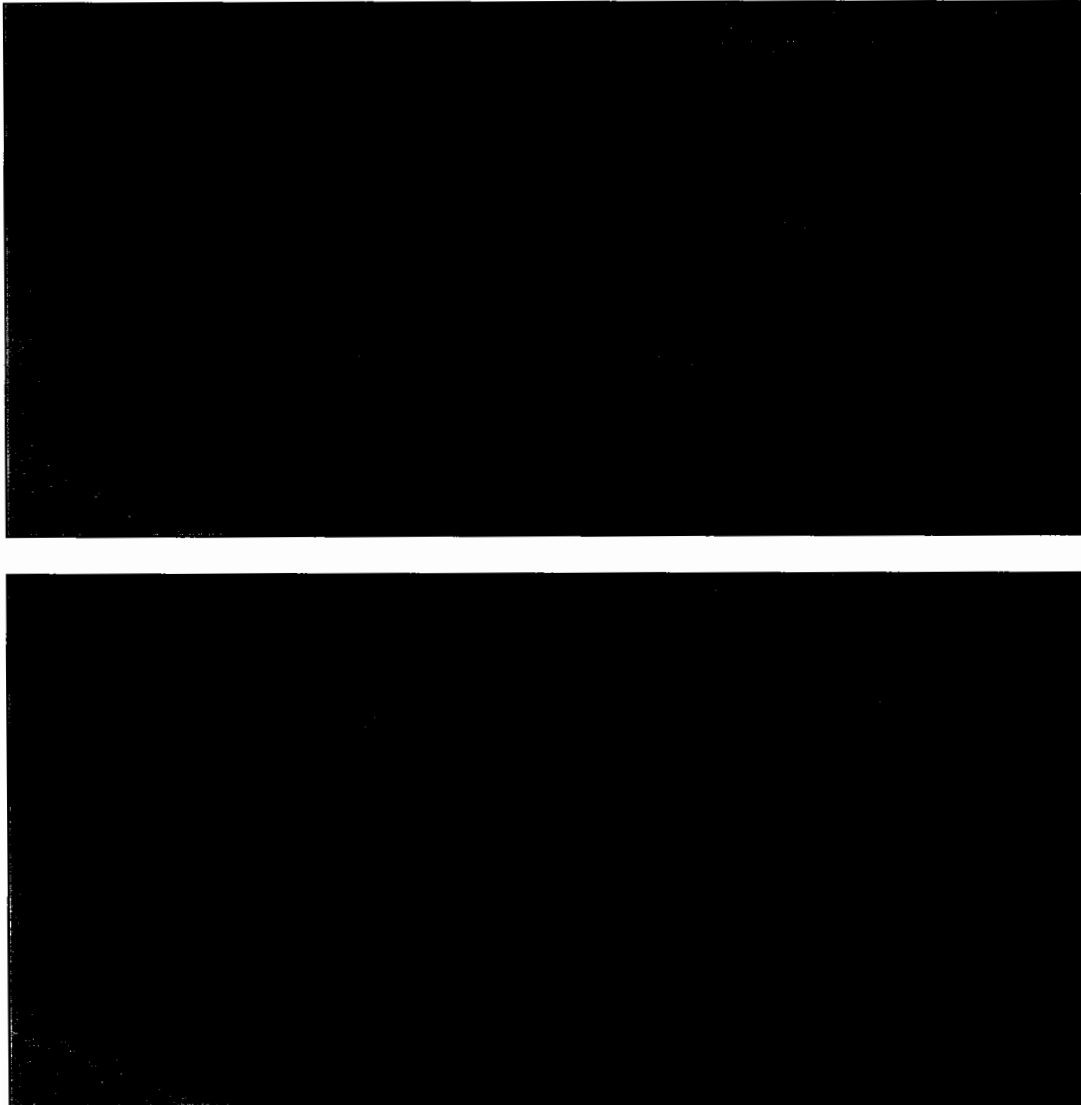


Figure A1-3. 2D images of the terrain squeezed in above-below display format.

eye (wearing the liquid-crystal glasses) sees 60 fields of image per second, while the other 60 fields are prepared for the other eye, therefore, when the right eye sees an image, the left eye does not, and vice versa (Lipton, L. and L. Meyer, 1984).

APPENDIX 2. Determining the Length of a Vertical Curve

In determining a feasible curve length, crest and sag vertical curves are considered separately based on the assumption that whether the curve length is greater or less than the *SSD*. Safe stopping distance, *SSD*, is computed using Equation A2-1 (AASHTO, 1990). In this equation, *V* is the design speed (kilometer per hour), *t_r* is perception/reaction time of the driver in second (generally 2.5 seconds), *f* is the coefficient of vehicle braking friction, and *g* is the road grade in decimal percent.

$$SSD = \frac{V^2}{254(f \pm g)} + 0.278Vt_r \quad \text{A2-1.}$$

The required safe stopping distances for various road surface types with different braking coefficients can be obtained from AASHTO (1990). There is no specific value for *g* in determining the *SSD* on a vertical curve (AASHTO, 1990). It is generally suggested to use a grade between zero percent and a small negative grade (e.g. -3%) (Mannering and Kilareski, 1990).

In determining a feasible curve length, crest and sag vertical curves are considered separately based on the assumption that whether the curve length is greater or less than the *SSD*. Equations A2-2 and A2-3 indicate the formulation for length of the crest vertical curve as follows based on *SSD* (AASHTO, 1990):

$$Lv_{i-1} = 2SSD - \frac{404}{A_{i-1}} \quad \text{A2-2.}$$

when safe stopping distance is greater than the curve length (Figure A2-1), or:

$$Lv_{i-1} = \frac{A_{i-1}SSD^2}{404} \quad \text{A2-3.}$$

when safe stopping distance is less than the curve length (Figure A2-2).

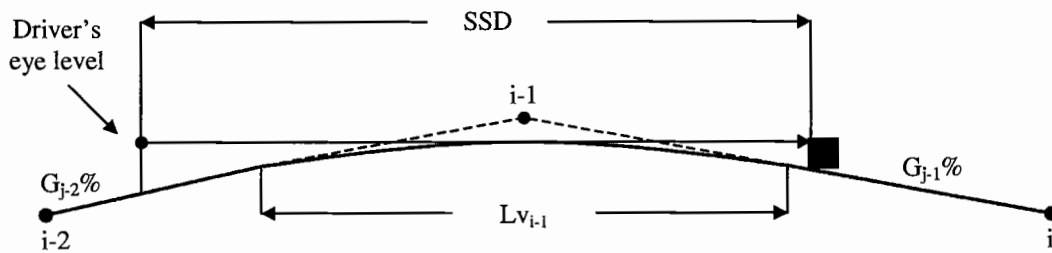


Figure A2-1. SSD is greater than the length of a vertical curve.

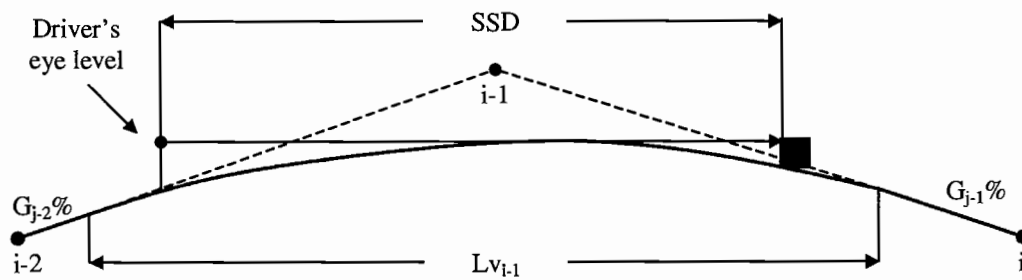


Figure A2-2. SSD is less than the length of a vertical curve.

The length of a sag curve, for a required SSD, is formulated in Equations A2-4 and A2-5 as follows (AASHTO, 1990):

$$Lv_{i-1} = 2SSD - \frac{122 + 3.5SSD}{A_{i-1}} \quad \text{A2-4.}$$

when safe stopping distance is greater than the curve length, or:

$$Lv_{i-1} = \frac{A_{i-1}SSD^2}{122 + 3.5SSD} \quad \text{A2-5.}$$

when safe stopping distance is less than the curve length.

APPENDIX 3. Safe Stopping Distance on a Horizontal Curves

The safe stopping distance is computed using Equation A2-1 in which the limiting speed of the vehicle around the horizontal curve, V , can be formulated considering vehicle weight, side friction force, centrifugal force, curve radius, side friction coefficient, and super elevation. Equation A3-1 is the simplified form of this formulation (Mannering and Kilareski, 1990).

$$V = 11.25\sqrt{R_v - 1(f_s + e)} \quad \text{A3-1.}$$

where f_s is the coefficient of side friction and e is the super elevation of the horizontal curve if it exists.

The AASHTO (1990) standards require that a driver should be able to see from an eye height of 1070 millimeters (about 3.5 feet) and stop before hitting an object of 150 millimeters (about 0.5 feet) at the mid-ordinate if a cut slope obstructs the line of sight on the horizontal curve. The general rule of the safe stopping distance around a horizontal curve is that the middle ordinate distance, M_s , must be visually clear, so that the available safe stopping distance is sufficient for the driver's line of sight (AASHTO, 1990). The equation for the middle ordinate of a simple horizontal curve is (Mannering and Kilareski, 1990):

$$M_s = R_v \left[1 - \cos \left(\frac{90SSD}{\pi R_v} \right) \right] \quad \text{A3-2.}$$

where R_v is the design curve radius minus the half of the road width (Figure A3).

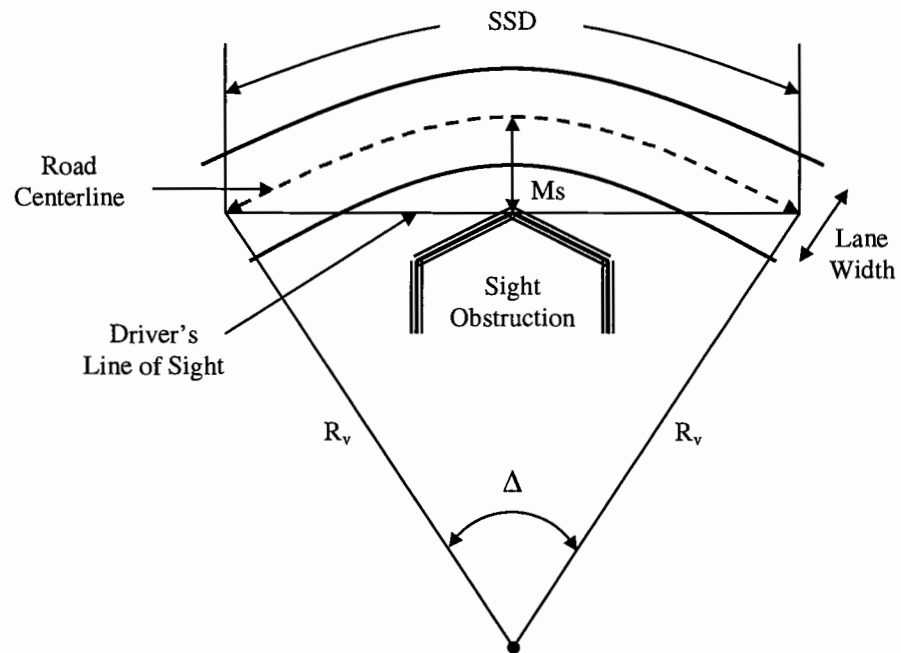


Figure A3. Safe stopping distance on a horizontal curve.

APPENDIX 4. Stream Crossing Angle

The stream-crossing angle, G_s , is computed using the horizontal angle of the road section, β_{j-1} (Equation 10), and the two consecutive stream points (s and $s-1$) that road section crosses between them. Equation A4 is used to compute G_s based on the specific conditions in Figure A4: $X_i > X_s$, $X_{i-1} < X_{s-1}$, $X_{s-1} < X_s$, $Y_i > Y_{s-1}$, $Y_{i-1} < Y_s$, $Y_{s-1} > Y_s$.

$$G_s = \beta_{j-1} + \arctan\left(\frac{|Y_s - Y_{s-1}|}{|X_s - X_{s-1}|}\right) \quad \text{A4.}$$

where X_s and Y_s are the coordinates of the stream point.

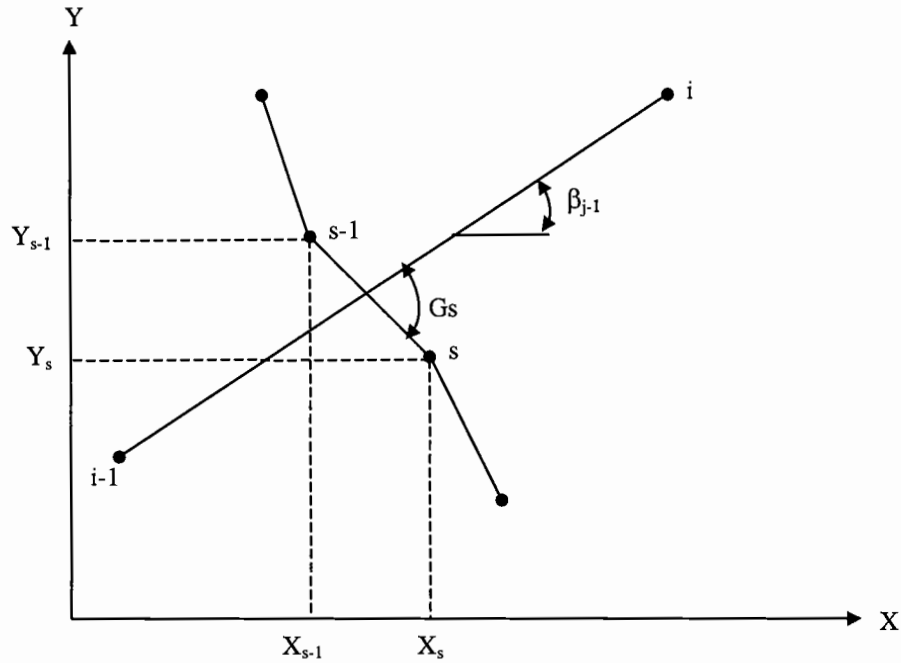


Figure A4. Elements of stream-crossing angle.

APPENDIX 5. Locating Station Points Along the Roadway

The Figure A5-1 shows the layout of a symmetrical vertical curve. In this figure, l is the user-defined horizontal distance between station points and v is the

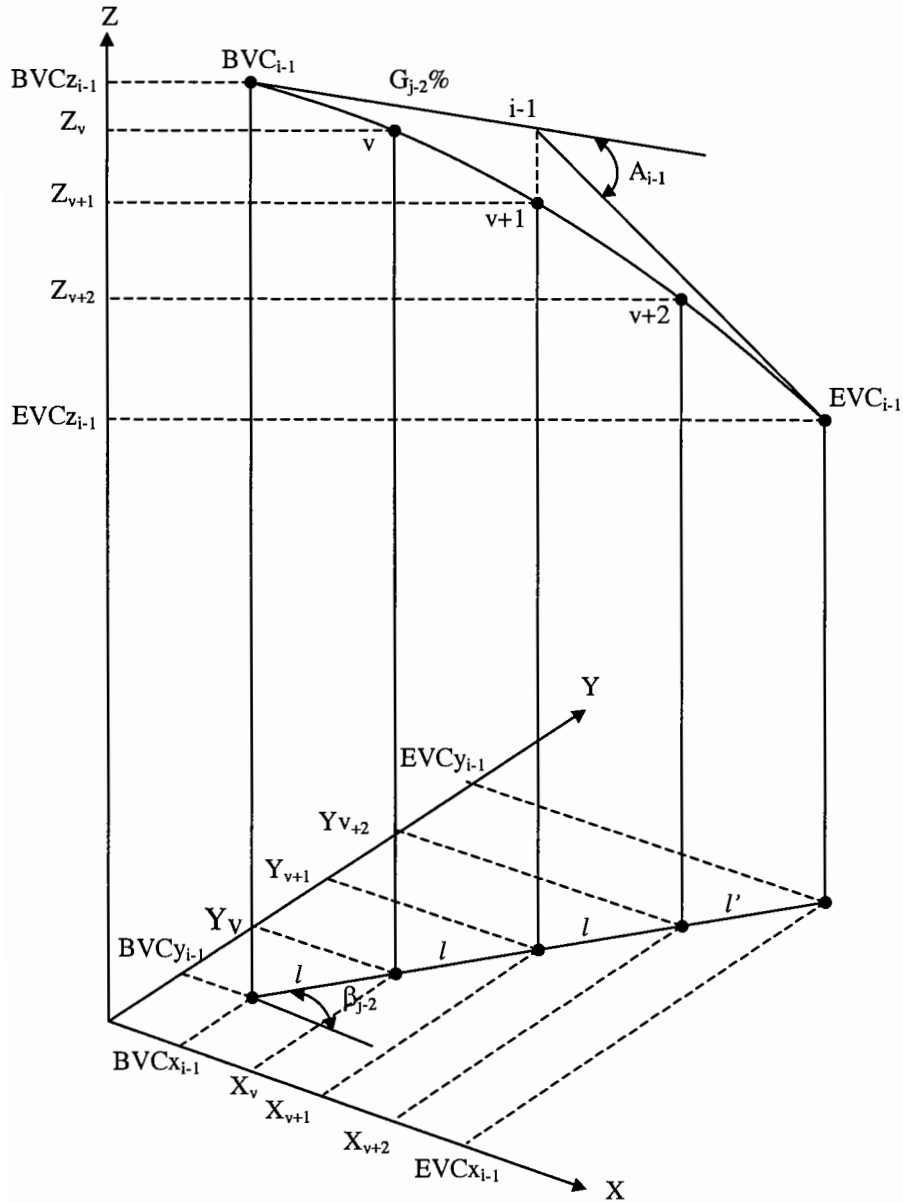


Figure A5-1. Layout elements of a vertical curve (crest).

parameter for numbering the station points along the vertical curve. X and Z axis represent the horizontal and vertical coordinates at any station point on the vertical curve. The coordinates of the station points (X_v and Y_v), are computed using the coordinates of the beginning point, the horizontal angle of the initial tangents, β_{j-2} , the road grade on the initial tangent, G_{i-2} , and the rate of change in grade, r . The value of r is positive in a sag curve and negative in a crest curve.

Equations A5-1 and A5-2 are the formulations for the coordinates of the first and the second station points, v and $v+1$, respectively. The elevation of the station point, Z_v , is computed using the standard parabolic formula (Hickerson, 1964).

$$\begin{aligned} X_{v=1} &= BVCx_{i-1} + \cos(\beta_{j-2})l \\ Y_{v=1} &= BVCy_{i-1} + \sin(\beta_{j-2})l \\ Z_{v=1} &= BVCz_{i-1} + G_{j-2}lv + (r(lv)^2/2) \end{aligned} \quad \text{A5-1.}$$

for the first point, v , and:

$$\begin{aligned} X_{v=2} &= X_{v=1} + \cos(\beta_{j-2})l \\ Y_{v=2} &= Y_{v=1} + \sin(\beta_{j-2})l \\ Z_{v=2} &= BVCz_{i-1} + G_{j-2}lv + (r(lv)^2/2) \end{aligned} \quad \text{A5-2.}$$

for the second point on the curve, $v+1$. The coordinates of the following station points are computed using the same method.

The control point of the horizontal curve is located based on the layout elements including curve radius, the coordinates of the beginning point, the horizontal angle of the initial tangents, β_{j-2} , the road grade on the curve, $G_{c_{i-1}}$ (Equation 13), and the degree of curve, d , which subtends a user-defined chord length, C . Figure A5-2

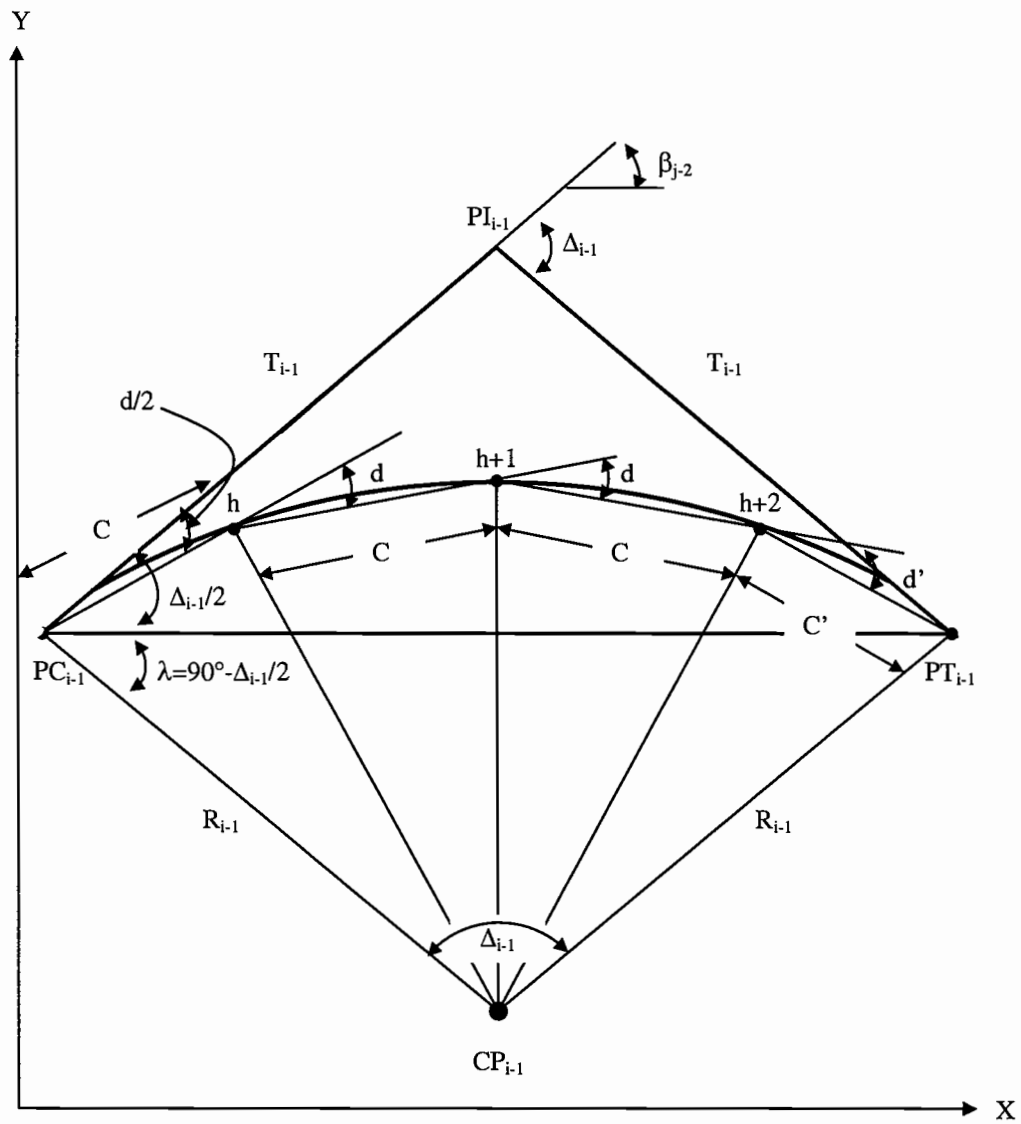


Figure A5-2. Layout elements of a horizontal circular curve (right-centered).

indicates layout elements of a circular horizontal curve. The degree of curve is formulated in the following equation (Hickerson, 1964).

$$d = \frac{C180^\circ}{R\pi} \quad \text{A5-3.}$$

In order to describe the method used to calculate the coordinates of the station points (X_h , Y_h , and Z_h) around the horizontal curve, the calculation for the first and the second points are presented in Equations A5-4 and A5-5 based on the specific geometric condition in Figure A5-2. In this figure, β_{j-2} happens to be equal to $\Delta_{i-1}/2$. h is the parameter for numbering the station points, and 0 at the beginning curve point.

$$\begin{aligned} X_{h=1} &= PCx_{i-1} + \cos(\beta_{j-2} - (d/2))C \\ Y_{h=1} &= PCy_{i-1} + \sin(\beta_{j-2} - (d/2))C \\ Z_{h=1} &= PCz_{i-1} + Gc_{i-1}C \end{aligned} \quad \text{A5-4.}$$

for the first point, h , and:

$$\begin{aligned} X_{h=2} &= X_{h=1} + \cos(\beta_{j-2} - (d+d/2))C \\ Y_{h=2} &= Y_{h=1} + \sin(\beta_{j-2} - (d+d/2))C \\ Z_{h=2} &= Z_{h=1} + Gc_{i-1}C \end{aligned} \quad \text{A5-5.}$$

for the second point on the curve, $h+1$.

The coordinates of the following station points are computed using the same method. The coordinates of the center point (CPx_{i-1} and Cpy_{i-1}) is also computed for each horizontal curve. Equation A5-6 indicates the formulation of CPx_{i-1} and Cpy_{i-1} , using the curve radius, angle λ in degree, and coordinates of the beginning point.

$$\begin{aligned} CPx_{i-1} &= PCx_{i-1} + \cos(\lambda)R_{i-1} \\ Cpy_{i-1} &= PCy_{i-1} - \sin(\lambda)R_{i-1} \end{aligned} \quad \text{A5-6.}$$

The model also records if the horizontal curve is right-centered (Figure A5-2), or left-centered. The coordinates of the two consecutive station points, on straight roadways are computed in Equations A5-7 and A5-8, respectively, based on the

specified conditions in Figure A5-3, in which t is the parameter for numbering the stations points on tangents and l is the horizontal distance between station points.

$$X_{t=1} = X_{i-2} + \cos(\beta_{j-1})l$$

$$Y_{t=1} = Y_{i-2} + \sin(\beta_{j-1})l$$

$$Z_{t=1} = Z_{i-2} + G_{j-1}l \quad \text{A5-7.}$$

for the first point, t , and:

$$X_{t=2} = X_{t=1} + \cos(\beta_{j-1})l$$

$$Y_{t=2} = Y_{t=1} + \sin(\beta_{j-1})l$$

$$Z_{t=2} = Z_{t=1} + G_{j-1}l \quad \text{A5-8.}$$

for the second point on the tangent, $t+1$.

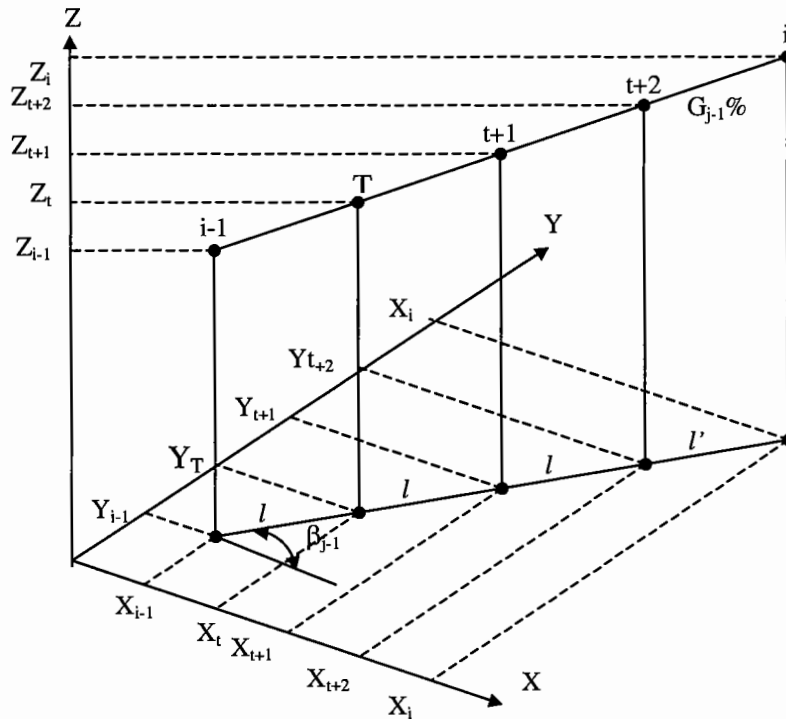


Figure A5-3. Layout elements of a straight roadway (tangent).

APPENDIX 6. Extracting Ground Elevations from the DEM

The ground elevation of any point (Z_{gp}) on the terrain can be computed as a function of X_p and Y_p coordinates of this point based on the DEM data file. The model searches through the DEM file and locates the elevation point (Z_{dem1}) that is the nearest to the point under consideration (Figure A6). Then, it locates other three elevation points to each side of this point and computes an average ground elevation of the terrain around the station point by evaluating the nearest elevation point and other points (Equation A6).

$$Z_{gp} = \frac{Z_{dem1} + Z_{dem2} + Z_{dem3} + Z_{dem4}}{4} \quad \text{A6.}$$

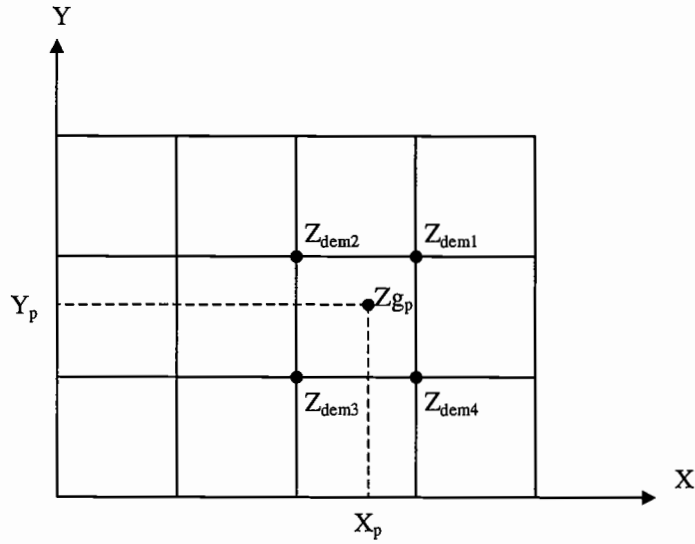


Figure A6. Estimation of the ground elevation at a station point.

APPENDIX 7. Determining Cross Section Types

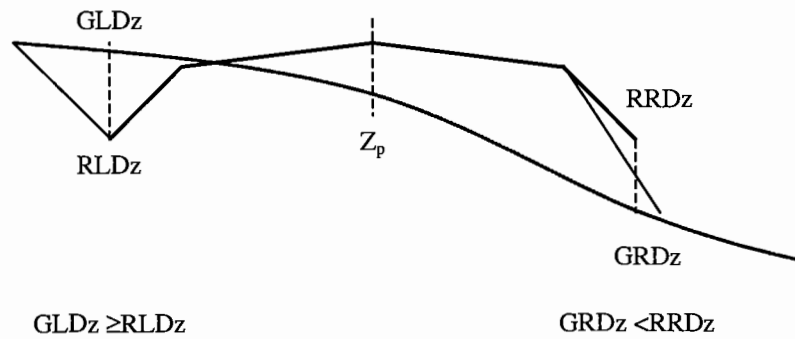
The cross sections used to set the road on the ground profile are cut and fill, through cut, and through fill sections (Figure A7-1). The current state of the model does not allow the designer to generate full bench type cross section since the horizontal alignment is fixed, once the station points are located along the roadway. The model determines the cross section types using a crowned type road surface (Figure A7-2) with two ditches as a measuring device.

In this figure, $RRDz$ and $RLDz$ are the road elevations at the right ditch point and left ditch point, respectively, while $GRDz$ and $GLDz$ are the ground elevations at the these points, respectively. The ditch depth, h_d , and ditch slope, g_d , are defined by the designer. The ditch length, l_d , is then equal to h_d/g_d . If a ditch relief culvert needs to be located, the model also designs the catch basin to allow access for cleaning. The catch basins should be constructed with a minimum bottom width of 1 meter.

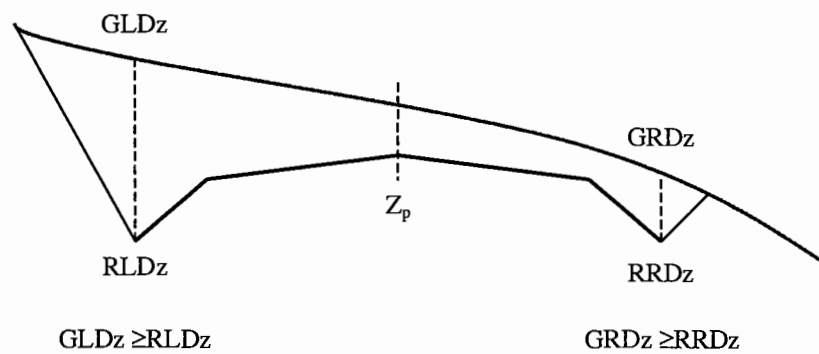
The model computes the road elevations $RRDz$ and $RLDz$ using the elevation at the centerline (Z_p), roadbed width, RBW , road surface slope, g_r in percent, and ditch dimensions (Equation A7-1). If the road stage is located on a right-centered horizontal curve, the model adds the curve widening to the right roadbed width.

$$\begin{aligned} RRDz &= Z_p - g_r RBW_r - h_d \\ RLDz &= Z_p - g_r RBW_l - h_d \end{aligned} \quad A7-1.$$

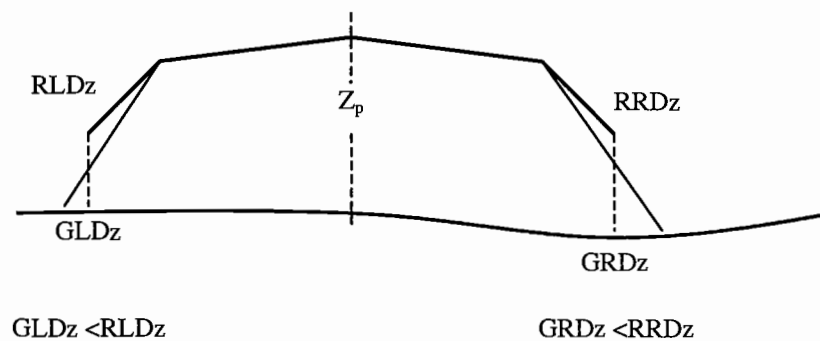
Using the DEM data, the ground elevations at the ditch points are computed as a function of their X and Y coordinates. Figure A7-3 shows the plan view of a sample cross section for a road stage located on a straight roadway. In this figure, RDx and



Cut and Fill Cross Section



Through Cut Cross Section



Through Fill Cross Section

Figure A7-1. The types of cross sections.

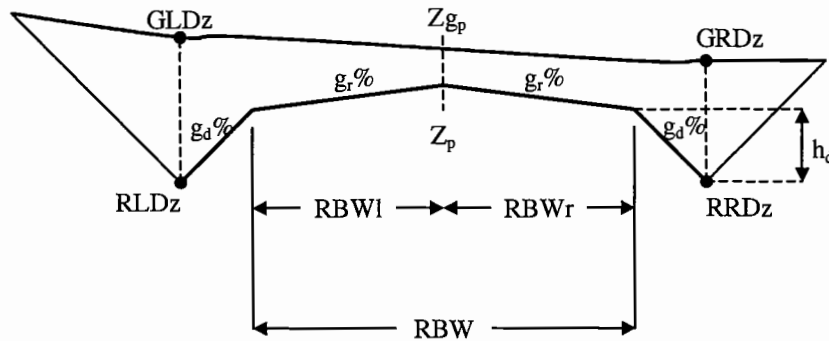


Figure A7-2. A crowned type road surface used as a scale in the model.

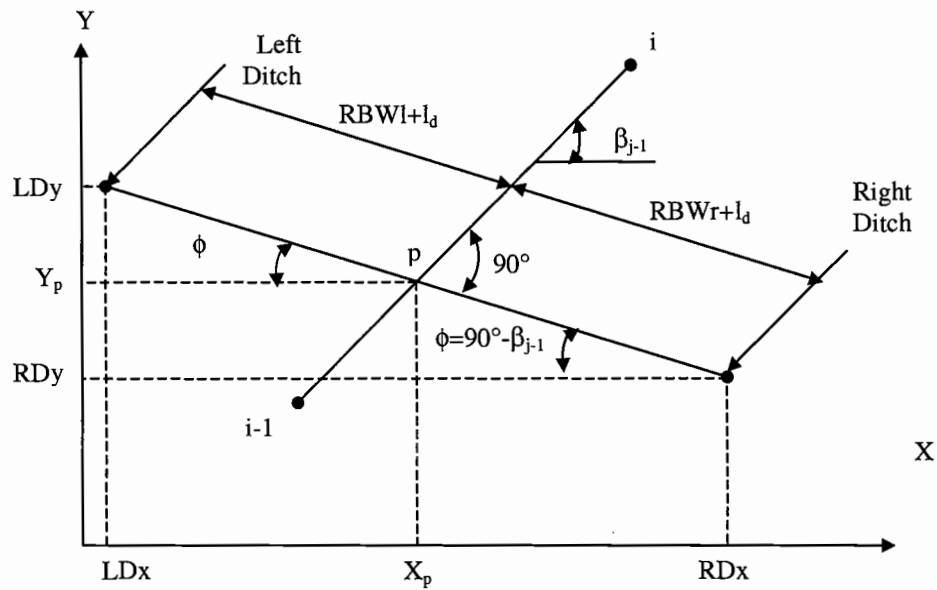


Figure A7-3. Geometry of a cross section on a straight roadway (tangent).

RDy represent the coordinates of the right ditch point, while LDx and LDy represent the coordinates of the left ditch point. The coordinates of ditch points are:

$$RDx = X_p + \cos(\phi)(RBWr + l_d)$$

$$RDy = Y_p - \sin(\phi)(RBWr + l_d)$$

$$LDx = X_p - \cos(\phi)(RBWr + l_d)$$

$$LDy = Y_p + \sin(\phi)(RBWr + l_d) \quad A7-2.$$

For the road stages located on a horizontal curve, the model considers the curve widening, CW , due to offtracking (Appendix 10) and clearing the middle ordinate distance for SSD (Appendix 11). The plan view of a sample cross section located around the horizontal curve is indicated in Figure A7-4. In this figure, the

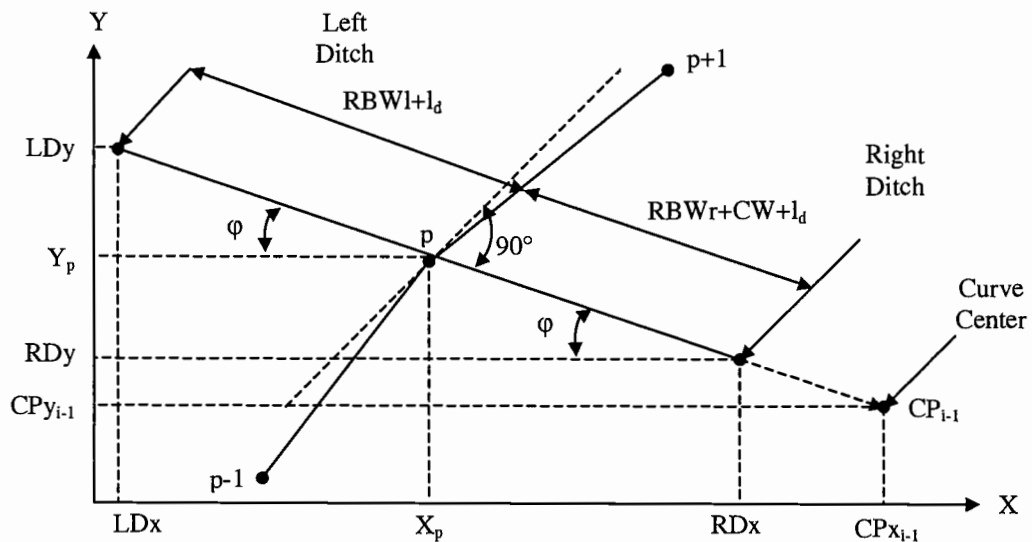


Figure A7-4. Geometry of a cross section on a right centered horizontal curve.

horizontal angle φ is computed using the coordinates of the current station point under consideration and the coordinates of the curve center:

$$\varphi = \arctan\left(\frac{|CPy_{i-1} - Y_p|}{|CPx_{i-1} - X_p|}\right) \quad A7-3.$$

then, the coordinates of ditch points are computed as follows:

$$\begin{aligned} RDx &= X_p + \cos(\varphi)(RBWr + CW + l_d) \\ RDy &= Y_p - \sin(\varphi)(RBWr + CW + l_d) \\ LDx &= X_p - \cos(\varphi)(RBWr + l_d) \\ LDy &= Y_p + \sin(\varphi)(RBWr + l_d) \end{aligned} \quad A7-4.$$

APPENDIX 8. Computing Cut and Fill Areas on Cross Sections

After determining the cross section types (Appendix 7), the cross sections are located and associated total cut and fill areas are computed on each station point. The model first divides the cross section area into five sections (right road side, left road side, cut slope, fill slope, and ditch) and evaluates them separately. Figure A8-1 and Figure A8-2 indicate the plan and profile view of a sample cut and fill cross section.

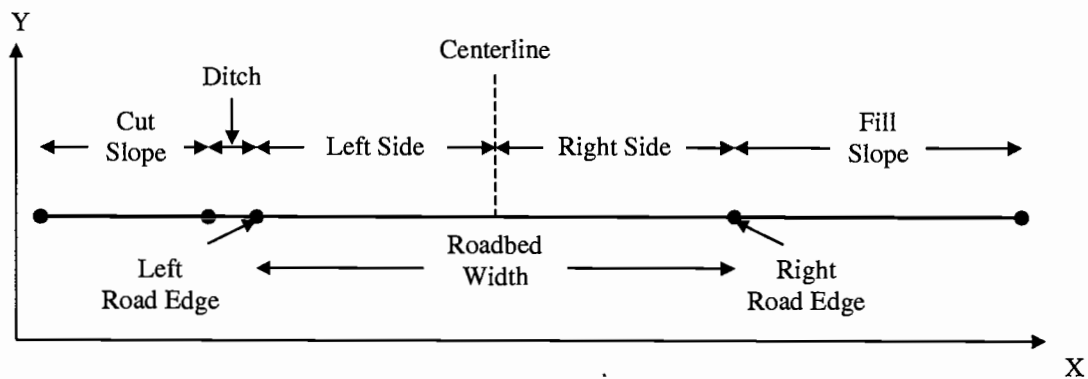


Figure A8-1. Plan view of the cut and fill cross section.

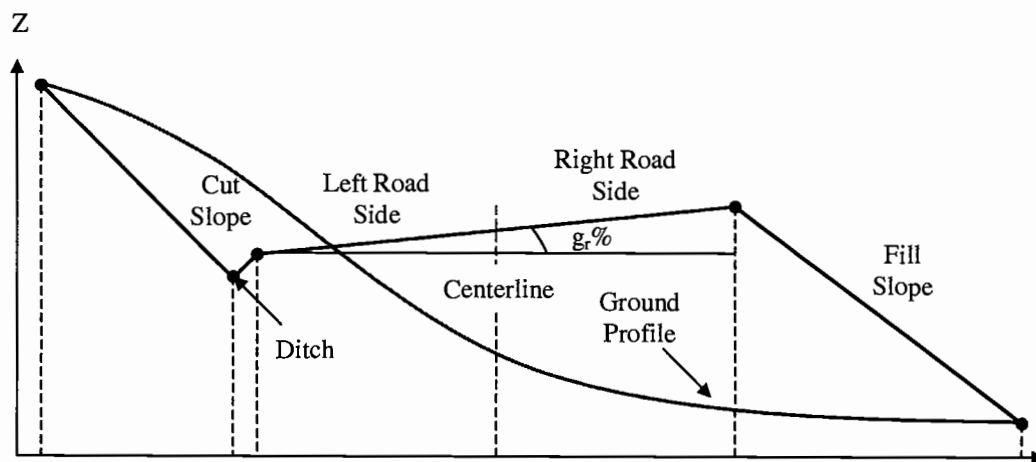


Figure A8-2. Profile view of the cut and fill cross section.

Right Road Side:

The model divides the right road side into lateral subsections by a specified length, L_{sub} , (e.g. 1 meter) as shown in Figure A8-3. In this figure, it is assumed that the road width is 4 meters and half of the road width is 2 meters in both sides. The model first compares the ground elevation, Z_{g_p} , and road elevation, Z_p , at the centerline (station point p). There are three cases that might occur:

Case 1: If $Z_{g_p} > Z_p$, three sub cases occur based on the comparison between ground elevation ($L1gz$) and the road elevation ($L1z$) at the first lateral point ($L1$).

(1) The model first computes $L1gz$ and $L1z$. $L1gz$ is computed as a function of X and Y coordinates of $L1$ based on DEM and the specific geometric conditions in Figure A8-1:

$$L1x = X_p + L_{sub}$$

$$L1y = Y_p$$

A8-1.

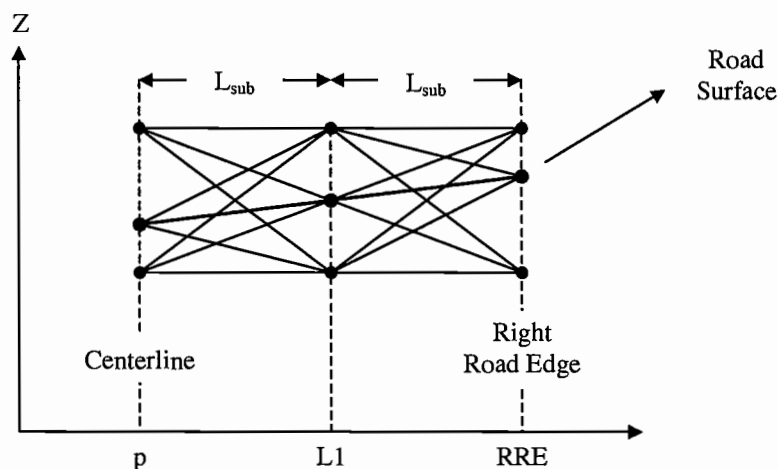


Figure A8-3. Cut and fill areas on right road side.

Then, the model computes $L1z$ in the following equation using road surface grade (g_r) and L_{sub} :

$$L1z = Z_p + g_r L_{sub} \quad A8-2.$$

If $L1gz > L1z$, the cut area is computed as follows:

$$Cut\ Area = L_{sub}(Z_{g_p} - Z_p)/2 + L_{sub}(L1gz - L1z)/2 \quad A8-3.$$

(2) If $L1gz = L1z$, the model computes the cut area as follows:

$$Cut\ Area = L_{sub}(Z_{g_p} - Z_p)/2 \quad A8-4.$$

(3) If $L1gz < L1z$, the cut and fill areas occur as indicated in Figure A8-4. The model first computes the distance x using the following equality:

$$\frac{x}{L_{sub} - x} = \frac{L1z - L1gz}{Z_{g_p} - Z_p}$$

$$x = \frac{L_{sub}(L1z - L1gz)}{(L1z - L1gz) + (Z_{g_p} - Z_p)} \quad A8-5.$$

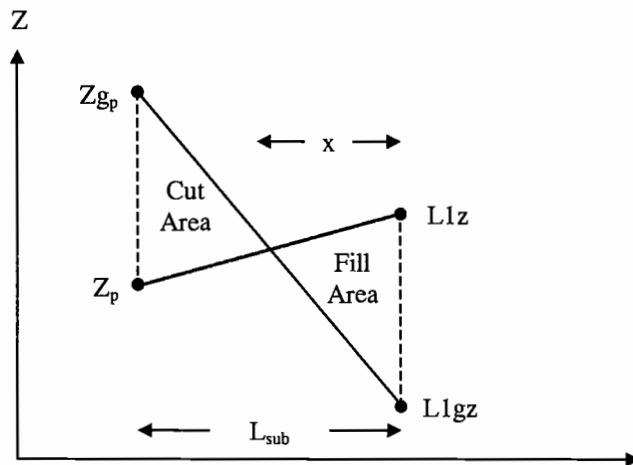


Figure A8-4. Case 1: Cut and fill area on right road side.

then, the model computes the cut and fill areas separately using the following equations:

$$\text{Cut Area} = (L_{sub}-x)(Z_{g_p} - Z_p)/2 \quad \text{A8-6.}$$

$$\text{Fill Area} = (x)(L1z - L1gz)/2 \quad \text{A8-7.}$$

The cut and fill area of the next subsection from L1 to right road edge is computed using the same method.

Case 2: If $Z_{g_p} = Z_p$, the following three sub cases occur:

(1) If $L1gz > L1z$, the model computes the cut area as follows:

$$\text{Cut Area} = L_{sub}(L1gz - L1z)/2 \quad \text{A8-8.}$$

(2) If $L1gz = L1z$, there is no cut or fill area occur.

(3) If $L1gz < L1z$, the model computes the fill area as follows:

$$\text{Fill Area} = L_{sub}(L1z - L1gz)/2 \quad \text{A8-9.}$$

Case 3: If $Z_{g_p} < Z_p$, the following three sub cases occur:

(1) If $L1gz > L1z$, the cut and fill areas occur as indicated in Figure A8-5. The model first computes the distance x using the following equality:

$$\begin{aligned} \frac{x}{L_{sub} - x} &= \frac{L1gz - L1z}{Z_p - Z_{g_p}} \\ x &= \frac{L_{sub}(L1gz - L1z)}{(L1gz - L1z) + (Z_p - Z_{g_p})} \end{aligned} \quad \text{A8-10.}$$

then, the cut and fill areas are computed as follows:

$$\text{Cut Area} = (x)(L1gz - L1z)/2 \quad \text{A8-11.}$$

$$\text{Fill Area} = (L_{sub}-x)(Z_p - Z_{g_p})/2 \quad \text{A8-12.}$$

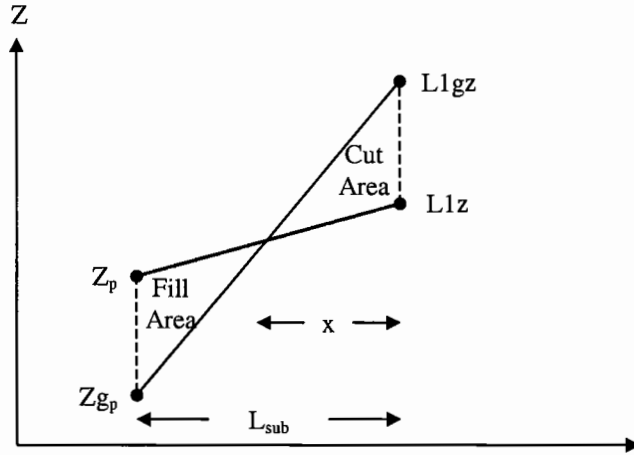


Figure A8-5. Case 3: Cut and fill area on right road side.

(2) If $L1gz = L1z$, the model computes the fill area as follows:

$$\text{Fill Area} = L_{sub}(Z_p - Z_{gp})/2 \quad \text{A8-13.}$$

(3) If $L1gz < L1z$, the fill area, consisting of two triangles, is:

$$\text{Fill Area} = L_{sub}(Z_p - Z_{gp})/2 + L_{sub}(L1z - L1gz)/2 \quad \text{A8-14.}$$

Left Road Side:

In the left road side, the model uses the same method used for the right road side. The illustration of the left road side is in Figure A8-6.

Ditch Section:

The model first computes the ground elevation, LRE_{gz} , and road elevation, LRE_z , at the left road edge (LRE) (Figure A8-7). LRE_z is computed as follows:

$$LRE_z = Z_p - g_r RBW/2 \quad \text{A8-15.}$$

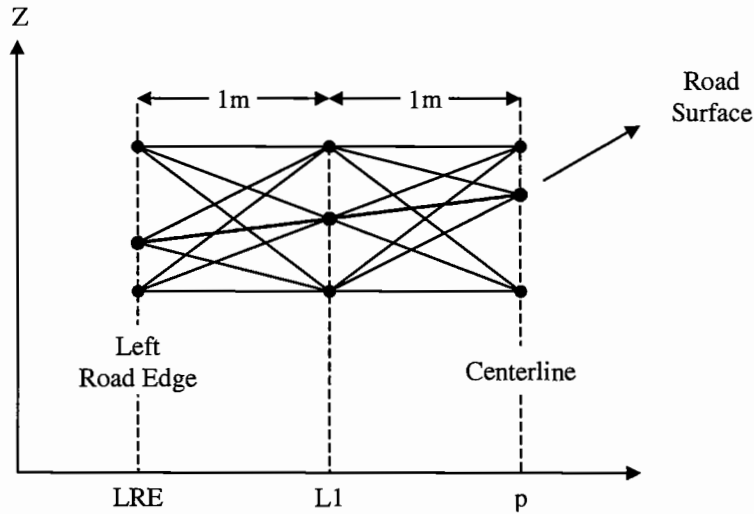


Figure A8-6. Cut and fill areas on left road side.

then, $LREg_z$ is computed as a function of X and Y coordinates of LRE based on DEM and the specific geometric conditions in Figure A8-1:

$$\begin{aligned} LREx &= X_p - RBW/2 \\ LREy &= Y_p \end{aligned} \quad \text{A8-16.}$$

The model compares the ground elevation, $LREg_z$, and road elevation, LRE_z , at the left road edge (LRE). There are three cases that might occur:

Case 1: If $LREg_z > LRE_z$, three sub cases occur based on the comparison between ground elevation (GLD_z) and the road elevation (RLD_z) at the left ditch (RLD).

(1) If $GLD_z > RLD_z$, the model first computes the ditch length, l_d , based on the given values of ditch depth, h_d , and ditch grade, g_d , (Figure A7-1):

$$L_d = h_d/g_d \quad \text{A8-17.}$$

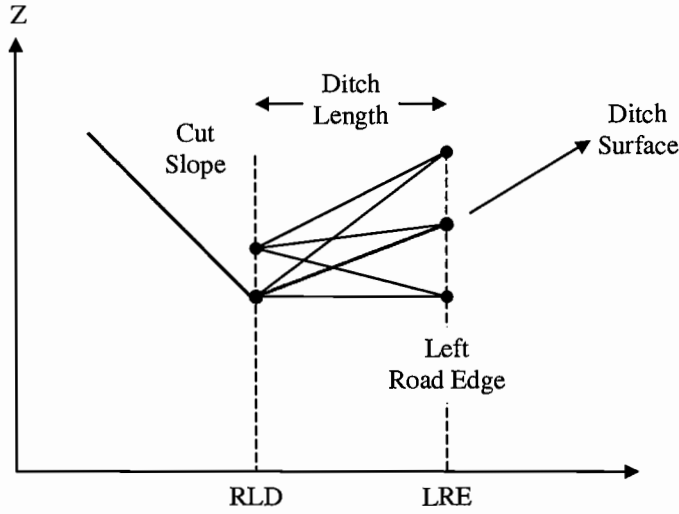


Figure A8-7. Cut and fill areas on ditch section.

then, the cut area, consisting of two triangles, is computed using the following equation:

$$\text{Cut Area} = L_d(GLD_z - RLD_z)/2 + L_d(LRE_{g_z} - LRE_z)/2 \quad \text{A8-18.}$$

(2) If $GLD_z = RLD_z$, the model computes the cut area as follows:

$$\text{Cut Area} = L_d(GLD_z - RLD_z)/2 \quad \text{A8-19.}$$

(3) If $GLD_z < RLD_z$, the cut and fill areas occur as indicated in Figure A8-8.

The model first computes the distance x using the following equality:

$$\frac{x}{L_d - x} = \frac{L1_{g_z} - L1_z}{RLD_z - GLD_z}$$

$$x = \frac{L_d(L1_{g_z} - L1_z)}{(L1_{g_z} - L1_z) + (RLD_z - GLD_z)} \quad \text{A8-20.}$$

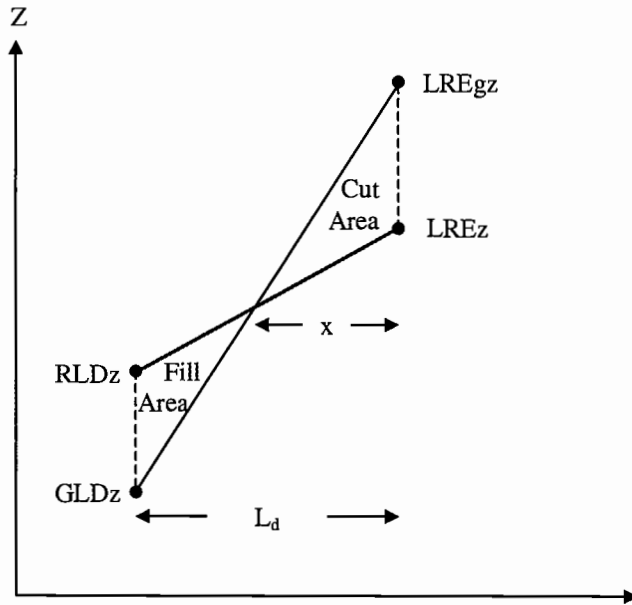


Figure A8-8. Case 1: Cut and fill area on ditch section.

then, the model computed the cut and fill areas separately using the following equations:

$$\text{Cut Area} = (x)(L1gz - L1z)/2 \quad \text{A8-21.}$$

$$\text{Fill Area} = (L_d - x)(RLDz - GLDz)/2 \quad \text{A8-22.}$$

Case 2: If $LREgz = LREz$, the following three sub cases occur:

(1) If $GLDz > RLDz$, the model computes the cut area as follows:

$$\text{Cut Area} = L_d(GLDz - RLDz)/2 \quad \text{A8-23.}$$

(2) If $GLDz = RLDz$, there is no cut or fill area occur.

(3) If $GLDz < RLDz$, the model computes the fill area as follows:

$$\text{Fill Area} = L_d(RLDz - GLDz)/2 \quad \text{A8-24.}$$

Case 3: If $LRE_{gz} < LRE_z$, three sub cases occur based on the comparison between ground elevation (GLD_z) and the road elevation (RLD_z) at the left ditch (RLD).

(1) If $GLD_z > RLD_z$, the cut and fill areas occur as indicated in Figure A8-9.

The model first computes the distance x using the following equality:

$$\frac{x}{L_d - x} = \frac{LRE_z - LRE_{gz}}{GLD_z - RLD_z}$$

$$x = \frac{L_d(LRE_z - LRE_{gz})}{(LRE_z - LRE_{gz}) + (GLD_z - RLD_z)} \quad \text{A8-25.}$$

then, the cut and fill areas are computed as follows:

$$\text{Fill Area} = (x)(LRE_z - LRE_{gz})/2 \quad \text{A8-26.}$$

$$\text{Cut Area} = (L_d - x)(GLD_z - RLD_z)/2 \quad \text{A8-27.}$$

(2) If $GLD_z = RLD_z$, the model computes the fill area as follows:

$$\text{Fill Area} = L_d(LRE_z - LRE_{gz})/2 \quad \text{A8-28.}$$

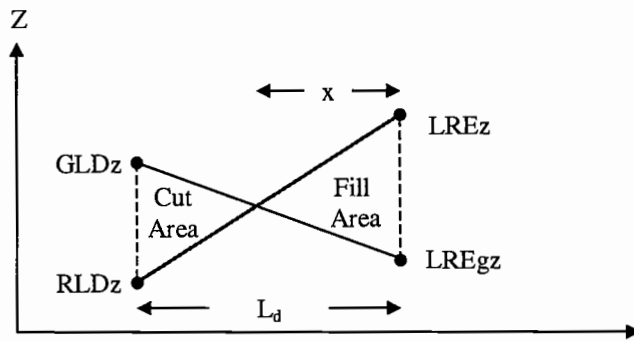


Figure A8-9. Case 3: Cut and fill area on ditch section.

(3) If $GLD_z < RLD_z$, the fill area, consisting of two triangles, is computed as follows:

$$Fill\ Area = L_d(RLD_z - GLD_z)/2 + L_d(LRE_z - LRE_g_z)/2 \quad A8-29.$$

If ditch relief culvert is located to carry roadway runoff from the ditch, the model considers a catch basin in the ditch. A catch basin is constructed with a minimum bottom width, CBW (e.g. 1 meter), between ditch point, RLD , and left cut slope point, LCS . Figure A8-10 indicates the minimum dimensions for a catch basin in the ditch.

The model first compares the ground elevation, GLD_z , and road elevation, RLD_z , at the ditch point (RLD). There are two cases that might occur:

Case 1: If $GLD_z > RLD_z$, three sub cases occur based on the comparison between ground elevation (GLC_z) and road elevation (RLC_z) at the first cut slope point (RLC).

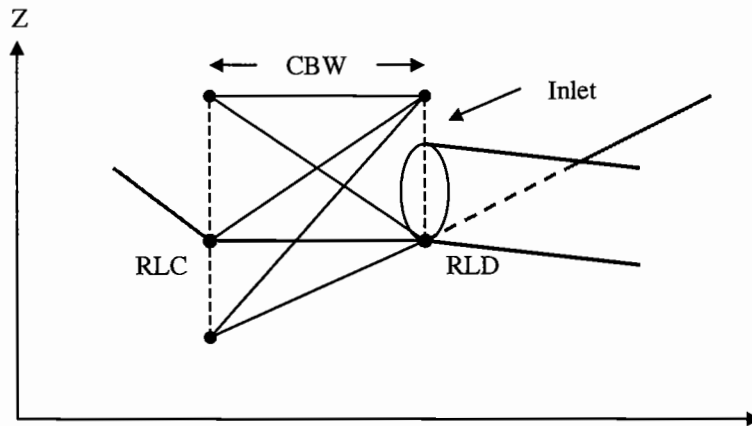


Figure A8-10. Cut and fill areas on the catch basin.

(1) The model first computes GLC_z and RLC_z . RLC_z is assumed to be equal to RLD_z . GLC_z is computed as a function of X and Y coordinates of RLC based on DEM and the specific geometric conditions in Figure A8-1:

$$RLC_x = RLD_x - CBW$$

$$RLC_y = RLD_y \quad A8-30.$$

If $GLC_z > RLC_z$, the cut area, consisting of two triangles, is:

$$Cut\ Area = CBW(GLD_z - RLD_z)/2 + CBW(GLC_z - RLC_z)/2 \quad A8-31.$$

(2) If $GLC_z = RLC_z$, the model computes the cut area as follows:

$$Cut\ Area = CBW(GLD_z - RLD_z)/2 \quad A8-32.$$

(3) If $GLC_z < RLC_z$, the cut and fill areas occur as indicated in Figure A8-11.

The model first computes the distance x using the following equality:

$$\frac{x}{CBW - x} = \frac{GLD_z - RLD_z}{RLC_z - GLC_z}$$

$$x = \frac{CBW(GLD_z - RLD_z)}{(GLD_z - RLD_z) + (RLC_z - GLC_z)} \quad A8-33.$$

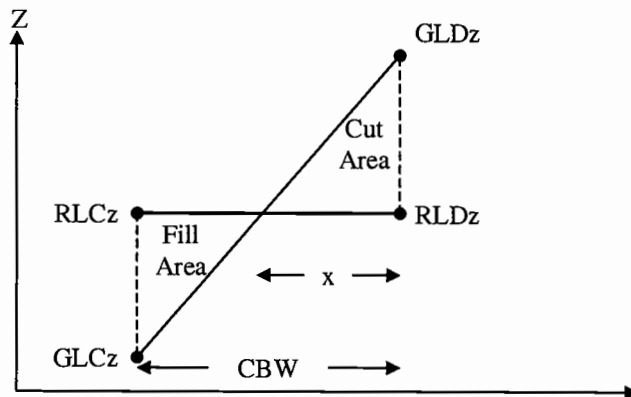


Figure A8-11. Case 1: Cut and fill area on a catch basin.

then, the model computes the cut and fill areas separately using the following equations:

$$\text{Cut Area} = (x)(GLD_z - RLD_z)/2 \quad \text{A8-34.}$$

$$\text{Fill Area} = (CBW-x)(RLC_z - GLC_z)/2 \quad \text{A8-35.}$$

Case 2: If $GLD_z = RLD_z$, the following three sub cases occur:

(1) $GLC_z > RLC_z$, the model computes the cut area as follows:

$$\text{Cut Area} = CBW(GLC_z - RLC_z)/2 \quad \text{A8-36.}$$

(2) If $GLC_z = RLC_z$, there is no cut or fill area occur.

(3) If $GLC_z < RLC_z$, the model computes the fill area as follows:

$$\text{Fill Area} = CBW(RLC_z - GLC_z)/2 \quad \text{A8-37.}$$

Cut Slope:

The model divides the cut slope into lateral subsections by a specified length, L_{sub} , (e.g. 1 meter) as shown in Figure A8-12. At each cut slope point, RLC , it compares the ground elevation, GLC_z , and cut slope elevation, RLC_z . If the ground elevation is greater than the cut slope elevation, the model moves to the next subsection.

Otherwise, it stops the iteration and computes the total cut area. In Figure A8-12, g_c is the grade on the cut slope in percent and h_c is the cut slope height. The model first determines the grade on the cut slope and maximum cut slope height, $Maxh_c$, based on the soil type data stored in the attribute data file. Cut and fill slopes should be constructed depending on the available soil and rock types on the cross sections.

The model compares the ground elevation, GLD_z , and road elevation, RLD_z , at the ditch point (RLD). There are two cases that might occur:

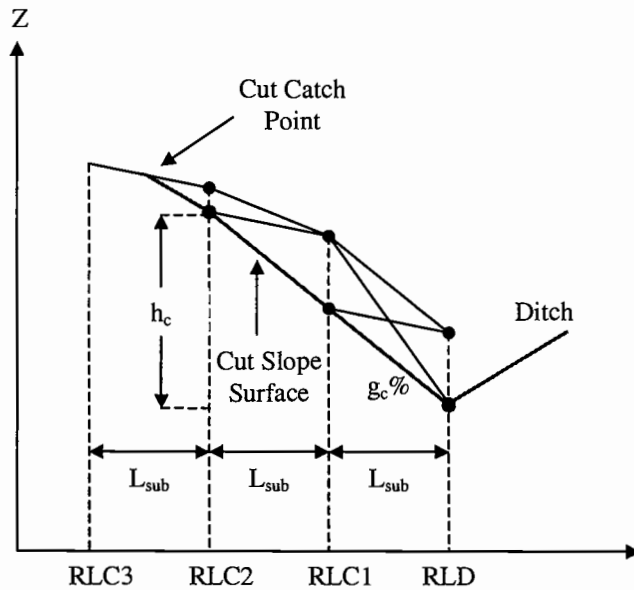


Figure A8-12. Cut and fill areas on cut slope section.

Case 1: If $GLDz > RLDz$, three sub cases occur based on the comparison between ground elevation ($GLC1z$) and the road elevation ($RLC1z$) at the first lateral point on the cut slope ($RLC1$).

(1) The model first computes $GLC1z$ and $RLC1z$. $GLC1z$ is computed as a function of X and Y coordinates of $RLC1$ based on DEM:

$$\begin{aligned} RLC1x &= RLDx - L_{sub} \\ RLC1y &= RLDy \end{aligned} \quad A8-38.$$

then, the model computes $RLC1z$ using cut slope grade, g_c , and L_{sub} :

$$RLC1z = RLDz + g_c L_{sub} \quad A8-39.$$

If $GLC1z > RLC1z$, the cut area is computed as follows:

$$Cut\ Area = L_{sub}(GLC1z - RLC1z)/2 + L_{sub}(GLDz - RLDz)/2 \quad A8-40.$$

(2) If $GLC1z = RLC1z$, the model computes the cut area as follows:

$$Cut\ Area = L_{sub}(GLDz - RLDz)/2 \quad A8-41.$$

then, the model stops the iteration and computes the total cut area.

(3) If $GLC1z < RLC1z$, it stops the iteration and computes the total cut area.

The cut area of the next subsections is computed using the same method.

Case 2: If $GLDz = RLDz$, the following three sub cases occur:

(1) If $GLC1z > RLC1z$, the cut area is computed as follows:

$$Cut\ Area = L_{sub}(GLC1z - RLC1z)/2 \quad A8-42.$$

(2) If $GLC1z = RLC1z$, there is no cut occurs.

(3) If $GLC1z < RLC1z$, it stops the iteration and computes the total cut area.

Penalty Costs on Cut Slopes:

If h_c is greater than the maximum cut slope height, $Maxh_c$, the model first considers increasing the grade of the cut slope, g_c , to a user-defined value of maximum grade, $Maxg_c$. If h_c becomes less than or equal to $Maxh_c$, the model considers locating curtain fence over the cut slope and computes its cost as a penalty cost (Figure A8-13). The area of the fence is computed based on the fence width (cut slope length, L_c) and length of the road stage, L_r , between two consecutive station points. The model estimates the cost of the fence by multiplying the fence area by a user-defined unit cost of the fence, C_{fence} in square meters.

$$Fence\ Cost = L_c L_r C_{fence} \quad A8-43.$$

After increasing the cut slope, if h_c is still greater than $Maxh_c$, the model considers constructing retaining wall. To compute cost of the wall, as a penalty cost,

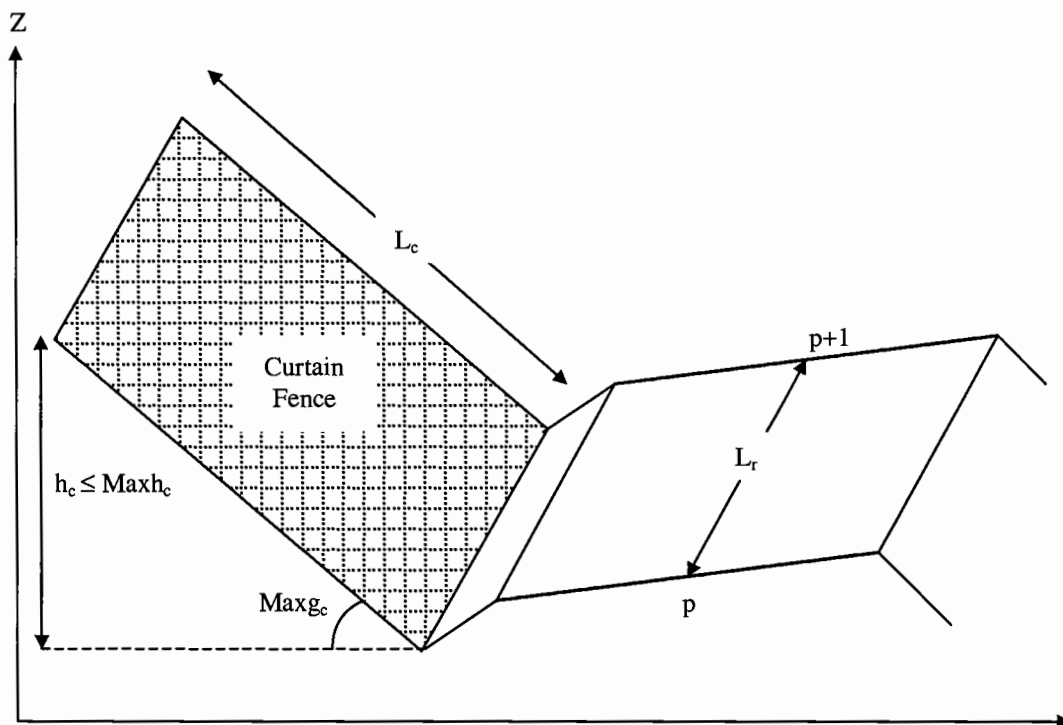


Figure A8-13. Locating curtain fence over the cut slope.

the model first computes the total wall volume, V_{wall} , and multiplies it by a user-defined unit cost of the wall, C_{wall} in cubic meters. Figure A8-14 indicates the geometry of the T-shape cantilever wall used in the model. In this figure, stem height, H_s , is computed as follows:

$$H_s = (GLD_z - RLD_z) - D_s \quad \text{A8-44.}$$

where D_s is a user-defined value for the minimum depth of the wall (e.g. 2 meters) in the ground. The thickness of the stem at the top, T_t , is usually at least 200 millimeters (Kramer, 1997). A minimum thickness of 300 millimeters is considered for footing,

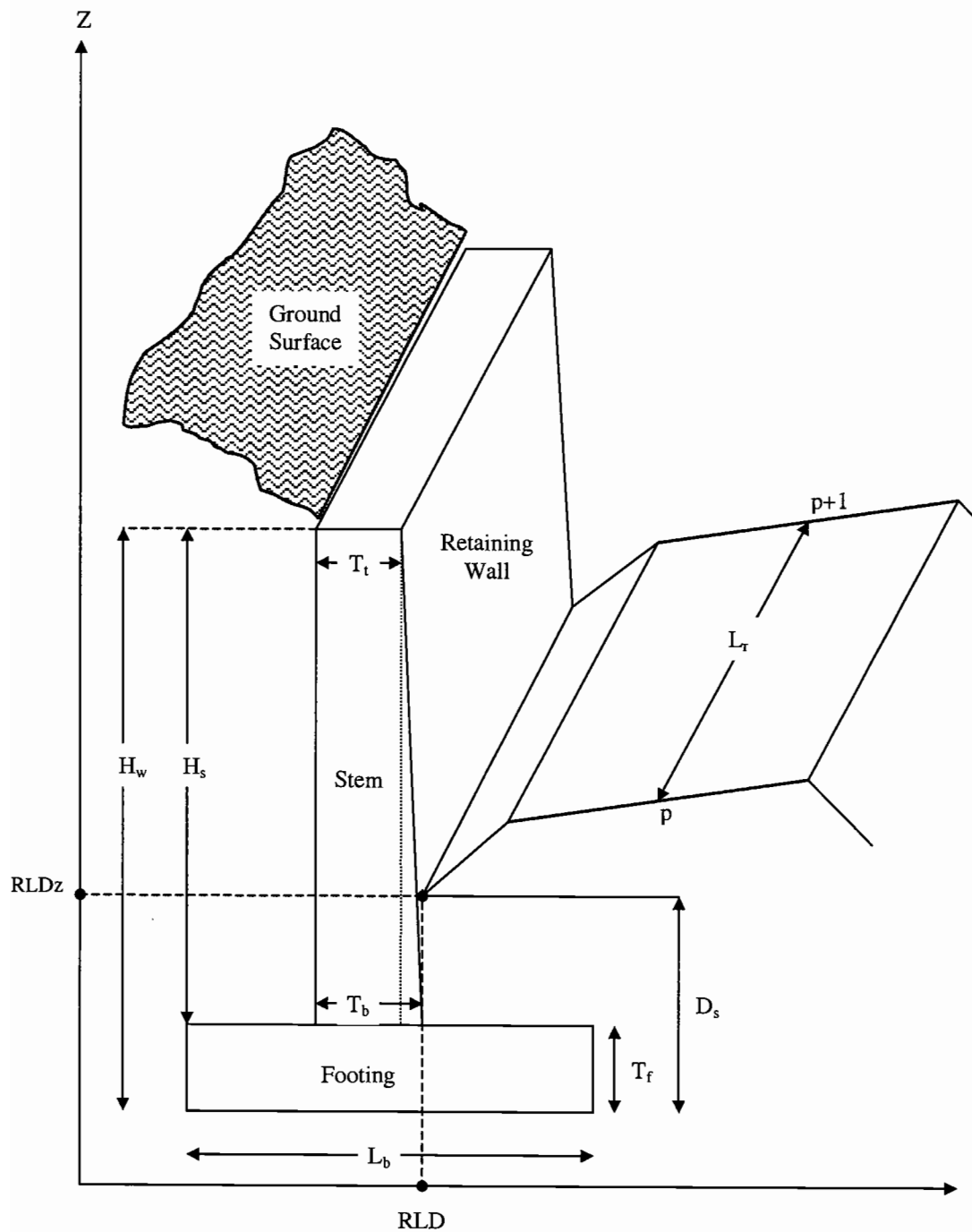


Figure A8-14. Geometry of a retaining wall.

T_f . The stem thickness at the base, T_b , is estimated to be equal to T_f . The footing thickness is assumed to be 8 % of H_w . Therefore, the variables are:

$$H_w = T_f / 0.08$$

$$H_s = H_w - T_f \quad \text{A8-45.}$$

The base length, L_b , is computed using Equation A8-46 (Kramer, 1997) developed for a simple special case without surcharge.

$$L_b = 1.5 \sqrt{k_a H_w^2 / 3} \quad \text{A8-46.}$$

where k_a , coefficient of active pressure, is computed based on the angle of internal friction, ϕ (Retaining Wall Design, 19XX):

$$k_a = \frac{1 - \sin \phi}{1 + \sin \phi} \quad \text{A8-47.}$$

The angle of internal friction is approximated based on the soil type. For example, ϕ is estimated as 30 degree for dry and dense silt type soil (Kramer, 1997).

Total wall volume, V_{wall} , is computed using the total wall cross section area and length of the road segment:

$$\text{Stem Area} = (T_t + T_b) H_s / 2$$

$$\text{Footing Area} = T_f L_b$$

$$V_{wall} = (\text{Stem Area} + \text{Footing Area}) L_r \quad \text{A8-48.}$$

then the model estimates the cost of the wall by multiplying the wall volume by a user-defined unit cost of the wall, C_{wall} in cubic meters.

$$\text{Wall Cost} = V_{wall} C_{wall} \quad \text{A8-49.}$$

Fill Slope:

In the fill slope, the model uses the same method used for the cut slope (Figure A8-15). The model divides the fill slope into lateral subsections. At each fill slope point, RRF , it compares the ground elevation, GLF_z , and fill slope elevation, RRF_z . If the ground elevation is less than the cut slope elevation, the model moves to the next subsection. Otherwise, it stops the iteration and computes the total fill area. In Figure A8-15, g_f is the grade on the fill slope in percent and h_f is the fill slope height. The model determines the grade on the fill slope and maximum cut slope height, $Maxh_f$, based on the soil type data stored in the attribute data file.

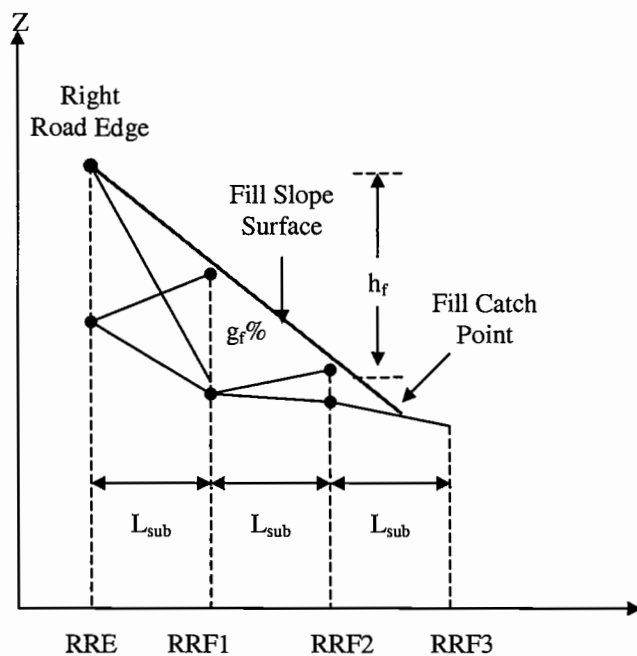


Figure A8-15. Cut and fill areas on fill slope section.

The model first computes the ground elevation, GRE_z , and road elevation, RRE_z , at the right road edge point (RRE). RRE_z is computed as follows:

$$RRE_z = Z_p + g_r RBW/2 \quad A8-50.$$

then, GRE_z is computed as a function of X and Y coordinates of RRE based on DEM and the specific geometric conditions in Figure A8-1:

$$\begin{aligned} RRE_x &= X_p + RBW/2 \\ RRE_y &= Y_p \end{aligned} \quad A8-51.$$

The model compares the ground elevation, GRE_z , and road elevation, RRE_z , at the right road edge point (RRE). There are two cases that might occur:

Case 1: If $GRE_z = RRE_z$, the following three sub cases occur:

(1) The model first computes $GRF1_z$ and $RRF1_z$. $GRF1_z$ is computed as a function of X and Y coordinates of $RRF1$ based on DEM:

$$\begin{aligned} RRF1_x &= RRE_x + L_{sub} \\ RRF1_y &= RRE_y \end{aligned} \quad A8-52.$$

then, the model computes $RRF1_z$ using fill slope grade, g_f , and L_{sub} :

$$RRF1_z = RRE_z - g_f L_{sub} \quad A8-53.$$

If $GRF1_z < RRF1_z$, the fill area is computed as follows:

$$Fill\ Area = L_{sub}(RRF1_z - GRF1_z)/2 \quad A8-54.$$

(2) If $GRF1_z = RRF1_z$, there is no cut occurs.

(3) If $GRF1_z > RRF1_z$, it stops the iteration and computes the total fill area.

The fill area of the next subsections is computed using the same method.

Case 2: If $GRE_z < RRE_z$, the following three sub cases occur:

(1) If $GRF1z < RRF1z$, the fill area is computed as follows:

$$Fill\ Area = L_{sub}(RREz-GREz)/2 + L_{sub}(RRF1z-GRF1z)/2 \quad A8-55.$$

(2) If $GRF1z = RRF1z$, there is no cut occurs.

(3) If $GRF1z > RRF1z$, it stops the iteration and computes the total fill area.

Penalty Costs on Fill Slopes:

If h_f is greater than the maximum fill slope height, $Maxh_f$, the model first considers increasing the grade of the fill slope, g_f , to a user-defined value of maximum grade, $Maxg_f$. If h_f becomes less than or equal to $Maxh_f$, the model locates the fill slope as described above. After increasing the fill slope, if h_f is still greater than $Maxh_f$, the model considers constructing retaining wall. To compute cost of the wall, as a penalty cost, the model first computes the total wall volume, V_{wall} , and multiplies it by a user-defined unit cost of the wall, C_{wall} in cubic meters. The model used the T-shape cantilever wall illustrated in Figure A8-14. In this figure, steam height, H_s , is computed as follows:

$$H_s = (GREz - RREz) - D_s \quad A8-56.$$

The retaining wall is also considered as a penalty cost when the distance from fill slope catch point to the stream channel is less than the required stream distance.

APPENDIX 9. Earthwork Volume

The earthwork volume is estimated using the average end-area method (Hickerson, 1964). This method is generally used in the field of forest road design due to its simplicity. The average end-area method tends to overestimate the volume (Hickerson, 1964). The length of the road stage between two consecutive cross sections must be kept adequately short to compute the earthwork volume more accurately particularly in rough and mountainous terrain, where the type of the cross sections change rapidly along the roadway. The model locates the cross sections at more frequent intervals (about 6 meters) to reduce this error. If the road stage is a transition stage in which the ground profile changes from cut to fill or fill to cut, the net volume is computed using the respective cut and fill designation. It is assumed that the earthwork allocation within the same road stage is made at no extra cost.

The net earthwork volume (V_{net}) between two cross sections (p and $p+1$) is computed by multiplying the distance between stations (L_r) by the average of the end cross section areas. If the road stage is cut (or fill) stage, V_{net} is (Hickerson, 1964):

$$V_{net} = \frac{A_p + A_{p+1}}{2} L_r \quad \text{A9-1.}$$

where A_p and A_{p+1} are the areas of the cross sections at station points p and $p+1$, respectively. When going from a cut and fill cross section to through cut or through fill cross section at the next road station, the model determines the run-out distance. Figure A9-1 indicates the typical road stage where cross sections are going from cut and fill to through cut. In this figure, L_{fill} is fill run-out distance, $A_{cut_{p+1}}$ is the cut area

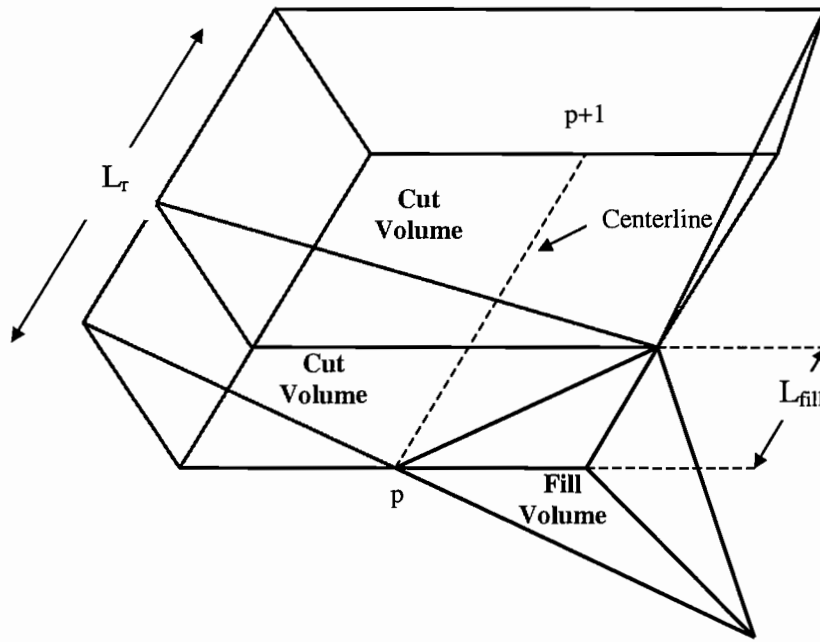


Figure A9-1. Earthwork Volume: cut and fill section to through cut section.

at station point $p+1$, and A_{fill_p} and A_{cut_p} are fill and cut areas at station point p , respectively. The fill run-out distance is (Lecklider et al., 1971):

$$\frac{A_{fill_p}}{A_{fill_p} + A_{cut_{p+1}}} = \frac{L_{fill}}{L_r}$$

$$L_{fill} = \frac{A_{fill_p} L_r}{(A_{fill_p} + A_{cut_{p+1}})} \quad \text{A9-2.}$$

The model computes cut volume (V_{cut}) and fill volume (V_{fill}) at the road stage as follows (Lecklider et al., 1971):

$$V_{cut} = \frac{(A_{cut_p} + A_{cut_{p+1}}) L_r}{2} \quad \text{A9-3.}$$

$$V_{fill} = \frac{A_{fill_p} L_{fill}}{3} \quad \text{A9-4.}$$

then, net volume (cut) $V_{net} = V_{cut} - V_{fill}$. When going from through fill cross section to through cut cross section at the next road station or vice versa, the model determines the cut run-out and fill run-out distances, L_{cut} (Figure A9-2) (Lecklider et al., 1971):

$$L_{cut} = \frac{Acut_{p+1}L_r}{(Acut_{p+1} + Afill_p)} \quad A9-5.$$

$$L_{fill} = \frac{Afill_pL_r}{(Afill_p + Acut_{p+1})} \quad A9-6.$$

The model computes V_{cut} and V_{fill} in Equation A9-7 and A9-8. If $V_{cut} > V_{fill}$ there is cut, and if $V_{cut} < V_{fill}$ there is fill. Otherwise, there is no cut or fill.

$$V_{cut} = \frac{Acut_{p+1}L_{cut}}{3} \quad A9-7.$$

$$V_{fill} = \frac{Afill_pL_{fill}}{3} \quad A9-8.$$

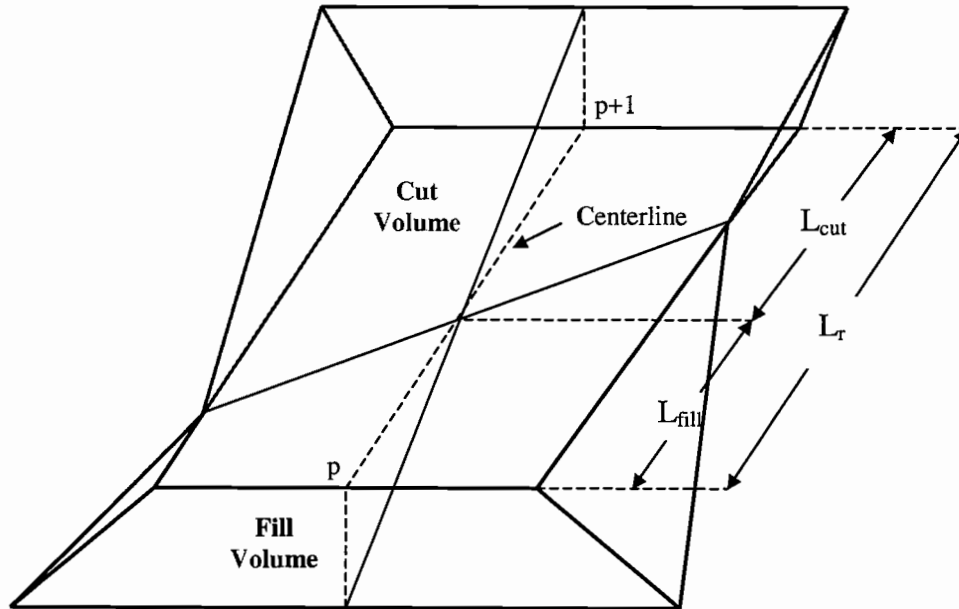


Figure A9-2. Earthwork Volume: through fill to through cut section.

APPENDIX 10. Offtracking around the Horizontal Curve

When traveling around the horizontal curve, the rear wheels of the vehicles do not track in the same path as the front wheels, which is called offtracking. To accommodate the offtracking of the rear wheels, extra road width is required on the inside of the curve (Figure A10). The required curve widening depends on various factors such as vehicle dimensions, curve radius, and the central angle of the curve.

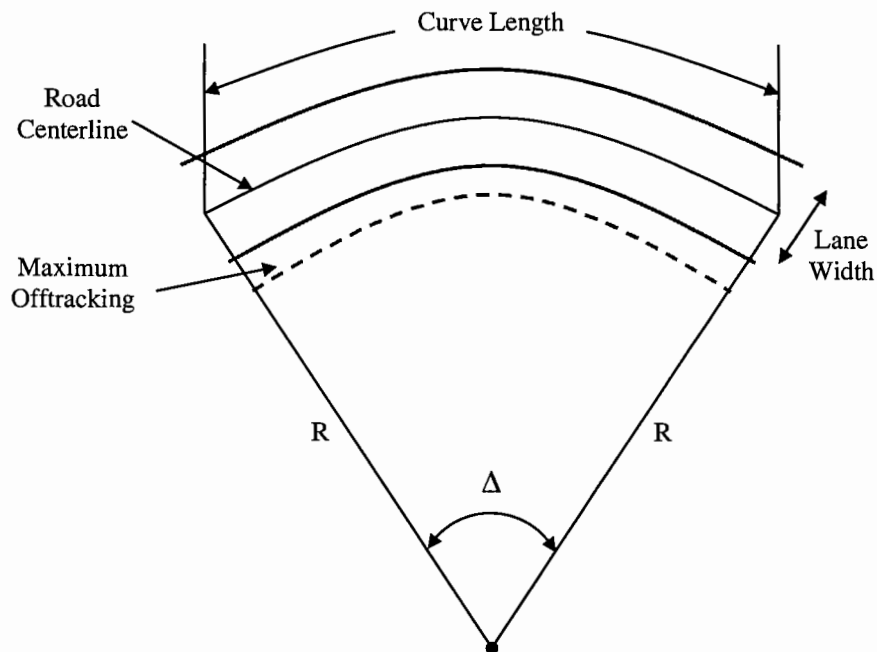


Figure A10. Maximum offtracking on a horizontal curve.

To predict offtracking, the model employs an empirical method, developed by USDA Forest Service to provide the designers with quick, easy, and relatively

accurate results. The following formulation used in the model (Cain and Langdon, 1982):

$$O.T. = (R - \sqrt{R^2 - L^2}) \left[1 - \exp^{(-0.015\Delta \frac{R}{L} + 0.216)} \right] \quad A10-1.$$

where $O.T.$ is total vehicle offtracking, Δ is the central angle in degree, R is radius at the centerline of the roadway, and L is the length of tractor plus trailer. The length of tractor is computed in Equation A10-2 based on the length of the wheel base of a vehicle unit, L :

$$L = \sqrt{L_1^2 - L_2^2 + L_3^2} \quad A10-2.$$

where L_1 is wheel base of the tractor, L_2 is the length of the stinger measured from the middle of the tractor rear duals to the end of the stinger, and L_3 is bunk to bunk distance minus the length of the stinger.

APPENDIX 11. Clearing the Middle Ordinate Distance for SSD

The general rule of the safe stopping distance around a horizontal curve is that the middle ordinate distance, Ms , must be visually clear, so that the available safe stopping distance is sufficient for the driver's line of sight (Figure 11-1). The AASHTO (1990) standards require that a driver should be able to see from an eye height of 1070 millimeters (about 3.5 feet) and stop before hitting an object of 150 millimeters (about 0.5 feet) at the mid-ordinate. On forest roads, 600 millimeters (about 2 feet) of object height at the middle ordinate point is generally used. In the model, the designer defines the object height, h_{obj} (Kramer, 1993).

The model first computes the height of the cut slope at the middle ordinate point by calculating the difference between ground elevation at the mid-point, Zg_m and road surface elevation at middle curve point, Zr_m . Equation A11-1 is used to compute Zr_m based on the elevation at the beginning point of the curve, PCz_{i-1} , curve length Lh_{i-1} , and road grade around the curve, Gc_{i-1} (Figure A10-1).

$$Zr_m = PCz_{i-1} + Gc_{i-1}(Lh_{i-1}/2) \quad \text{A11-1.}$$

The ground elevation at the middle ordinate point is computed as a function of its X_m and Y_m coordinates based on DEM data. The model computes X_m and Y_m coordinates based on the coordinates of the beginning point (PCx_{i-1} and PCy_{i-1}) and ending point (PTx_{i-1} and PTy_{i-1}) of the curve as follows:

$$\begin{aligned} X_m &= PCx_{i-1} + (PTx_{i-1} - PCx_{i-1})/2 \\ Y_m &= PCy_{i-1} + (PTy_{i-1} - PCy_{i-1})/2 \end{aligned} \quad \text{A11-2.}$$

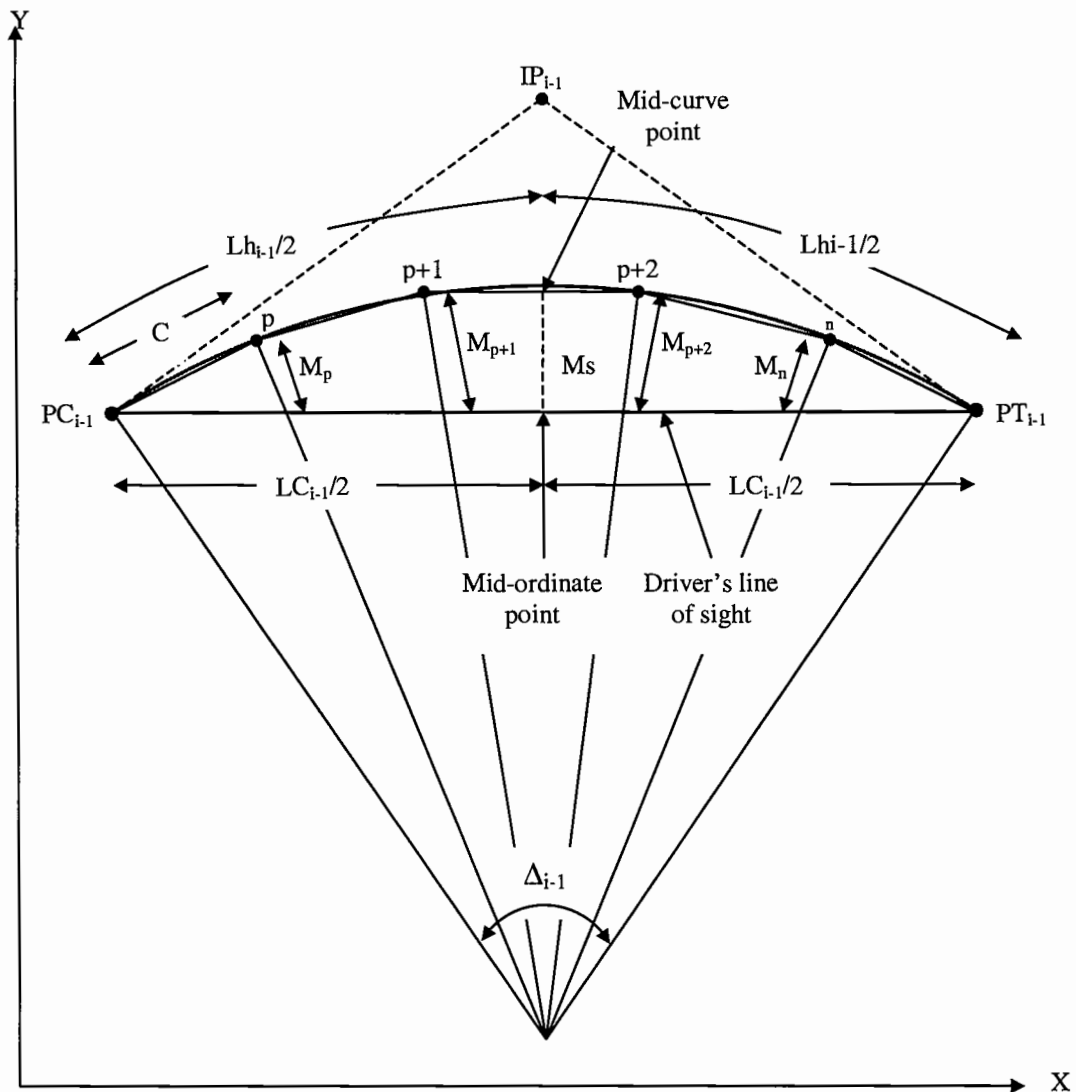


Figure A11-1. Clearing the middle ordinate distance for SSD.

If cut slope height is higher than h_{obj} , the model lays back cut slope from road edge to the driver's line of sight to provide minimum safe stopping distance. In order to layback the cutslope, the horizontal distance of M_p from each station point, p , to the line of sight is computed (Figure A11-2).

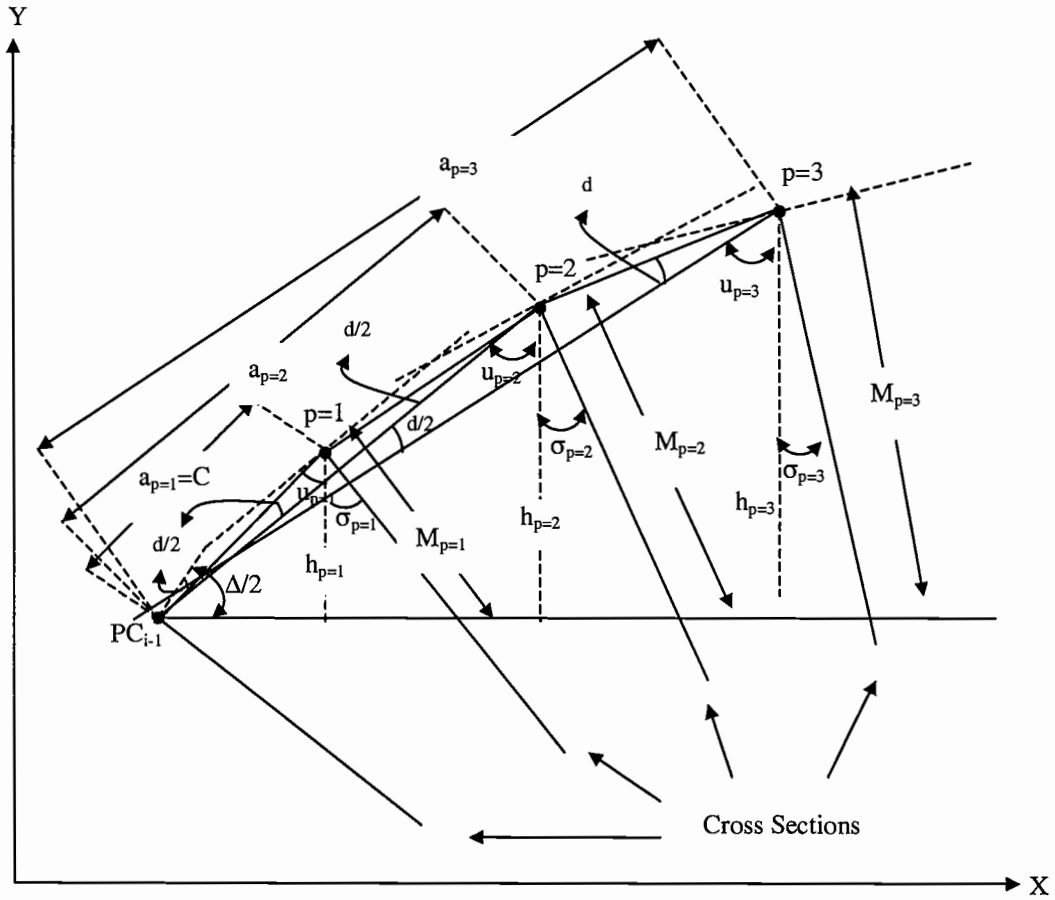


Figure A11-2. Computing M_p distances.

The model first computes the angle $u_p = 90 - (\Delta/2 - d/2)$, then, the formulation of σ_p is simplified as follows:

$$\sigma_p = 90 - d/2 - u_p$$

$$\sigma_p = \Delta/2 - pd \quad \text{A11-3.}$$

In Figure A11-1, h_p can be computed by using following equalities:

$$h_p = \sin(\Delta/2 - (pd/2))a_p \quad \text{A11-4.}$$

$$h_p = \cos(\sigma_p)M_p \quad \text{A11-5.}$$

If Equation 11-4 and 11-5 are combined with respect to h_p in order to compute M_p as follows:

$$\sin(\Delta/2 - (pd/2))a_p = \cos(\sigma_p)M_p$$

$$M_p = \frac{\sin(\Delta/2 - (pd/2))a_p}{\cos(\sigma_p)} \quad \text{A11-6.}$$

In the first station point, $a_{p=1}$ is equal to user defined value of chord distance, C . The model computes the $a_{p=2}$ using Equation A11-7 based on the specific geometric conditions in Figure A11-3.

$$a_{p=2} = 2\cos(d/2)C \quad \text{A11-7.}$$

Then, a general formula of a_p for the rest of the station points along the curve is developed. Figure A11-4 shows the elements of the formulation used to compute a_p

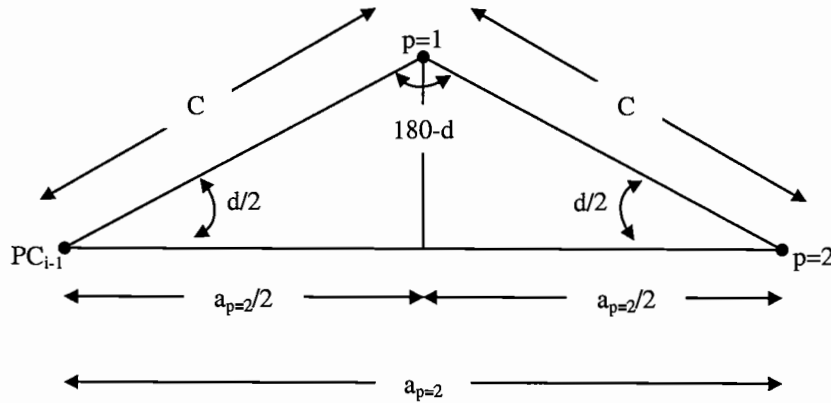


Figure A11-3. $a_{p=2}$ distance between PC and the second station point on the curve.

at station point three and following stations. The formulation for a_p at the 3rd, the 4th, and n th station points are developed as follows:

$$\text{Station point 3 } (p=3): \quad a_{p=3} = a_{p-2} + 2\cos((p-1)d/2)C \quad \text{A11-8.}$$

$$\text{Station point 4 } (p=4): \quad a_{p=4} = a_{p-2} + 2\cos((p-1)d/2)C \quad \text{A11-9.}$$

$$\text{Station point } n \text{ } (p=n): \quad a_{p=n} = a_{n-2} + 2\cos((n-1)d/2)C \quad \text{A11-10.}$$

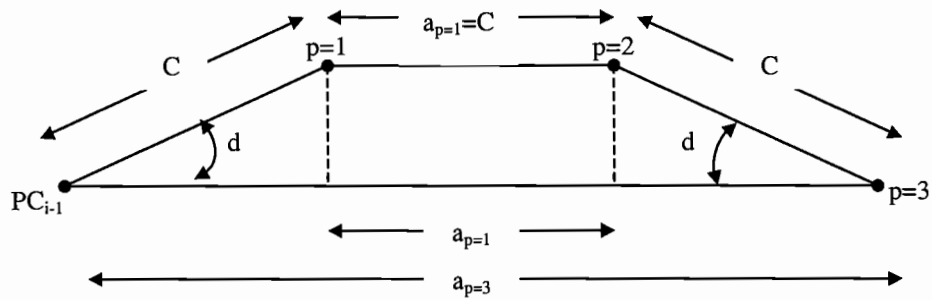


Figure A11-4. $a_{p=3}$ distance between PC and the third station point on the curve.

APPENDIX 12. Clearing and Grubbing Limits

The first step in the road construction process is clearing the trees, brushes, and stumps from the road right of way. The clearing and grubbing area (CA_r) at road stage r is computed based on the average clearing width of two consecutive stations and the distance between these stations.

$$CA_r = CW_{avr}L_r \quad A12-1.$$

where CW_{avr} , average clearing width, is estimated as follows:

$$CW_{avr} = \frac{CW_p + CW_{p+1} + 4EW}{2} \quad A12-2.$$

Figure A12 indicates the elements of clearing area. The model considers the extra clearing width (EW) of 1.5 meters (about 5 feet) beyond the catch points to assure that stumps and live trees will not fall off the cut bank and onto the road.

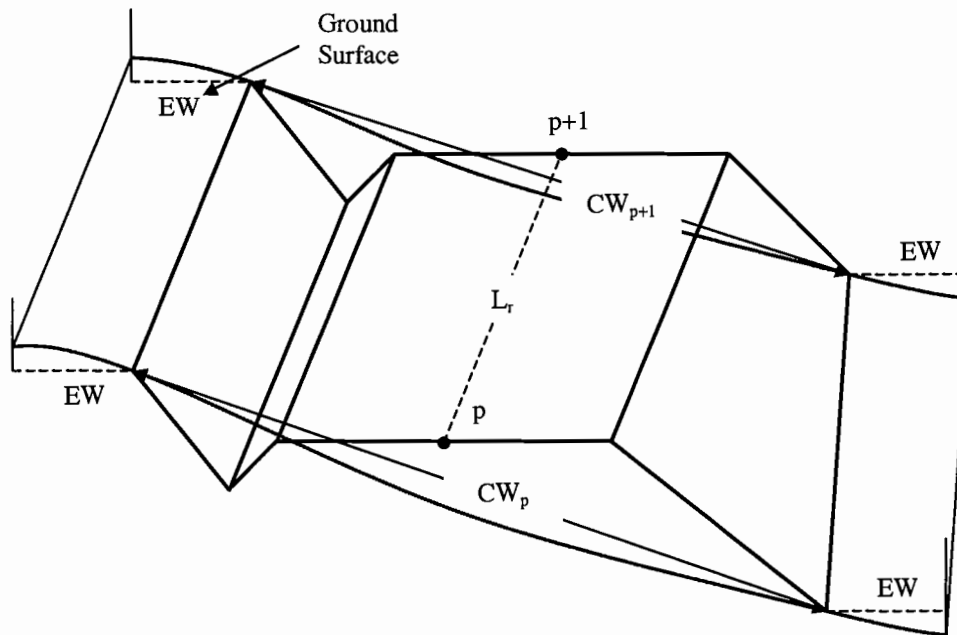


Figure A12. Clearing and grubbing limits.

After determining locations of the culverts, the model estimates the culvert length, L_c . It is required that there is at least 0.3-meter (about 1 foot) fill over the top of the culvert inlet. Besides, the slope of the culvert flow line, g_{fl} , must be at least 2% to prevent sediment and debris from accumulating inside the culvert barrel. The model considers a maximum slope of the flow line, $Maxg_{fl}$ (e.g. 45%) to help disperse erosive energy of the falling water on the downspouts. Maximum culvert length, $MaxL_c$, is also considered to provide continuous water movement through the culvert. The formulation is presented for a culvert located on a sample cut and fill cross section (Figure A13-2). The culverts are skewed by a user-defined angle to efficiently direct the water into the culvert entrance and reduce debris blockage of the culvert inlet. In the model, the perpendicular distance (L_{perc}) at the road cross section is used

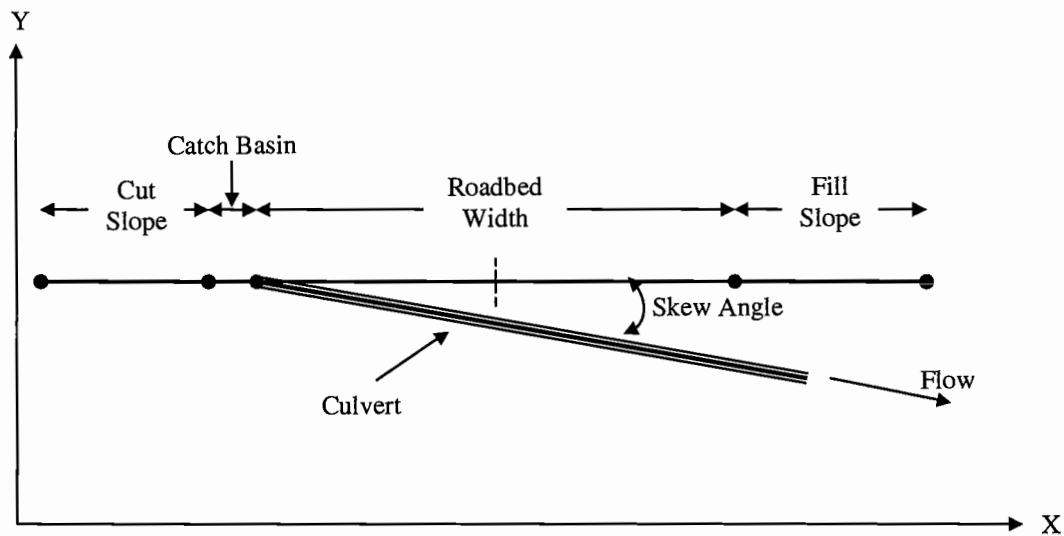


Figure A13-2. Plan view of the culvert on the cut and fill cross section.

as a reference for a culvert location, then, the final culvert length is computed based on this perpendicular distance and skew angle:

$$L_c = L_{per_c} / \cos(\text{Skew}) \quad \text{A13-3.}$$

In calculating the culvert length, the model considers two possible scenarios:

Scenario 1: The model locates the culvert as shown in Figure A13-3. In this figure, RRF_{last} is the catch point at the fill slope, and RLD is the location of the ditch point. In the previous sections, the formulations for the coordinates (X , Y , and Z) of these two points are presented earlier. The model first computes L_{per_c} :

$$L_{per_c} = \sqrt{(RRF_{xlast} - RLD_x)^2 + (RRF_{y_{last}} - RLD_y)^2} \quad \text{A13-4.}$$

then, L_c is computed using equation A13-3. The model considers adding a user-defined extra length of L_{ext_c} into the culvert length beyond the fill. If $L_c > \text{Max}L_c$,

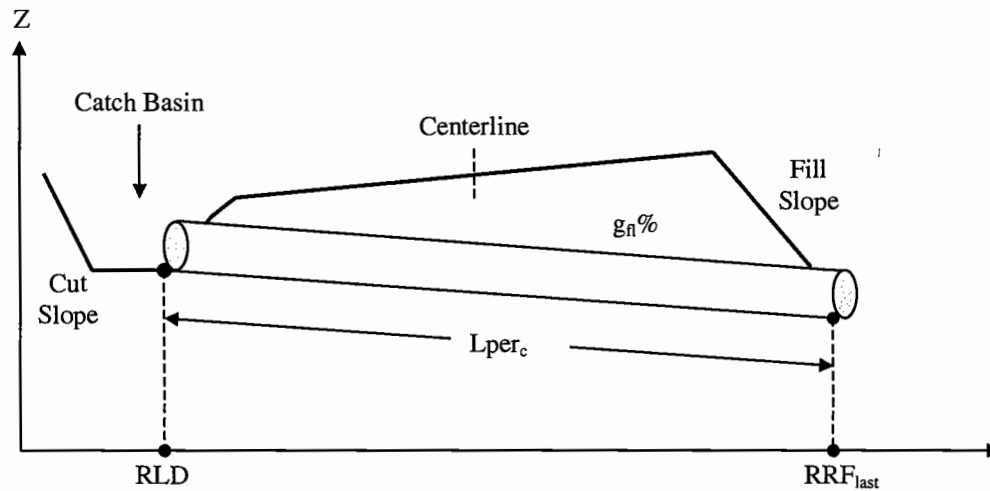


Figure A13-3. Scenario 1: Geometry of a ditch relief culvert.

model moves to the second scenario. Otherwise, it keeps the current culvert length and computes g_{fl} :

$$g_{fl} = \frac{RLDz - RRFz_{last}}{L_{perc}} \quad A13-5.$$

If $g_{fl} > Maxg_{fl}$, model moves to the second scenario. Otherwise, it saves the current culvert length as the final length.

Scenario 2: If $L_c > MaxL_c$ or $g_{fl} > Maxg_{fl}$ in the first scenario, the model locates the culvert as shown in Figure A13-4. In this figure, the slope of the flow line is 2%, CP is the catch point of flow line at the fill slope, L_h is the distance between

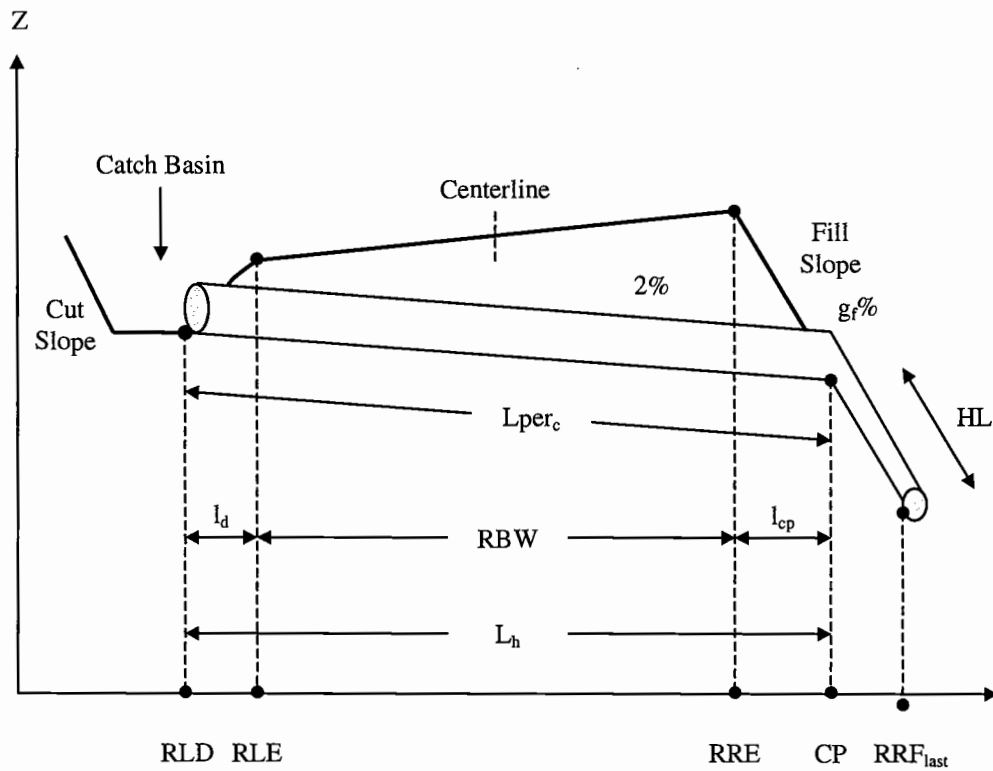


Figure A13-4. Scenario 2: Geometry of a ditch relief culvert.

ditch point and CP , l_{cp} is the distance between right road edge and CP , and HL is the length of the half-round culvert section attached below the outlet of a relief culvert outlet. In the previous sections, the formulations for the coordinates (X , Y , and Z) of points RRE and RLD , and for ditch length (l_d) are presented earlier. The ground elevation at CP can be computed using following equations:

$$CPz = RREz - l_{cp}g_f \quad A13-6.$$

$$CPz = RLDz - L_h 0.02 \quad A13-7.$$

where $L_h = l_d + RBW + l_{cp}$. l_{cp} is formulated as follows:

$$l_{cp} = L_h - l_d - RBW \quad A13-8.$$

then the following equality is derived using Equation A13-6 and A13-7:

$$RREz - l_{cp}g_f = RLDz - L_h 0.02 \quad A13-9.$$

When l_{cp} in Equation A13-9 is replaced by its equality in Equation A13-8, L_h can be stated as follows:

$$L_h = \frac{RREz - RLDz + (l_d + RBW)g_f}{g_f - 0.02} \quad A13-10.$$

then the model computes CPz using Equation A13-7 and L_{perc} in Equation A13-11:

$$L_{perc} = \sqrt{(RLDz - CPz)^2 + L_h^2} \quad A13-11.$$

Finally, the length of the half-round culvert section is computed as follows:

$$HL = \sqrt{(CPz - RRFz_{last})^2 + \left(\frac{CPz - RRFz_{last}}{g_f} \right)^2} \quad A13-12.$$

The model considers hand-placed riprap material on the catch basin and on the downspout area (Figure A13-5). The amount of rock is defined by the user. If the culvert is placed close to the stream crossing, the model uses the machine-placed method where the rocks are dumped on the fill slope area and on the downspout. The model computes the volume of the machine-placed riprap based on the dimensions of the fill slope and length of the road stage, L_r . It is assumed that the riprap material is located along the roadway for a length of a road stage. Figure A13-6 illustrates a machine-replaced riprap installation on a road stage crossing a stream. In this figure, w_{rr} is user-defined width of the riprap material on the road template. The volume of the riprap material is estimated using the average fill slope height of the road stage on the both sides, h_{f1} and h_{f2} :

$$V_{rr} = w_{rr}(h_{f1} + h_{f2})L_r \quad \text{A13-13.}$$

where h_{f1} is computed by taking the average of left fill height of two consecutive road stations while h_{f2} is the average of right fill height of these stations.

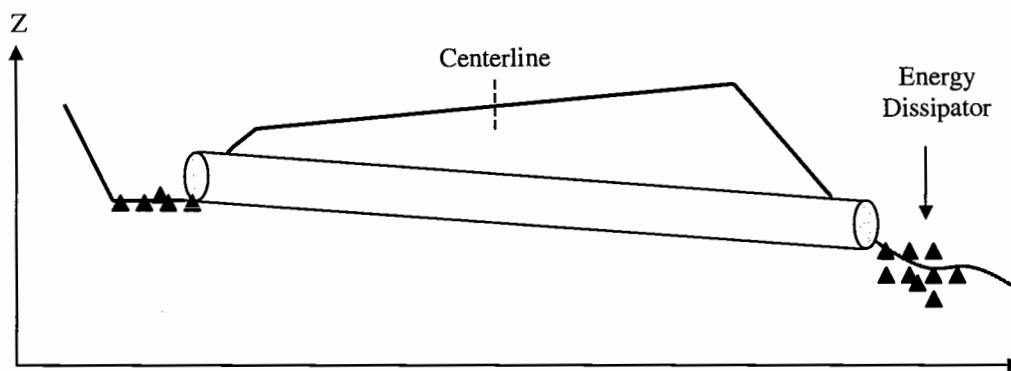


Figure A13-5. Hand-placed riprap material.

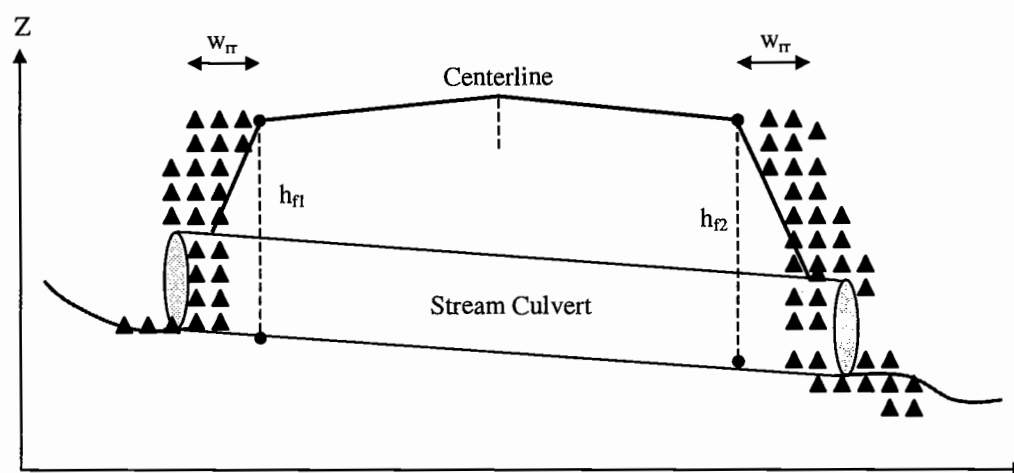


Figure A13-6. Machine-placed riprap material.

APPENDIX 14. Surfacing Cost Components

The model computes required amount of surfacing material based on the dimension of the road section and estimated surfacing depth. The quantity of the traction surface material and base course is computed separately. Figure A14 illustrates the road surfacing elements of a sample road stage located between two identical consecutive cross sections. In this figure, RW is road width (travel way), TSW is the surfacing width at the bottom of the traction surface (or at the top of the base course), g_c (e.g. 1:1) is the side slope of the surface material, and h_{ts} and h_{bc} are the height of the traction surface and base course, respectively. h_{ts} and h_{bc} are

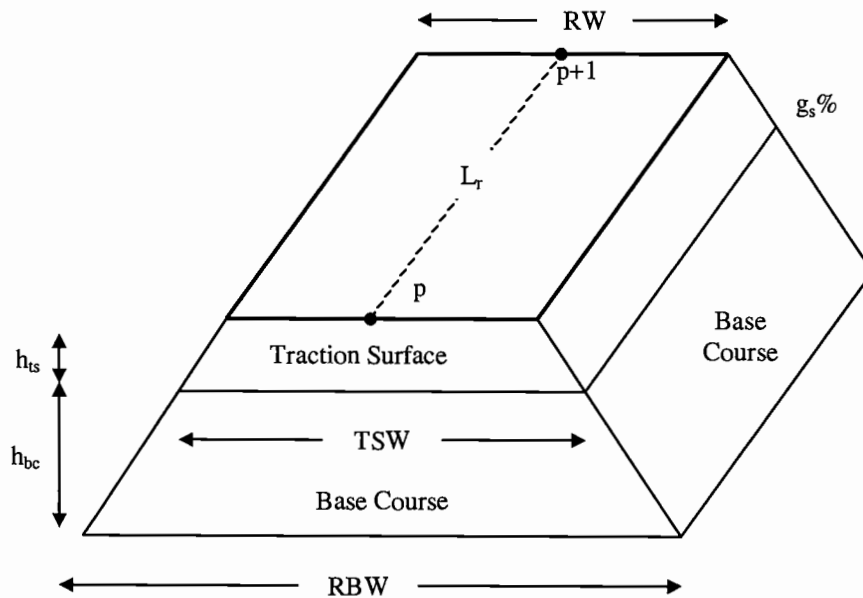


Figure A14. Elements of the aggregate surfacing.

determined based on the soil type at the road stage. TSW at station point p is computed as follows:

$$TSW = RW + 2(h_{ts}/g_c) \quad A14-1.$$

The following formulations are used to compute the cross section areas of the traction surface (A_{ts}) and base course (A_{bc}):

$$A_{ts} = (RW + TSW)h_{ts}/2 \quad A14-2.$$

$$A_{bc} = (TSW + RBW)h_{bc}/2 \quad A14-3.$$

then the quantity of the surfacing material for traction surface (Q_{ts}) and base course (Q_{bc}) are computed as follows:

$$Q_{ts} = A_{ts}h_{ts}(1 + c_{ts}) \quad A14-4.$$

$$Q_{bc} = A_{bc}h_{bc}(1 + c_{bc}) \quad A14-5.$$

where c_{ts} and c_{bc} are the compaction rate (in percent) of the material used for traction surface and base course, respectively.

After estimating the quantity of the surfacing material, the model computes components of the surfacing cost including rock purchasing or production cost, hauling cost, processing costs (compacting, mixing, and placing) and testing cost. In the model, it is assumed that the surfacing material is purchased from a local rock sources. The purchasing cost, C_p (including loading cost), can be defined by the designer based on the local economic data. If surface rock is obtained from natural sources, the total cost of rock production involving drilling, shooting, ripping, crushing, stockpiling, and loading can be estimated based on the local information, and replace the purchasing cost.

The hauling cost, C_h , is divided into fixed hauling cost and variable hauling cost. The fixed hauling cost (u_{fh}) per cubic meters is defined by the cost guide (USDA Forest Service, 1999) considering truck size, approximate legal load limit, and delay time. The variable hauling cost (u_{vh}) per cubic meters per kilometers based on round trip haul distance and average truck speed (loaded and empty) is also provided by the cost guide. The formulation of the total hauling cost is:

$$C_h = (Q_{ts} + Q_{bc})(u_{fh} + u_{vh}D_{mr}) \quad A14-6.$$

where D_{mr} is the distance (in kilometers) to the local resources. It is assumed that the hauling cost per cubic meters does not change by size of the rock hauled.

Processing of the surface material involves compacting, mixing, and placing activities. The processing cost, C_{pro} , is computed by multiplying the sum of the basic unit costs of these activities (u_p) by the total amount of surfacing material:

$$C_{pro} = u_p(Q_{ts} + Q_{bc}) \quad A14-7.$$

The testing cost, C_t , is divided into fixed testing cost and variable testing cost. The fixed cost per cubic meters of the surface material considered in the model is the cost of the Los Angeles Abrasion (LAR) test (Pearce, 1974) for wear. In LAR test, the suitability of the surfacing rock is tested in laboratories. The fixed testing cost (C_{ft}) is defined by the cost guide (USDA Forest Service, 1999). The variable testing costs include gradation and Sand Equivalent (SE) test costs. These tests are applied to make sure that the aggregate rocks are sufficiently durable and hard to resist fracturing under tire loads. The variable costs per cubic meters are also obtained from the cost guide. Therefore, the total testing cost is:

$$C_t = C_{ft} + u_{vt}(Q_{ts} + Q_{bc}) \quad \text{A14-8.}$$

where u_{vt} is the sum of the basic unit costs of the variable costs per cubic meters of the surfacing material. Finally, the total surfacing cost, C_s , is formulated in the following equation:

$$C_s = C_p + C_h + C_{pro} + C_t \quad \text{A14-9.}$$

APPENDIX 15. Seeding and Mulching Area

The seeding and mulching area (A_{sfm}) at road stage r is estimated based on the average width of bare cut and fill slopes (CFW_{avr}) of two consecutive stations and the distance between these stations (Figure A15).

$$A_{sfm} = CFW_{avr} L_r \quad A15-1.$$

where CFW_{avr} is estimated as follows:

$$CFW_{avr} = \frac{CSW_p + CSW_{p+1} + FSW_p + FSW_{p+1} + 4EW}{2} \quad A15-2.$$

where CSW_p and FSW_p are the lengths of the cut and fill slopes at station point p , respectively. The model considers the extra clearing and grubbing width (EW) of 1.5 meters beyond the catch points.

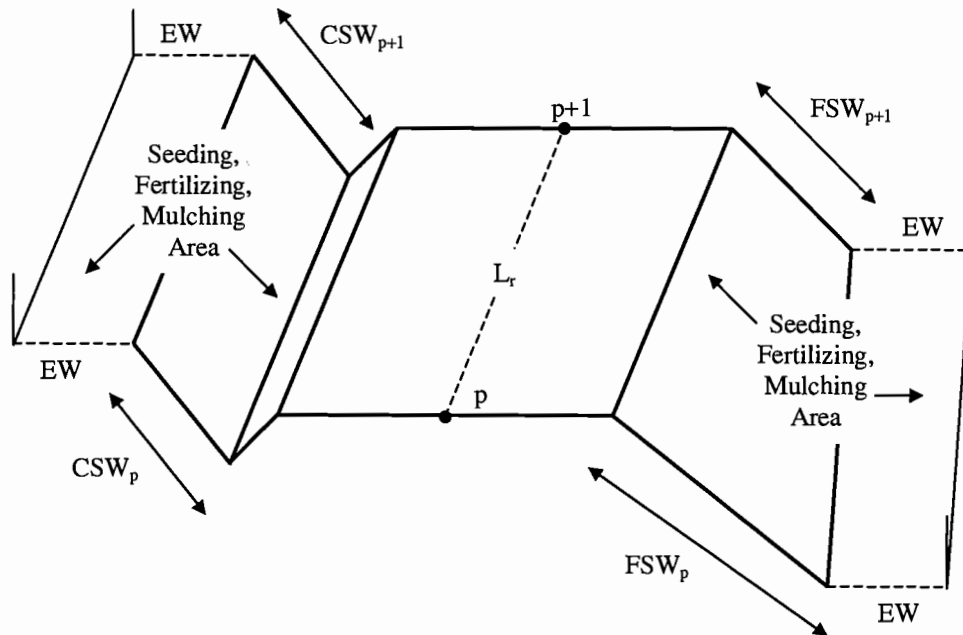


Figure A15. Seeding and mulching area.

APPENDIX 16. Vehicle Performance

The characteristics of the vehicle are defined by the designer during the data preparation process. These characteristics include engine specifications (horsepower, brake horsepower, and fuel consumption rate), vehicle weight (loaded and unloaded gross weight), and tire data (width, diameter, tire slip, load factor, inflation rate, maximum acceptable tire wear rate, and weight distribution).

The model computes the vehicle speed at the each road stage using tire weight distribution, flywheel power, gross thrust, and total resistance. The tire weight distribution of a sample truck (stinger type with trailer) is shown in Figure A16-1 (Botha et al. 1977). In this figure, tire types are identified as steering wheels (*S*), drivers (*D*), and trailers (*T*). The flywheel power data can be obtained from the engine performance tables. The tractive force per tire is computed as follows (Mannering and Kilareski, 1990):

$$F = \mu W$$

16-1.

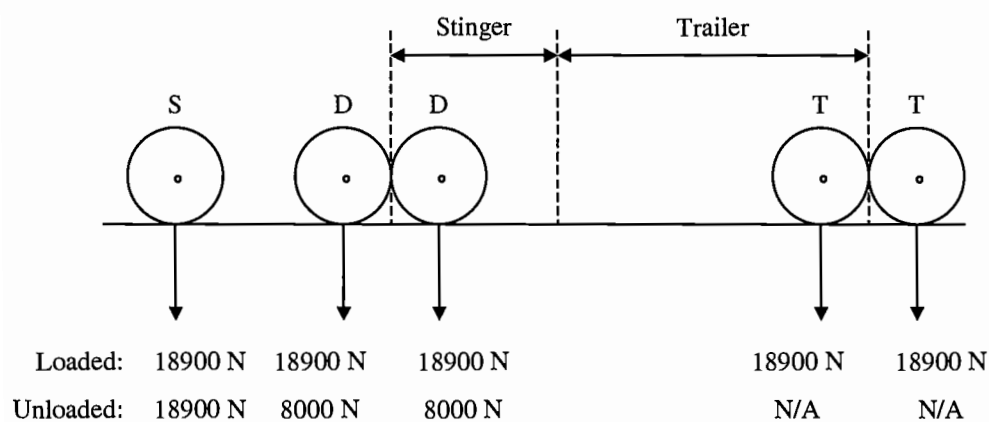


Figure A16-1. Dynamic wheel load distribution on stinger type truck (loaded).

where F is gross thrust in Newton, W is the dynamic wheel load normal to soil surface in Newton, and μ is the coefficient of road adhesion. The coefficient of adhesion for gravel forest road is about 0.36 (Sessions et al., 1986).

The total resistance includes grade resistance and rolling resistance. Air resistance is excluded due to low speed of logging trucks traveling on low volume forest roads. Grade resistance is computed based on the gross vehicle weight (GW in kilogram), and road grade (G in percent) (Mannering and Kilareski, 1990):

$$R_g = GW(G) \quad 16-2.$$

then the model computes the rolling resistance using the following equation (Mannering and Kilareski, 1990):

$$R_r = GW(f_r) \quad 16-3.$$

where the coefficient of rolling resistance (f_r) varies depending on the road surface type. The vehicle uphill speed (V in meters per minute) is calculated based on constant velocity, horsepower (pwr) and estimated tire slip (s) as follows:

$$V = \frac{60000pwr}{(1+s)R_g + R_r} \quad 16-4.$$

The limiting speed of the vehicle around the horizontal curve is computed using Equation A3-1, considering vehicle weight, side friction force, centrifugal force, curve radius, side friction coefficient, and super elevation. The vehicle downhill speed (V in meters per minute) is determined using the engine brake horsepower available ($Bpwr$):

$$V = \frac{60000Bpwr}{R_g - R_r}(1+s) \quad 16-5.$$

where V must produce sufficient net thrust to overcome the sum of the resistances.

The vehicle speed also has to be less than or equal to the maximum design speed defined by the designer.

After determining the vehicle speed for each road stage along the road section, total road section is divided into the subsections in which the difference between the highest and the lowest vehicle speed must be less than a user-defined increment speed, V_{inc} (e.g. 85 meters per minute). For each subsection, the lowest vehicle speed is assigned as the average vehicle speed of this subsection as indicated in Figure A16-2, in which $V_2 - V_1 < V_{inc}$ in the first subsection, $V_3 - V_1 \geq V_{inc}$ in the second subsection, and $V_3 - V_4 \geq V_{inc}$ in the third subsection. The travel time is computed using the vehicle speeds of three consecutive subsections, V_b , V_m , and V_e . The acceleration (AR) and

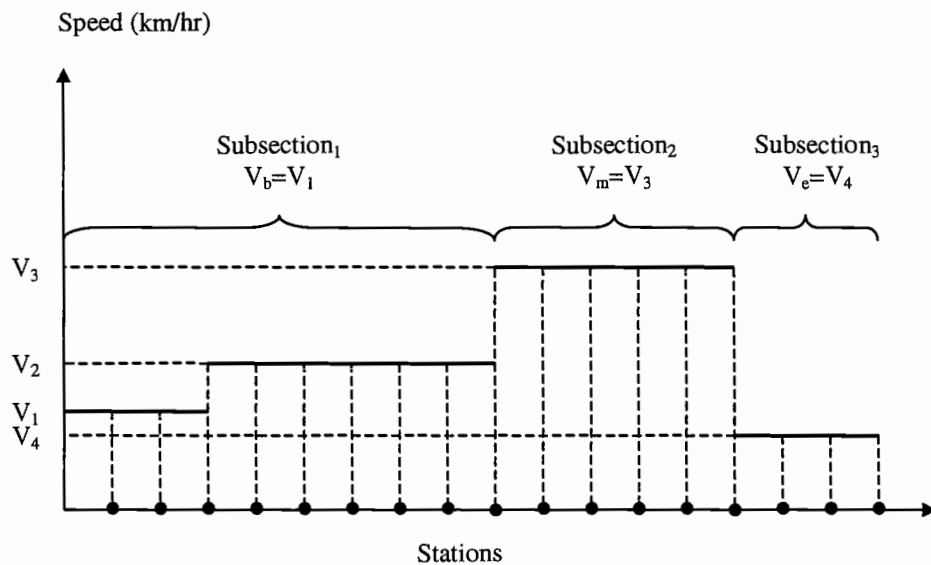


Figure A16-2. Determining subsections using vehicle speed.

deceleration rates (DR) of the vehicle in meters per minute are used to compute accelerating and decelerating time, respectively.

The model computes the travel time considering following cases:

Case 1: If $V_b < V_m < V_e$ (Figure A16-3), travel time (in minutes) in the beginning (t_b) subsection is computed as follows:

$$t_b = \frac{L_b}{V_b} \quad \text{A16-6.}$$

where L_b is length of the beginning subsection in meters. The model considers the accelerating distance (AD) and time (AT) in the middle and ending subsections. The accelerating distance in the middle subsection is (Mannering and Kilareski, 1990):

$$AD_m = \sqrt{\frac{V_m^2 - V_b^2}{2AR}} \quad \text{A16-7.}$$

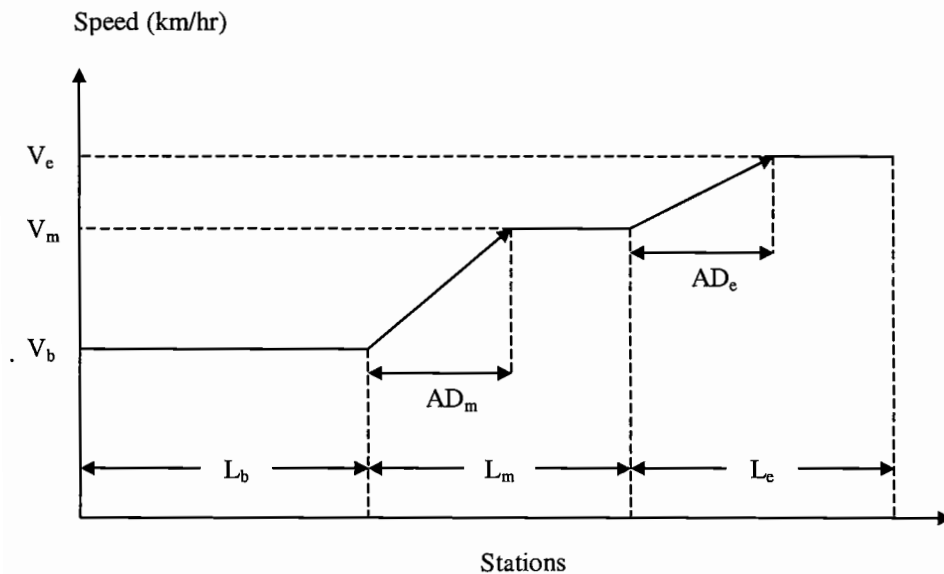


Figure A16-3. Case 1: Determining travel time.

then, the model computes the accelerating time using the following equation

(Mannering and Kilareski, 1990):

$$AT_m = \sqrt{\frac{2AD_m}{AR}} \quad \text{A16-8.}$$

The total travel time for the middle subsection is computed using the following equation:

$$t_m = AT_m + \frac{L_m - AD_m}{V_m} \quad \text{A16-9.}$$

In the ending subsection, the accelerating distance (AD_e) and time (AT_e) is computed using the same manner in Equation 16-7 and 8, respectively.

Case 2: If $V_b < V_m > V_e$ (Figure A16-4), travel time in the beginning and ending subsections is computed using the same manner in Equation 16-6. The model

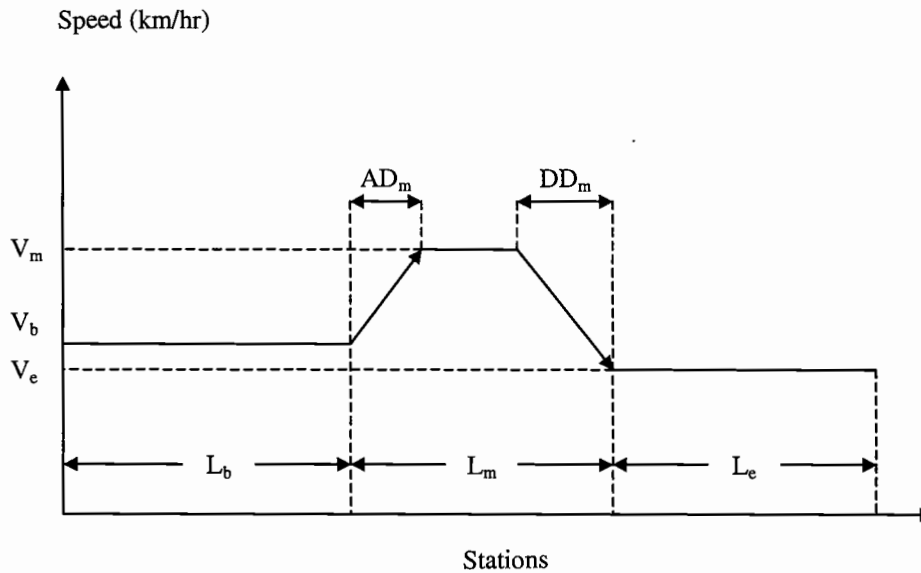


Figure A16-4. Case 2: Determining travel time.

computes the travel time, considering accelerating and decelerating times (DT_m) in the middle subsection. The accelerating distance and time can be computed using the same manner in Equation A16-7 and 16-8. The decelerating distance is:

$$DD_m = \sqrt{\frac{V_e^2 - V_m^2}{2DR}} \quad \text{A16-10.}$$

then, the decelerating time is computed as follows (Mannering and Kilareski, 1990):

$$DT_m = \sqrt{\frac{2DD_m}{DR}} \quad \text{A16-11.}$$

Finally, the total travel time for the is computed using the following equation:

$$t_m = AT_m + DT_m + \frac{L_m - AD_m - DD_m}{V_m} \quad \text{A16-12.}$$

If $AD_m + DD_m > L_m$, then the model computes a new speed as follows:

$$V_m = \frac{V_b + V_m + V_e}{3} \quad \text{A16-13.}$$

then, it repeats the computation of total travel time using this new speed, V_m .

Case 3: If $V_b > V_m > V_e$ (Figure A16-5), travel time in the ending subsection is computed using the same manner in Equation 16-6. The model computes the travel time in both beginning and middle subsections using the same manner in Equation 16-10 to 16-13.

Case 4: If $V_b > V_m < V_e$ (Figure A16-6), travel time in the middle subsections is computed using Equation 16-7. The model considers the decelerating distance and time in the beginning subsection (Equation A16-10 and 16-11), while the accelerating distance and time is computed in the middle subsection (Equation A16-7 and 16-8).

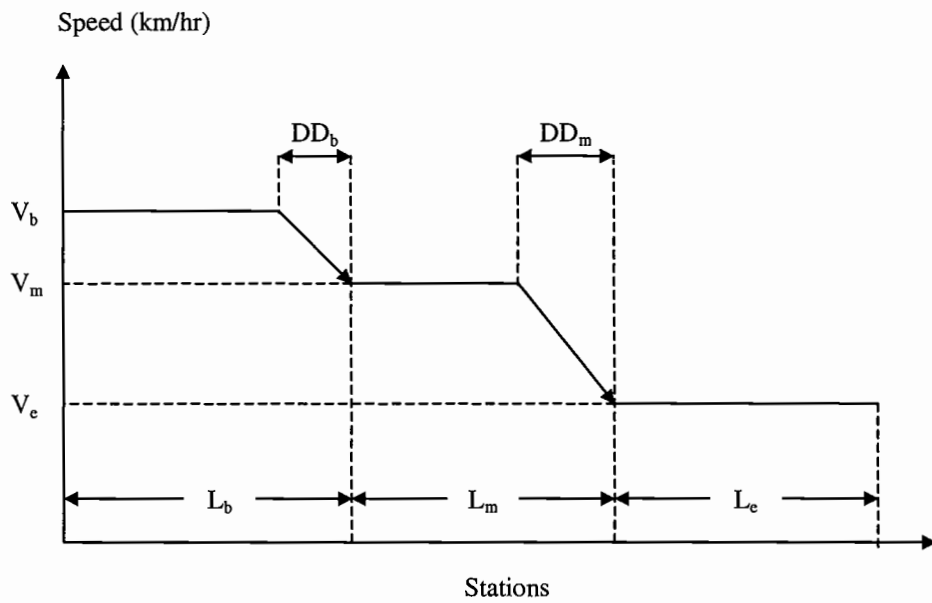


Figure A16-5. Case 3: Determining travel time.

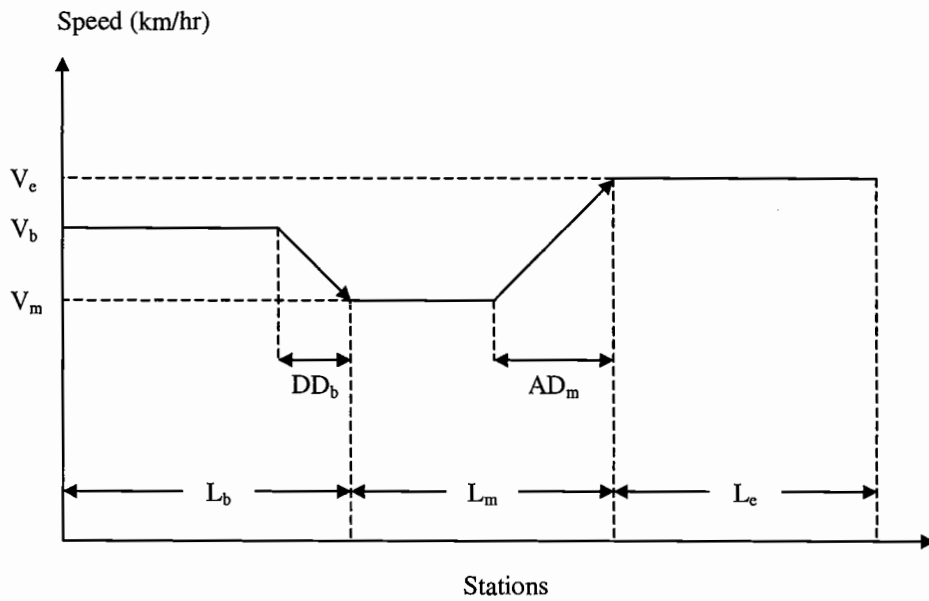


Figure A16-6. Case 4: Determining travel time.

In the model, when a truck travels from the beginning point of the road to the landing, it is assumed that the exiting vehicle speed is equal to zero, while the entering speed equal to the speed at the first subsection. When a truck travels from the landing to the beginning point, the entering speed becomes zero and exiting speed is equal to the speed at the first subsection.

APPENDIX 17. Vehicle Cost Calculation

The machine rate is usually divided into ownership, operating, and labor costs (Sessions, 1992). The ownership costs includes actual equipment purchase cost (new or used), salvage value, depreciation costs, the cost of interest or opportunity cost, insurance premium, property tax, and license and storage fees of the equipment. Operating costs include the cost of fuel, lube and oil, equipment maintenance and repair, and tire replacement. Labor costs components include wages, draws, and salaries, social security, federal unemployment insurance, state unemployment insurance, workmen's compensation, health insurance, and labor burden factor. In the data preparation section, the designer defines these cost components based on the local economic data. In the model, the fuel cost and tire cost are computed separately based on fuel consumption rate and tire wear rate, respectively. The machine rate is computed using the following procedure of straight-line method:

Ownership Costs:

Initial Purchase Price, P

Salvage Value, S (e.g. some % of P)

Economic Life in year, N

Straight-line Depreciation, D :

$$D = (P-S)/N \quad 17-1.$$

Scheduled Machine Hour, SMH (e.g. 2000 hr.)

Productive Machine Hour, PMH :

$$PMH = SMH(1+Utilization) \quad 17-2.$$

Average Annual Investment, AAI :

$$AAI = [((P-S)(N+1))/(2N)] + S \quad 17-3.$$

Interest Rate or Rate of Opportunity Cost, r (e.g. 12 %)

Property Tax Rate, T_r (e.g. 3%)

Insurance Rate, I_r (e.g. 3%)

Interest per year = $rAAI$

Property Tax per year = $T_r AAI$

Insurance per year = $I_r AAI$

Total Ownership Cost = (Depreciation + Interest + Tax + Insurance)/ SMH

Operating Costs:

Percent of Equipment Depreciation for Maintenance and Repair, d_r

Maintenance and Repair Cost per $SMH = (d_r D)/SMH$

Total Operating Cost = Maintenance and Repair Cost/ SMH

Labor Costs:

Hourly Wages per SMH

Labor Burden Factor in percent, LB

Total Labor Cost = Hourly Wages(1+ LB)

Fuel and Tire Costs:

First, the following equation is used to compute the energy delivered to the wheels by the engine, Y_e in horsepower-hour (Botha et al. 1977):

$$Y_e = \frac{LFL_r}{274390} \quad 17-4.$$

where LF is the total longitudinal force at the wheels, L_r is the length of the road stage, and 274390 is used to convert meter-kilogram to horsepower-hour.

The fuel consumption of the vehicle is computed by multiplying the engine energy output by the user-defined value of the fuel consumption rate in liter per horsepower-hour. Then, the model computes the fuel cost using the current price of the fuel per liter. In the model, it is assumed that the tire wear does not greatly vary depending on the road grade. Therefore, the amount of tire wear is estimated by multiplying the maximum acceptable tire wear rate (in cubic millimeter per meter) by the length of the road stage. The model computes the tire wear cost using the adequate price of the tire per cubic millimeter based on the local economic data.

APPENDIX 18. Road Sediment Delivery Prediction

The model adopts the equations used in the SEDMODL, estimating average annual volume of sediment delivered to a stream from the road segments, (Boise Cascade Corporation, 1999). When the designer interprets the results of sediment predictions, there are number of limitations of the model that should be kept in mind. It is assumed that all roads are in-slope with ditch, and roads are over two years old. The model tends to over-predict the sediment predictions if the attribute data (stream, soil etc.) is not accurate and road template information (road length, cut slope, etc.) are incomplete.

The average annual volume of sediment delivered to a stream from each road segment is estimated using the formulations developed depending on the empirical relationships between road surfacing, road use, road template, road grade, vegetative cover, and delivery of eroded sediment to the stream channel (Beschta 1978, Reid and Dunne 1984, and WDNR 1995). Total sediment delivered from each road segment in tons per year is predicted from two road sediment sources; road tread and cutslope:

$$\text{Tread Sediment} = GE_r S_f T_f G_f P_f D_f L_r RW$$

$$\text{Cutslope Sediment} = GE_r CS_f h_c D_f L_r \quad \text{A18-1.}$$

where GE_r is geological erosion rate in kilogram per cubic meter per year, S_f is tread surfacing factor, T_f is traffic factor, G_f is road grade factor, P_f is precipitation factor, D_f is delivery factor, L_r is length of the road segment in meter, RW is road width in meter, CS_f is cutslope cover factor, and h_c is cutslope height in meter. The values for

the variables used in the formulation are obtained from the previous research and listed in the data tables (Boise Cascade Corporation, 1999).

Geological Erosion Rate:

The geological erosion rate is determined based on the geologic information such as dominant lithology and age. Table A18 indicates some of the erosion rates listed in SEDMODL documentation (Boise Cascade Corporation, 1999) for 1:5000,000 scale geologic maps of Idaho, Washington, and Oregon (Bond and Wood 1978, Huntting et al. 1961, Walker and MacLoed 1991).

Table A18. Geologic erosion rates based on lithology and age.

Lithology	Geologic Age of Formation				
	Quaternary	Tertiary	Mesozoic	Paleozoic	Precambrian
Basalt	15	15	30	30	30
Andesite	15	15	30	30	30
Ash	50	50	50	50	50
Tuff	50	50	30	30	30

Delivery Factor:

The sediment model computes the erosion delivery factor for each road stage based on the proximity of roads to streams (WDNR 1995). It is assumed that a road

segment that deliver directly to streams results a delivery factor of 1 (i.e. at stream crossings). A road segment within 30 meters and 60 meters of a stream results a delivery factor of 35 percent and 10 percent, respectively (i.e. at roads parallel to streams). The road segments that are located further than 60 meters do not deliver sediment to streams (i.e. sediment do not reach the stream).

The stream distance between a road stage and the closest stream point is determined based on the stream data in attribute file. The model first locates the coordinates of the middle point of the road stage under consideration. Then it computes the horizontal distances from this point to the stream points listed on the attribute data file, and keeps the shortest distance as the stream distance. Figure A18

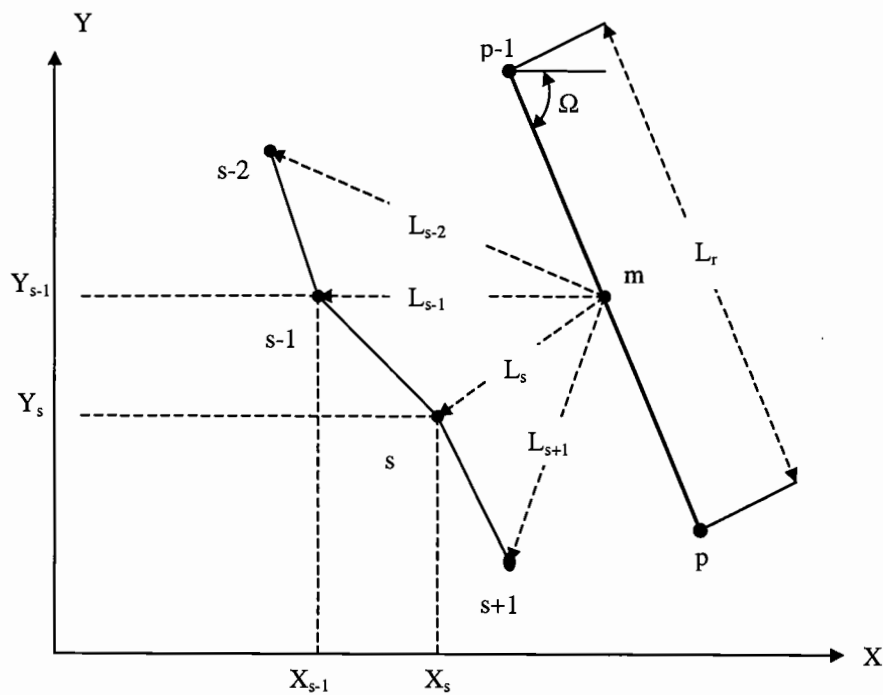


Figure A18. Determining stream distance.

indicates the elements of stream distance from a road stage r , located between two consecutive station point, $p-1$ and p .

The model first computes the coordinates of the middle point of the road stage, m , based on angle of Ω , and X and Y coordinates of the station points:

$$\begin{aligned} X_m &= X_{p-1} + L_r \cos(\Omega) / 2 \\ Y_m &= Y_{p-1} - L_r \sin(\Omega) / 2 \end{aligned} \quad \text{A18-2.}$$

The distances from middle point to the stream points are computed. Following equation indicates a sample stream distance computation for stream point s :

$$L_s = \sqrt{(X_s - X_m)^2 + (Y_s - Y_m)^2} \quad \text{A18-3.}$$

then, it compares all the stream distances (i.e. L_{s-2} , L_{s-1} , L_s , L_{s+1} etc.) and keeps the shortest one. In the case illustrated in Figure A18, the stream distance is L_s since it is the shortest stream distance.

Other Factors:

The sediment model provides the user with the surfacing factors of various surface types based on the previous research. The surfacing factors of gravel, pitrun, and native surface used in the model are 0.2, 0.5, and 1, respectively (WDNR 1995). Traffic factors of various road classes are listed in the road class table. The data on this table are obtained from average measurements taken during road erosion inventory studies (Reid and Dunne 1984 and WDNR 1995). In this table, traffic factors of primary, secondary, and spur roads are 10, 2, and 1, respectively. The road slope factors are assigned to each road stage based on the road grade. For road stages

with grade of less than 5 percent, 5 to 10 percent, and greater than 10 percent, the road grade factors are 0.2, 1, and 2.5, respectively (Reinig et al. 1991). In the model, precipitation factor is computed using the following formula based on the average annual precipitation in the basin, P_{avr} in millimeters (Reid, 1981):

$$P_f = \left(\frac{P_{avr}}{150mm} \right)^{0.8} \quad \text{A18-4.}$$

The cutslope cover factor as percent of vegetative or rock cover on cutslopes are also included into the sediment prediction equation based on the local conditions on the watershed (WDNR 1995). Road width, length of the road stage, and cutslope height in the model is computed based on the road template information.

APPENDIX 19. Optimizing Vertical Alignment

In the model, vertical alignment is optimized using the simulated annealing technique, which is easy to implement and it provides the designer with a good quality/near optimal solution. There are a number of generic decisions that must be done implementing this method to solve a specific problem. These decisions include the initial temperature (t_0), the cooling rate (α), and the stopping condition. In most of the combinatorial optimization problems, maximum number of iterations is defined as a stopping condition, an initial temperature determined by a few experiments, and a geometric cooling rate of 0.95 usually provides reasonable solutions (Reeves, 1993).

In the model, a trial road alignment generated by tracing the possible path using the computer cursor on the 3D image of the terrain is used as the initial solution, s_0 . Then, the model generates an alternative road alignment by changing the elevation of the initial solution in a randomly selected control point by a specified value (e.g. ± 0.5 meters) within the elevation range of the control points. If this new alignment obeys all the geometric and environmental constraint, it is kept by the model as new feasible solution, s . Otherwise, the model generates other alternatives till finding a feasible solution. Figure A19 indicates the description of simulated annealing method implemented in the model. In this figure, $nrep$ is the user-defined number of iteration before adjusting the temperature, and x is a random number between 0 and 1.

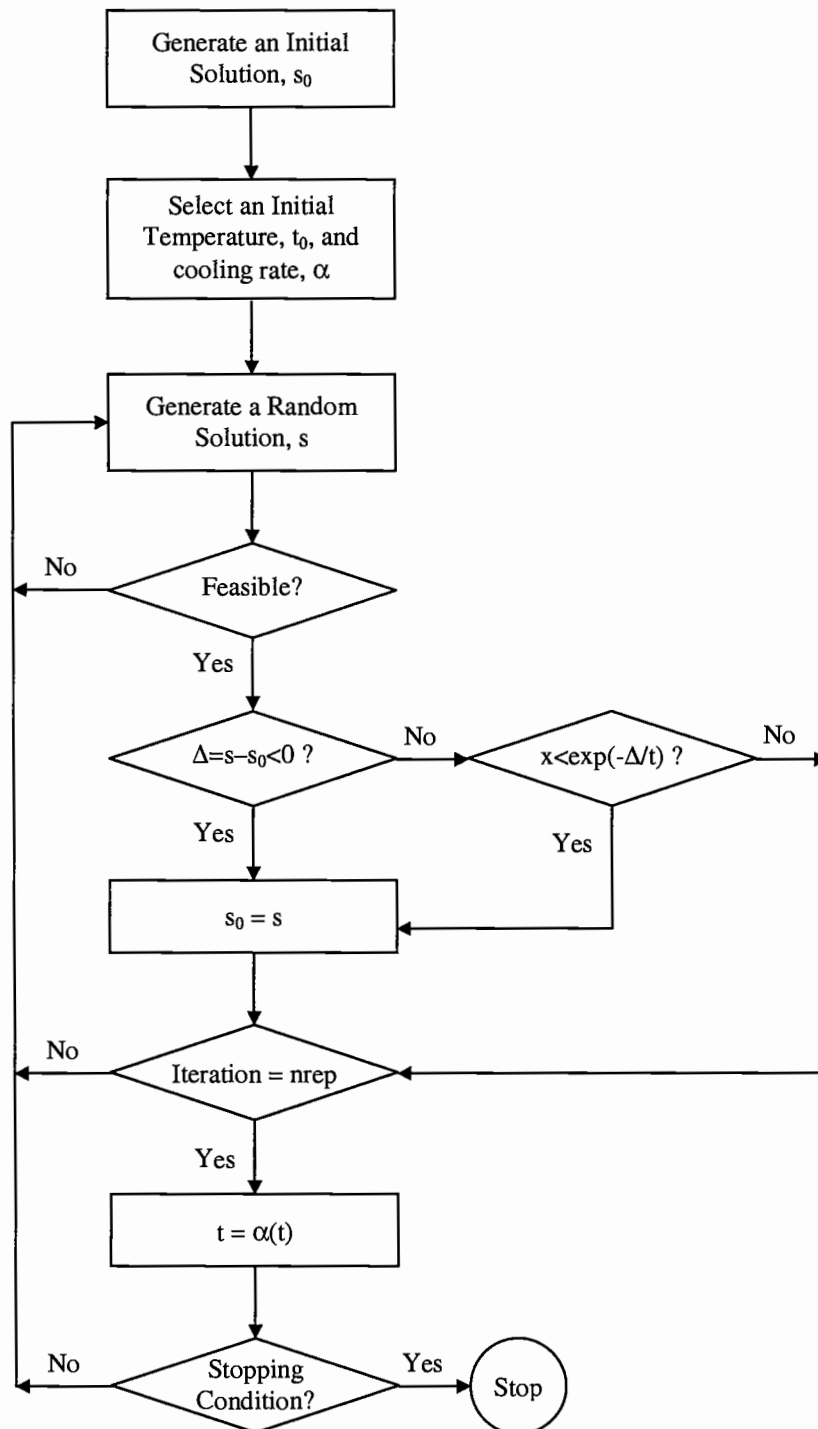


Figure A19. Flow of the simulated annealing method.

APPENDIX 20. Turnout Design Geometry

Turnouts are used for vehicle passage on one-lane, two-direction roads. In the model, they are located on the right or left side of the tangents where the terrain allows. In the common practice, turnouts have to be intervisible with a maximum road distance of 300 meters between turnouts (AASHTO, 1990). In shorter spur roads, it is not very important that the turnouts are intervisible because speeds are reduced, and most logging operations use citizen band radio communications. Typical turnout dimension geometry is shown in Figure A20 (AASHTO, 1990). In this figure, L_{TO} is the length of turnout, L_{TL} is the transition length, and W_{TO} is the turnout width. The turnout should be at least 3 meters in width and 15 meters long with a 7-meter transition at each end.

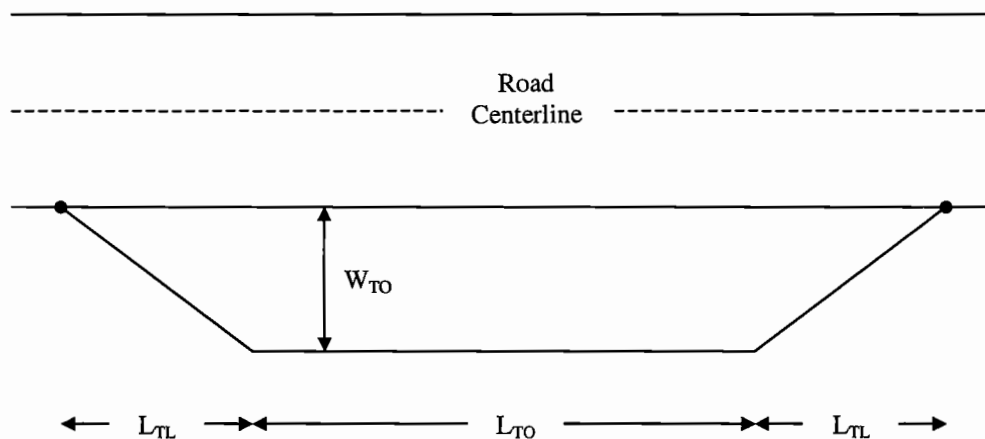


Figure A20. Elements of a turnout geometry.

